5-2011

Stealth Carbon Nanotubes: Strategies to Coat Carbon Nanotubes to Prevent Opsonization and Improve Biodistribution

Nalinikanth Kotagiri
University of Arkansas

STEALTH CARBON NANOTUBES: STRATEGIES TO COAT CARBON NANOTUBES TO PREVENT OPSONIZATION AND IMPROVE BIODISTRIBUTION

STEALTH CARBON NANOTUBES: STRATEGIES TO COAT CARBON NANOTUBES TO PREVENT OPSONIZATION AND IMPROVE BIODISTRIBUTION

A dissertation submitted in partial fulfillment
of the requirements for the degree of
Doctor of Philosophy in Cell and Molecular Biology

By

Nalini Kotagiri
AndhraMedicalCollege
Bachelor of Medicine and Bachelor of Surgery, 2000

May 2011
University of Arkansas

ABSTRACT

Carbon nanotubes (CNT) have recently been in the limelight for its potential role in disease diagnostics and therapeutics. Even before these medical applications can be realized, there is a need to address issues like opsonization, phagocytosis by macrophages and sequestration to liver and spleen for eventual elimination from the body. We believe coating CNT with biocompatible and opsonin resistant moieties will not only help CNT in traversing the blood stream to reach the target organ, but also improve biodistribution tremendously. We set out to achieve this by firstly identifying a new compound, mAmp, which is a fluorescent derivative of the antibiotic, Ampicillin. Besides possessing a varied plethora of properties that complements CNTs already superlative traits, mAmp also affords opsonin resistance to CNT. We wanted to test and compare the four categories of opsonin repellants that we employed: synthetic – Polyethylene glycol (PEG), semisynthetic – mAmp, seminatural – Dextran sulfate (DSS) and natural – Protein A (PrA) + Factor H (FH). We developed novel strategies to conjugate these moieties to CNT and in the process also implemented attachment of Antibodies, specific recognition moieties, to these hybrids to make them ready for precision targeting downstream.

Of the four materials used, DSS posed considerable difficulties in achieving a pure DSS-CNT hybrid mainly due to its size and lack of defined purification strategies to separate polysaccharides in a mixture. We responded to this challenge by devising a simple lectin based affinity chromatography system that employs CNT as the support material. As proof of principle we tested the four hybrids on *Staphylococcus aureus*, in

their ability to evade the bacterium in the absence of specific antibody and ability to specifically attach to the bacterium in its presence. We then tested the particles on human macrophages in the presence of opsonins, C3b and IgG. It was henceforth proved that coating CNT with the opsonin resistant moieties provided excellent immunity versus macrophages and considerable stealth character to CNTs.

This dissertation is approved for
Recommendation to the
Graduate Council

Dissertation Director:

_____

Dr. Jin-Woo Kim

Thesis Committee:

_____

Dr. Douglas D. Rhoads

_____

Dr. Joshua Sakon

_____

Dr. Russell J. Deaton

_____

Dr. Steve Tung

DISSERTATION DUPLICATION RELEASE

I hereby authorize the University of Arkansas Libraries to duplicate this dissertation when needed for research and/or scholarship.

Agreed _____

Nalini Kotagiri

Refused _____

Nalini Kotagiri

ACKNOWLEDGEMENTS

Starting my research career as a doctoral student after the culmination of my medical education was challenging, to say the least. It required a fresh outlook, acquisition of new skillsets, deriving satisfaction from the most fleeting of experiences – experimental result and preparing for a career in academia. My advisor, Dr. Jin-Woo Kim, has been an excellent role model all throughout my graduate studies. Just like as in the ancient vedic system of *Gurukul*, he has been a mentor, father figure, big brother and friend to his students; constantly guiding, yet not over-imposing. It was through his broad outlook and attention to detail; I understood the importance of good experimental design to follow-up a good idea and expand its scope to its full potential. I thank him for providing me with the intellectual wherewithal and freedom to independently pursue the research topic of my choice. He has led by example and kept me motivated through my stint as a graduate student, to which I will be ever grateful.

My peers, Ju Seok Lee and Jeong Hwan Kim, have been the source of constant encouragement and support during my graduate studies. Ju Seok played a critical part during the entirety of my stay in the Bio/Nano Technology Lab. When I first started, the hands on skills in handling various laboratory equipment was directly acquired from him. During the final months of my dissertation, he played an active part in helping me finish my tissue culture experiments. Jeong Hwan, his zest for research and positive outlook has constantly rubbed off on me and helped me be a better researcher. More than anything, Ju Seok and Jeong Hwan have been great and trustworthy friends.

I thank my committee members, Dr. Douglas Rhoads, Dr. Russell Deaton, Dr. Steve Tung and Dr. Joshua Sakon for their utmost patience shown during my PhD qualifying examination and final defense. They have been very supportive during the entirety of my course and have time and again provided valuable guidance and information.

I would very much like to thank Dr. Jackson Lay for his invaluable suggestions and assistance in helping me decipher the structure of mAmp. Without his continued interest and expertise in the project it would have been very difficult to pursue the molecular analysis of the compound and in all probability would have delayed my dissertation even further.

John Judkins, Tom Garrison and Chase Darr have been valuable lab members and friends. Discussions and exchanges of information with them have made me look into various aspects of data analysis with a different perspective. I would also like to thank Jason Clendenin and Husein Rokadia with whom I have collaborated on diverse projects. Associating with them has helped me broaden my understanding of various disciplines and improve my skillset.

My deepest gratitude to my parents, who have been patient and supportive from the very beginning. I thank them heart fully for always being with me in mind and spirit even through the most difficult of times in spite of the physical distance.

Finally, special thanks to my wife Shruti for her love and patiently enduring this journey with me and for truly being the “better half”.

DEDICATION

To my parents,

Murali Krishna Rao Kotagiri and ***Seetayamma***

and

To my wife,

Shruti

---

with love

TABLE OF CONTENTS

CHAPTER 1

Introduction

The last decade has seen the emergence of a new field of medicine aptly termed Nanomedicine that utilizes nanoparticles and similar materials in that dimension range to diagnose and treat afflictions of the human body. Its logical that an intravenous route will be the preferential mode of administering the nanoparticles and given that most end capillaries measure not more than 5-6 microns in diameter it can be safely assumed nanoparticles are preferred over microparticles to prevent aggregation. Please note that a nanoparticle is a loose terminology applied to engineered particles and for lack of a naming convention to classify the different architectures that can be manufactured. Some of the common architectural shapes are rods, spheres (hollow and solid) and tree like. The uniqueness of nanoparticles comes from their dimensions (1nm-100nm) which are larger than atoms and smaller than cells (Buzea et al., 2007). This allows for engineered nanoparticles to be designed in such a way that they tag specific cells, such as tumor cells, and enable monitoring and destruction of the respective cell type. Such specificity and precision in targeting individual cells is an encouraging departure from drugs that systemically target even normal cells leading to undesired side effects (Davis, 2007). Besides this the different varieties of nanoparticles bring something unique to the table that warranted their physical, chemical and optical characterization in the first place, such as fluorescence, ease of conjugation to ligands and optical responsiveness to Ultraviolet (UV) and Near Infrared (NIR) and Infrared (IR) radiation (Sokolov et al., 2007; O'Connell et al. 2002). Research groups interested in biomedical applications of these

nanoparticles have the luxury to choose from their signature properties to suit their individual needs and tune them accordingly for the desired effect. One of the nanomaterials that attracted our attention was carbon nanotubes (CNT), prompted mainly due to recent revelations on three vital traits required for *in vivo* diagnostic and therapeutic purposes. One, even though there have been mixed reports about the toxicity of CNT, intravenous injection in animal models have yielded encouraging results concerning its biocompatibility (Maynard et al., 2004; Huczko and Lange, 2001; Huczko et al., 2005; Lam et al. 2004; Warheit et al., 2004; Shvedova et al., 2005; Yokoyama et al. 2005; Sato et al. 2005; Poland et al., 2008; Schipper et al., 2008; Lewinski et al., 2008). Two, after favorable attachment to ligands CNT have shown high degree of specificity to targeted cells and tissue (Zharov et al., 2005; Kam et al., 2005; Panchapakesan et al., 2005). Three, CNT have demonstrated a high degree of internalization into a wide range of cells and couldintracellularly traffic through different cellular barriers (Pantarotto et al., 2004; Bianco et al., 2005). Above all, its CNTs signature property, NIR radiation absorption and thermal excitability, is what enables effective tracking and localization of the nanoparticles *in vivo*(O'Connell et al. 2002).

Carbon Nanotubes:

Carbon nanotubes (CNT) are hollow cylindrical tubes with high aspect ratios corresponding to 100-300nm in length for processed CNT and up to 2-5 microns for unprocessed CNT, and diameter of 1-2nm (Iijima, 1991). Ever since their discovery in 1991 they have attracted a lot of attention due to their unique structure and properties.

They are known to be one of the most versatile nanomaterial around as they exhibit superlative electronic, electrical, optical, thermal, magnetic, mechanical and recently, biological properties (Baughman et al., 2002).

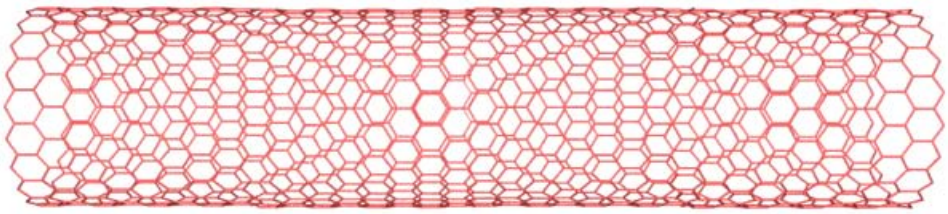

Figure 1.1. Illustration of Carbon nanotube

We shall focus on the optical, thermal and biological properties of CNT since they are pertinent to the successful design and implementation of the *in vivo* photothermal response. CNT exhibit band-gap fluorescence in the 800 to 1600nm wavelength of the near infra-red spectrum (O'Connell et al. 2002). Photo-excitability of CNT in the near IR range is of extreme significance for biological applications since living cells and tissues are virtually transparent to near IR radiation in the range of 750-1200nm (Konig, 2000). Hence the near IR responsiveness of CNT makes them ideal candidates for bioimaging and in vivo IR laser targeting. Besides the ability to absorb and fluoresce near IR radiation, CNT act as perfect heat sinks whereby they confine the generated heat in its clusters, thus reducing heat loss to the surroundings (Kim et al., 2007). This critical property of CNT can eventually help in reducing extensive damage to the surrounding normal tissue, by localizing the heat to small pockets around itself (Kam et al., 2005;

Panchapakesan et al., 2005). CNT also have a high melting point of approximately 2000^{o}F, which would ensure negligible loss of structural integrity during the photothermal therapy. The combined optical and thermal properties have encouraged us to perform experiments on in vitro bacterial photothermal damage using Nd:Yag IR laser pulses. The results demonstrated the viable use of CNT as not only effective targeting agents but also as high-affinity biomolecular interactive agents. CNT possess the ability to passively transport itself, spontaneously through the cell membrane of animal cells as was shown in some *in vitro* studies recently (Pantarotto et al., 2004; Bianco et al., 2005). Henceforth, CNT have been demonstrated to act as transfection agents to transport DNA, RNA and other small biological moieties inside cells (Kam et al., 2005; Lu et al., 2004). The ability of CNT to interface with many of the biopolymers as well as living cells on the whole, has prompted the wide array of bio-medical experiments (Kim et al., 2004). It has been reported that cell culture experiments using cardiomyocytes and pristine CNT have yielded no toxicity data, and CNT was concluded biocompatible (Garibaldi et al., 2006). A step further into performing real world practical biomedical application using CNT yielded encouraging results. CNT attached with folate moieties were made to selectively target tumor cells *in vitro,* followed by irradiation with short IR laser pulses (Kam et al., 2005).Effective tumor cell destruction was observed.

The most important reason behind using CNT as an *in vivo* vector is its shapeand structure. The rod shaped CNT with high aspect ratio (ratio of length and diameter) provides ample surface area and conformation to the attachment of ligands in multiple ways. For example the ends/tips of CNT can be used to attach certain ligands and the sidewalls can be used to attach a different type of ligand if desired. This allows for

multifunctionality and myriad ways to design applications where such traits are highly required. The architecture and surface chemistry of CNT allows for ligands to be attached in four different ways: covalent, noncovalent hydrophobic attraction, noncovalent π–π stacking and noncovalent electrostatic attraction (Yang et al., 2007). Covalent bonding of ligands to CNT is performed using the carboxyl functional groups (COOH) that are introduced during the processing of pristine CNT as a result of acid induced oxidation (Bahr and Tour, 2002; Hirsch, 2002)]. The COOH groups on CNT's surface can be used to form amide linkages with ligands possessing amino groups. We however refrained from using this chemical coupling due to the purported effect of disrupting the electronic property of CNT and mostly due to the indeterminate number of COOH groups that can be introduced on the CNT, which is highly random and cannot be controlled. A given CNT can have COOH groups introduced on its entire surface or only partially which will interfere with downstream control of ligand attachment which we wish to attain. For any particle that is chosen for an *in vivo* diagnostic and therapeutic application, we believe it's imperative that coating of ligand on its surface has to be complete and uniform so that the actual surface of the particle that will come in contact with the surrounding fluids is minimal. This will allow for efficient transportation and biodistribution of the particle. This will be the underlying theme throughout this work and will be discussed at length in the next chapters. Non covalent hydrophobic attraction is possible between the hydrophobic sidewalls of CNT and hydrophobic moieties or domains located in ligands (Zheng et al., 2003; Balavoine et al., 1999; Star et al., 2002; Kotagiri and Kim, 2010), for example there are many hydrophobic domains located in proteins which unfold and interact with other hydrophobic materials. Certain moieties that possess free π electrons,

aromatic compounds generally and highly conjugated systems, can stack on the sidewalls of CNT without directly coming in contact with the surface (Chen et al., 2001; Kim et al., 2006). It is CNTs unique electronic structure that makes such a versatile bonding possible due to the presence of delocalized π electrons. In more cases than not the compound π stacking on CNT is a low MW compound and acts a crosslinker to attach larger and more complex ligands to CNT. Processed CNT, CNT oxidized using acids, possess numerous charged groups on their sidewalls such as carboxyl and sulphonic acid which can be used to electrostatically bind to other charged moieties (Bahr and Tour, 2002). This is a very vague conjugation scheme as it requires a high degree of control over the solutions and compounds used to prevent any cross interactions with other charged groups that is not intended. We have employed all the noncovalent conjugation schemes listed above for attaching ligands to CNT, as will be discussed in the later chapters. It is hard to imagine any other competing nanoparticle to have such a varied and suitable repertoire of properties for biomedical applications. Gold nanoparticles, quantum dots, titanium oxide particles have their own pros and cons, however it's CNTs right mix of structure, shape, optical properties and their behavior in biological environment make them a frontrunner amongst contemporary nanoparticles for suggested biomedical applications.

Despite of all these advantages demonstrated by CNT they also possess certain disadvantages that make them difficult materials to process and handle. CNT have a high propensity to bundle up due to the van der Waals attractive forces existing between the individual tubes (Niyogi et al., 2002). This leads to complex entanglements that make them very difficult to disperse in solutions. The sp^2 chemical bonding and architecture also make them hydrophobic thereby resulting in extremely low solubility in aqueous

solutions. It's common knowledge that all living systems are water based and therefore aqueous solubility is a prerequisite for any potential biomedical applicability. Making pristine CNTs, which are manufactured and supplied as dry powder form, from an extremely long, bundled and hydrophobic state into a shortened, individual and hydrophilic state will be the first challenge we address in chapter 3. Even though many strategies to render CNT hydrophilic such as treatment with surfactants, Triton X and Sodium dodecyl sulfate (SDS), have been implemented, we still found it essential to come with a unique and novel solution to make the CNT not only water soluble but also biocompatible. Surfactants usually are considered to be toxic to animal cells as they denature the cell membrane and eventually lead to cell disruption (Partearroyo et al., 1990).

Nanomedicine:

The quest of many pharmaceutical companies is the development of novel drug delivery systems as it has been a pressing issue to deliver the correct dose to a specific site. The failure of traditional therapeutics in delivering precise and controlled amounts of drug to a specific site has often lead to severe unwanted side effects as a result of administering excessively high doses. This is where novel nanomaterials such as CNT are poised to deliver due to their ability to translocate to the specific site after proper functionalization. This new modality in therapeutics through precision targeting will reduce systemic side effects and improve patient compliance. Usually nanoparticle based therapeutics is reliant on carefully selecting the right type of nanoparticle wherein the nanoparticle serves

simply as a vector to carry the therapeutic agent such as anti-tumor drugs to a specific tumor site. To cite a few examples, the FDA has approved some nanoparticulate and microscale drug delivery systems (DDS): Abraxane (Paclitaxel conjugated to albumin particles), AmBisome (Amphotericin B liposome), Myocet (Doxorubicin liposome), Elestrin (Estradiol complexed to calcium phosphate nanoparticles) etc. (Bajwa, 2008). The common theme in the list of nanoparticulate formulations approved by FDA is that almost all of them have the active component (the therapeutic agent) as the functionalized conjugate and the carrier serves only for translocating it to the specific site. We intend to use CNT not only as a vector but also as a diagnostic and therapeutic agent due to its unique optical and thermal properties respectively.

Generally good therapeutic and clinical success can be achieved if four important parameters can be satisfied: increased blood residence time, low toxicity, high specificity and excretability. From the moment the particle is injected intravenously till it is completely excreted, it will have to defy the natural order of things (it's understandably an engineered 'foreign' material) and perform functions autonomously and effectively. We approach the selection and design of the nanoparticle with these in perspective, fully understanding that each phase is connected to the other and interdependent on each other's success. Surface functionalization of CNT will aid in improving the parameters: blood residence time, toxicity and specificity directly and have a somewhat lower influence on the excretability. This is because the glomerular capillaries in the kidney filter based on the size of the particles, predominantly. It has been reported recently that CNT that are shortened and well dispersed pass through the glomerular membrane and get excreted through the renal system (Lacerda et al., 2008; Ruggiero et al., 2011)). Since

we have developed and perfected processes to render CNT short, unbundled to the basic dimension and extremely water soluble we are confident that they will behave accordingly [25]. Our focus and expertise is in the area of functionalizing CNT so that they have longer blood residence time, have negligible to no toxicity and are specific to a particular cell/tissue type for precision targeting. There have been many reports over the years on ways to coat CNT with peptides such as folate receptors (targeting tumors), aptamers and cell specific antibodies and these studies have successfully demonstrated tumor regression and ablation over the course of the treatment (Kam et al., 2005). Alongside it is but natural to address the issue of toxicity as it goes hand in hand with the functionalization of the CNT, when the appropriate ligands for site specific delivery are being selected. However, there is a glaring lack of any concerted study on how CNTs blood circulation times can be improved. There have been some sporadic reports on functionalizing CNT to improve the bio distribution in mice (Liu et al., 2007), but none that studies the interaction of CNT with the very cells in the bloodstream that prevent this from happening, macrophages. We believe it is important to put a magnifying glass on the environment inside the blood vessels where possible rejection/acceptance of the introduced ‘foreign’ CNT might be happening. Studying the micro milieu for such events rather than whole body bio distribution will shed light on the complex factors and their interplay that are involved with this phenomenon. The entirety of this work will be focused on developing strategies and ways to coat CNT to prevent the interaction with macrophages and improving blood circulation times and in the process also address the biocompatibility and specific targeting issues by using biocompatible ligands and cell specific antibodies.

Need for Stealth:

The immune system is a defense mechanism of the human body against invading pathogens and foreign materials and works on the basic self/non self-discriminatory rule. Anything considered harmful including cells of the human body are quickly eliminated. In 1908 Elie Metchnikoff and Paul Ehrlich shared the Nobel Prize for their pioneering contributions, innate immunity and adaptive immunity respectively. Innate immunity is a rather broad term used to indicate non-specific immune response and adaptive immunity indicates a specific immune response. The nonspecificity of innate immunity makes it the first line of defense against invading pathogens and foreign materials, whereas the specificity of adaptive immunity makes it the second line of defense and affords long term protection against the pathogen (Alberts et al., 2002). The innate immune system is comprised of an anatomical barrier, a cellular and humoral division, each having their specific roles in preventing and early control of any invasion of the human body by pathogens and foreign particles (Male et al., 2006)

The anatomical barriers to infection are the epidermal cells of the skin, mucous lining of the gastrointestinal tract and the enzymes and secretions of sebaceous, lacrimal and salivary glands such as lysozyme and saliva (Male et al., 2006).

The humoral component of the innate immune system is the next barrier to any potential infection, which has managed to get past the anatomical barriers specified above. It is common knowledge that any infection is accompanied by classical signs of acute inflammation such as edema (accumulation of serum) and subsequent suppuration (pus formation). The first phase of edema is mainly due to the components present in the

serum, such as complement factors, immunoglobulins, interleukins, coagulation factors and interferons. These serum proteins flood the inflammation site and start associating with the pathogen/foreign material and subsequently aid in recruiting the heavy machinery i.e macrophages and monocytes. Macrophages and monocytes are larger cells that can phagocytize the invaders and sequestrate them to liver and spleen for further processing and eventual excretion. Therefore the main role of the humoral branch of the innate immune system is to act on the invading pathogen/foreign material and associate with them so that they can be tagged by the cellular component of the innate immune system. The complement system serves two roles: it tags the pathogen/foreign material also known as opsonization and recruits cells of the cellular component, monocytes and macrophages (Kinoshita, 1991). There are more than 20 serum proteins which constitute the complement system and the ones that interest us and are pertinent to this study are the proenzymes which when activated by pathogens/foreign material cleave certain complement proteins to yield complement factors that act as opsonins (Sahu and Lambris, 2001). C3b and C4b are the only complement factors that act as opsonins and the rest have varied roles which is outside the scope of the present study (Male et al., 2006). Likewise Immunoglobulins is a large family of plasma proteins that also flood the infection site and tag the invaders. However, only the IgG fraction of the immunoglobulins serves as opsonins. C3b and IgG therefore are the two most abundant and important opsonins present in human serum that mediate majority of the downstream immunological responses to potential pathogens (Male et al., 2006).

The cellular component is constituted by cells like macrophages, monocytes, eosinophil and natural killer cells. Of these, tissue macrophages and monocytes are

primarily recruited to the sites of infection and invasion and are responsible for the intracellular killing of pathogens/foreign material (Adams and Hamilton, 1984). Tissue macrophages are found in the liver, spleen and bone marrow where the extraneous particles generally end up (Demoy et al., 1999). Before that happens the newly recruited monocytes differentiate into macrophages in the blood serum and work to phagocytize the foreign particle after being tagged by opsonins, and eventually are sequestered to the end organs such as liver and spleen for excretion. Phagocytosis is a phenomenon where substances exterior to the cell are engulfed by macrophages for intracellular digestion or sequestration to liver and spleen. It is an irreversible and active mechanism that involves receptor mediated uptake via an opsonin dependent manner or non opsonin dependent manner (Panyam and Labhasetwar, 2003). Non receptor or passive endocytosis otherwise called pinocytosis, does not involve any receptors (Tabata and Ikada, 1990). In mice opsonin independent receptor based phagocytosis of liposomes has been reported (Liu et al., 1995). We however are interested in processes taking place in the human body, where only opsonin dependent receptor based phagocytosis takes place (Liu et al., 1995). Hence we will emphasize and discuss in more detail this particular type of phagocytosis. Macrophages are decorated with a wide arsenal of receptors hooked to the plasma membrane: (1) Receptors for complement factor C3b (2) Receptors for the F_c portion of immunoglobulins (3) Receptors to mannose/fucose and other bacterial surface polysaccharides (Patel and Moghimi, 1998; Kiwada et al., 1998; Kamps and Scherphof, 1998; Sparrow et al., 1989). Once the pathogen/foreign material that has already been tagged by opsonins comes in contact with macrophages they are rapidly recognized by the receptors which then initiates the phagocytotic process where the particle is engulfed

by the macrophage for intracellular digestion. Any undigested particles end up in the liver and spleen and are eventually excreted (Moghimi et al., 2001).

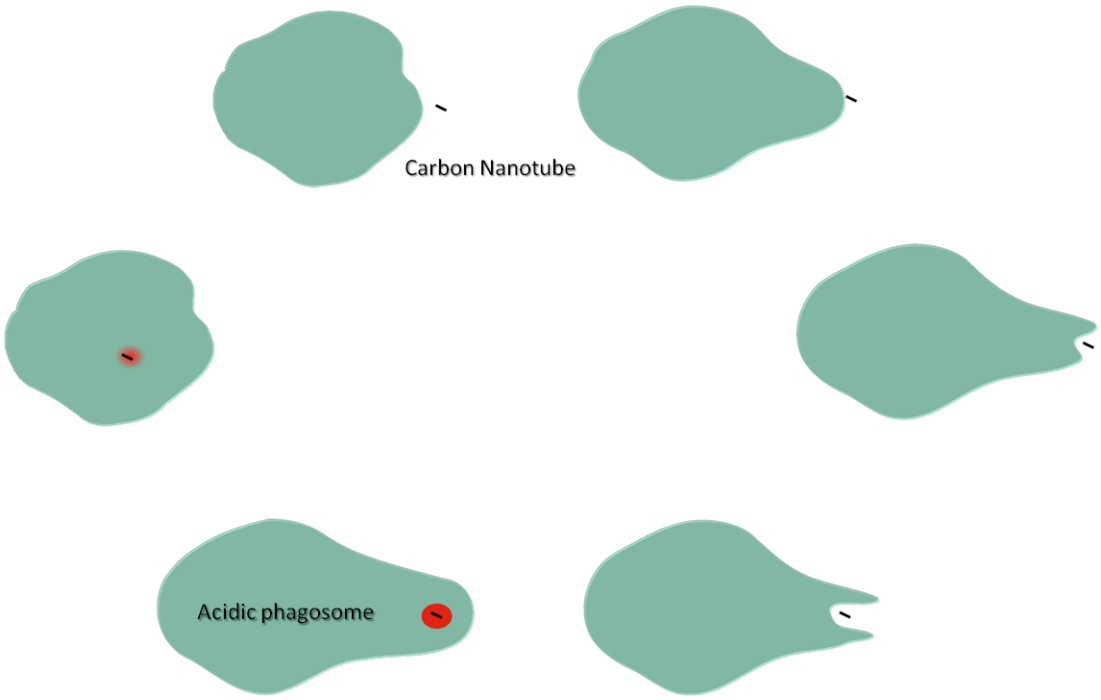

Figure 1.2. Schematic of endocytosis of CNT by macrophages

It can then be safely agreed that CNT (an engineered foreign particle) would suffer the same fate as any pathogen entering the blood stream. Opsonins C3b and IgG which are present in blood in substantial quantities will readily attach to the hydrophobic sidewall of CNT and tag them for macrophage targeting. Macrophages have receptors for the F_c portion of IgG and Complement receptor 1 (CR1) for C3b. Newly recruited macrophages will recognize the opsonins on the surface of CNT through the respective receptors and commence the process of phagocytosis to finally completely engulf the

CNT and initiate intracellular digestion. Being non-biodegradable, the CNT laden macrophages will ultimately make it to their graveyards, liver and spleen. It is here the fate of the intravenously injected CNT will be sealed as they have already been diverted from their original destination (tumor) and will be eventually excreted. This is a very common trend observed amongst intravenously injected polymeric and metallic nanoparticles lately (Puisieux et al., 1994; Stolnik et al., 1995).

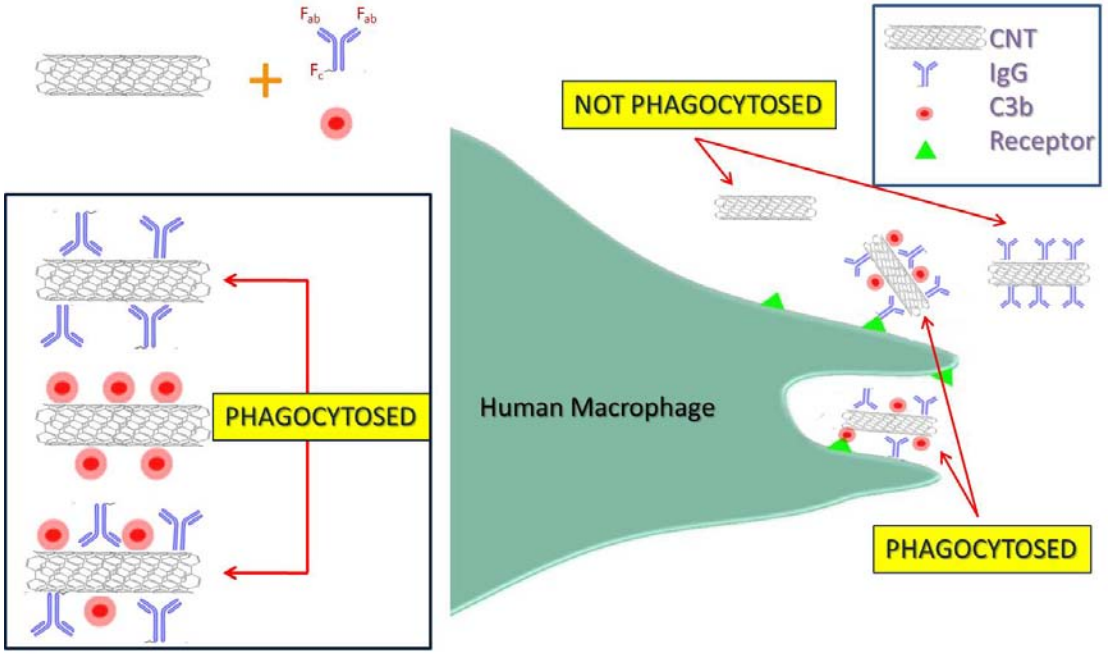

Figure 1.3. Schematic of endocytosis of an opsonized CNT by a macrophage.

Even in reports where whole body bio distribution studies are conducted, after amenable functionalization with ligands that prolong blood residence times, there are a high percentage of nanoparticles that could end up in the liver and spleen because

materials injected in bulk to improve bioavailability often aggregate and precipitate down. More often than not this is the case in such studies as the only way to effectively monitor the location of the particles is to have a high enough concentration to be able to trace them. Therefore the solution to improve blood residence time is to devise novel ways to coat CNT with biocompatible ligands which prevent attachment of opsonins to CNT by acting as a shield and individually assess their performance *in vitro,* which simulates the micro environment of the confined space of the blood vessel where such events take place in matter of seconds after injection. The fate of CNT is decided in the first few minutes after intravenous injection where opsonins flood the area and readily tag the particle if not coated effectively. The shielding of the ligand is a crucial step in rendering the CNT transparent to opsonins and deceiving the innate immune response to make believe it is not foreign. If this battle versus the humoral and cellular component of the innate immune system can be controlled and won we believe the war against the disease/tumor can be easily fought. By designing and manufacturing 'stealth' CNT we are ensuring the vital link between its manufacturing and application is not in peril. The success of any diagnostic or therapeutic precision targeting system cannot be foreseen by overlooking the stealth mechanics of the given particle. With this conviction and awareness we actively pursued novel and unconventional ways to render CNT transparent using different classes of coating materials and also an optical based method to develop stealth CNT. But before we delve into that topic and the materials employed, acquaintance with the factors and principals involved that normally decide the stealth behavior of a particle is warranted.

CHAPTER 2

Literature Review - Biocompatibility, functionalization, biodistribution and physicochemical characteristics governing opsonin attachment and macrophage uptake

Biocompatibility:

The importance of cytotoxicity of xenobiotics, like CNT, gains prominence given that it could be used for biomedical applications. A wide array of cell types have been used to characterize the cytotoxicity of CNTs and the data has been inconsistent and inconclusive to say the least (Jos et al., 2009; Belyanskaya et al., 2007; Pan et al., 2007; Worle-Knirsch et al., 2006; Wick et al., 2007). Part of the reason being the lack of standard and customized techniques to assess CNT toxicity. For example, use of different cell types and diverse doses of CNT for each study by different research groups has only lead to lack of consensus on this issue. It has been shown that viability studies of cells incubated with CNTs and assessed using the commonly used MTT assay (3-(4,5-dimethylthiazol-2-yl)-2,5-diphenyltetrazolium bromide) yielded false positives due to the physical attraction of SWNT with MTT-formazan crystals, thereby interfering with the viability study (Worle-Knirsch et al., 2006). However, the use of its water soluble counterpart, WST-1 (2-(4-iodophenyl)-3-(4-nitrophenyl)-5-(2,4-disulfophenyl)-2H-tetrazolium) yielded a more plausible result as no SWNT-salt aggregations was observed. Besides these factors, parameters such as CNT surface property and presence/absence of impurities also influence cytotoxicity studies to a great extent.

CNT surface property:

The surface chemistry of unprocessed CNT is extremely hydrophobic which leads to formation of large agglomerates due to the van der Waals attractive forces. These rope-like agglomerates were found to be more cytotoxic than well dispersed SWNT on MSTO-211H cells, even more than asbestos (Wick et al., 2007). Therefore the need for well dispersed CNT for biomedical applications cannot be more overemphasized. CNTs are capable of forming well dispersed suspensions in aqueous solutions after oxidation in acid solution mainly due to the formation of carboxyl groups (Vivekchand et al., 2005). Even higher degree of aqueous solubility can be attained by functionalizing the sidewalls with hydrophilic moieties such as polymers. Studies on Chinese hamster ovary (CHO) cells and Jurkat human T-lymphoma cells using glycopolymer coated SWNT and unfunctionalized SWNT have demonstrated lower cytotoxicity for the functionalized SWNT (Chen et al., 2006). Also, unfunctionalized SWNT provoked secretion of proinflammatory cytokines by macrophages in comparison to amino group functionalized SWNT (Dumortier et al., 2006). Functionalization of CNT sidewall can be achieved through covalent and noncovalent methods, each having their own advantages and disadvantages generally. However for biomedical applications *in vitro* and *in vivo*, noncovalent method is preferable due to lower cytotoxicity and preservation of CNTs structural and electronic integrity. Studies using covalently conjugated streptavidin-SWNT demonstrated extensive cell death of human promyelocytic leukemia HL 60 cells after 2 days (Kam et al., 2004). Whereas no such effect was noticed with noncovalently conjugated streptavidin-SWNT even after 5 days (Kam and Dai, 2005). Therefore,

noncovalently functionalized, biopolymer coated and well dispersed SWNT were employed throughout the experiments in order to minimize cytotoxicity of SWNT.

CNT impurities:

CNTs synthesized by the arc-discharge process contain a high degree of catalytic impurities such as Fe, Co and Ni (Vivekchand et al., 2005). The cytotoxicity of these metals is well known and well documented. Pulskamp et al. (2007) showed that rat macrophages and human A549 lung cells when exposed to unpurified CNTs released reactive oxygen species intracellularly due to cell oxidative stress. Other cytotoxic effects include apoptosis, decreased adhesiveness and inhibition of proliferation of human embryo kidney cells; increased intracellular lipid hydroperoxides and lowering of low molecular weight thiols in murine macrophages; lower cell proliferation rate in human epidermal keratinocytes (Shvedova et al., 2003; Kagan et al., 2006; Cui et al., 2005). The most commonly used method to remove the impurities involves acid treatment of CNTs to oxidize the catalysts. As a result of this procedure carboxyl and hydroxyl groups are introduced on the CNT sidewalls (Vivekchand et al., 2005). It has been shown that purified CNT are more cytotoxic when compared to unpurified CNT as demonstrated on human intestinal cells Caco-2 (Jos et al., 2009). This can be attributed to the carboxyl and hydroxyl groups on the CNT surface. It can therefore be reemphasized that rendering CNTs soluble in aqueous solutions does not guarantee the biocompatibility of CNT. Hence, it is imperative that further functionalization of the CNT surface is needed in order to shield the sidewall from the surrounding environment.

Functionalization of CNTs:

Functionalization of CNTs can be achieved through covalent and noncovalent methods. It was discussed in the previous section how covalently modified SWNT were more cytotoxic than noncovalently modified SWNT. Besides demonstrating higher cytotoxicity, covalent modification of SWNT also disrupts its structural, π -electron configuration and photoluminescence properties (Liu et al., 2009). Therefore, covalent modification strategies have been essentially excluded in this work for the reasons cited above. To preserve the sp^2 nanotube structure, chemical adsorption of functional moieties is preferred. π-π stacking, hydrophobic attraction, electrostatic and hydrogen bonding are some of the noncovalent interactions that are involved in stabilizing the functional moieties on the CNT surface. Surfactants such as sodium dodecyl sulfate (SDS) and Triton-X form stable suspensions of CNT in aqueous solutions by forming micelles where the aliphatic chain of the surfactant interacts with the hydrophobic surface of the CNT (Wang et al., 2004). The chemical adsorption of the surfactant can be reversed if the concentration is lower than the critical micelle concentration. Polysaccharides such as starch have been shown to wrap on the CNT surface through hydrophobic interaction (Star et al., 2002). The iodine molecule in the starch-iodine complex undergoes displacement by CNT, thereby enabling the hydrophobic domains of starch to interact with the hydrophobic sidewall of CNT. Another example of hydrophobic interaction is the adsorption of phospholipid-PEG moieties to CNT (Liu et al., 2007). The two hydrocarbon chains adsorb on the CNT sidewall and the hydrophilic PEG groups renders CNT water soluble and biocompatible.

Aromatic compounds, due to their unique structure possess π electrons that complement the π electron lattice of CNT. This results in π-π stacking of the aromatic rings on the CNT sidewall. Pyrene is one such aromatic compound with the versatility to attach functional groups at one terminal for conjugation with various ligands. It has been demonstrated that proteins can be conjugated to CNT through an amino group reactive pyrene derivative (Chen et al., 2001). The same π-π stacking mechanism can be used to helically wrap DNA on CNT, for making them soluble in aqueous solutions and also enable separation of metallic CNT from semiconducting CNT (Zheng et al., 2003). The helical isoalloxazine assembly of a low molecular weight compound, Flavin mononucleotide (FMN) hydrogen bonds with the CNT chirality and helps in improving CNT dispersity and aqueous solubility (Ju et al., 2008). Due to the ease of use and control afforded by noncovalent modification of CNT, we have extensively used π-π stacking, hydrophobic and electrostaticattraction to conjugate a wide variety of compounds, polymers and biomolecules on the CNT sidewall.

Biodistribution:

High biodistribution, prolonged circulation time and low clearance rate of CNT is an essential prerequisite for proposed biomedical applications like tumor targeting and drug delivery. After intravenous injection, CNT's blood residence time, organ biodistribution and accumulation and clearance half-life are highly dependent on its surface characteristics and coating. The first biodistribution profiling of SWNT in mice was performed by Wang et al. (2004) where hydroxylated SWNT were shown to be rapidly

removed from circulation and distributed evenly throughout the body. The blood clearance half-life was 49mins. Cherukuri et al. (2006) reported that SWNT dispersed using Pluronic F108 surfactant had a blood circulation half-life of only 1h, as most of the SWNT predominantly accumulated in the liver. Singh et al. (2006) demonstrated SWNT conjugated to a chelating agent, diethylentriaminepentaacetic (DTPA), accumulated in kidneys (10.5% injected dose (ID)), muscle (6% ID) and skin (2% ID) 30min post i.v. injection. The blood clearance rate was 3.5h. Almost similar blood clearance rate was observed by McDevitt et al. (2007) on using 1,4,7,10-tetraazacyclododecane-1,4,7,10-tetraacetic acid (DOTA), a more potent chelating agent compared to DTPA, conjugated to SWNT. The DOTA-SWNT conjugate accumulated in kidneys (8.3% ID), liver (17.8% ID), spleen (14.3% ID) and bone (2.26% ID) after 3h post injection. PEGylation of nanoparticles has been extensively employed to render the xenobiotics resistant to opsonins, macrophages and RES in general. Currently it is the most popular agent to prevent nonspecific adsorption of blood proteins *in vivo*. Liu et al. (2007) reported branched PEG-phospholipid (PL) with MW 2000, 5400 and 7000 conjugated to SWNT had varied blood circulation and biodistribution profiles. As the degree of branching increased from 2k – 7k MW, there was increase blood circulation half-life from 0.5h – 7h. Raman measurement on hepatic sequestration showed a decreasing trend, 70% ID/g for 2k PEG-PL-SWNT and 30% for 7k MW PEG-PL-SWNT, at 24h post injection. Therefore, higher degree of branching of PEG leads to more uniform and complete coating of SWNT surface which leads to lower hepatic and splenic uptake and higher blood circulation half-life. The blood residence time of PEG did not continue to demonstrate an upward trend beyond 7k MW PEG.

This clearly demonstrates the need to sheath the CNT surface from the external environment by ensuring most and if possible the entire surface is coated with the functionalizing agent. Also, there is a need for more coating materials that have PEG like properties in preventing opsonization and RES sequestration. This will give more options to researchers to coat various kinds of xenobiotics for *in vivo* applications.

Physicochemical characteristics governing opsonin attachment and macrophage uptake:

Size matters:

Physiological and anatomical parameters such as blood transport, tissue diffusion, hepatic filtration and renal excretion along with size of fenestrae in end capillaries dictate that size of the particles is an important factor to ensure prolonged circulation times for nanoparticles and high therapeutic efficacy (Alexis et al., 2008). It was shown in recent biodistribution studies that polystyrene particles ranging from 50nm to 500nm, larger particles demonstrated higher levels of hepatic sequestration thereby hampering their circulation times (Nagayama et al., 2007). Since we are concerned about how nanoparticles interact with opsonins and macrophages the focus will be on how the radius of curvature which is determined by the size, will impact protein attachment and subsequent macrophage interaction. Harashima et al. (1994) and more recently Champion and Mitragotri (2006) have shown size of the nanoparticle is not as important a determining factor for phagocytosis as was thought to be. Instead it was found out that macrophages recognize nanoparticles as a function of number of opsonins attached rather

than the function of the size (Harashima et al., 1994). It was shown that smaller particles that have a high radius of curvature tend to offer less attachment sites for plasma proteins than larger particles with lower radius of curvature. Less opsonins on smaller particles translates to low phagocytic rate by macrophages and hence more stealth.

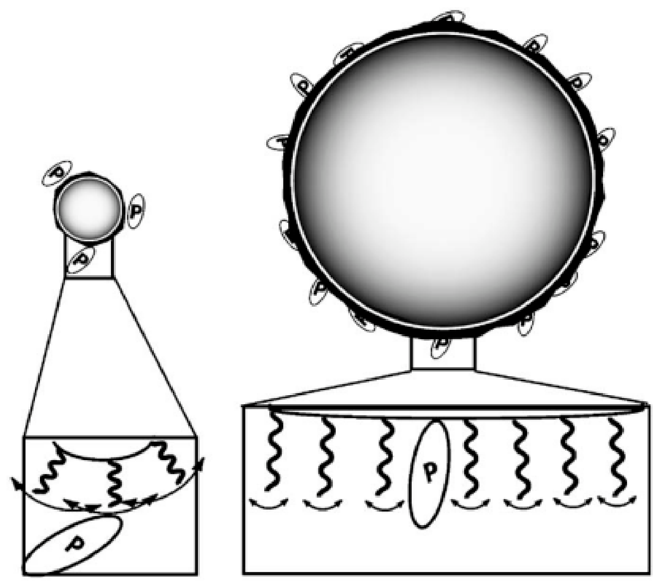

Figure 2.1. Schematic of size effect. P is protein. Reprinted from Vonarbourg et al.(2006). Copyright 2006 Elsevier Ltd.

Some authors have demonstrated that for particles less than 100nm, there is minimal to no uptake by macrophages whether they are coated or not by opsonins (Moghimi and Szebeni, 2003; Rudt and Muller, 1993). Therefore it can be concluded that particles with high radius of curvature, small size (< 100nm) the outcome is more promising compared to larger particles with low radius of curvature.

This augurs well for the CNT employed in our lab as we use Single walled carbon nanotubes (SWNT) which have an effective diameter of 0.8nm - 1.2nm and lengths that vary from 50nm - 150nm after processing. With such small diameter and high radius of curvature, SWNT is an ideal material to escape attachment by opsonins by itself without any extraneous functionalization and coating. However, the lengths have a propensity to show a lot of variation mainly due to the random nature of the shortening process employed.

Shape:

Recently Champion and Mitragotri (2006) have demonstrated that shape of the nanoparticles have a greater role than size in the process of phagocytosis by macrophages. Different shapes of polystyrene (PS) particles were synthesized and exposed to macrophages after opsonization with IgG. The Ω- angle was defined as the angle formed between the point of contact of the cell membrane and the particle.

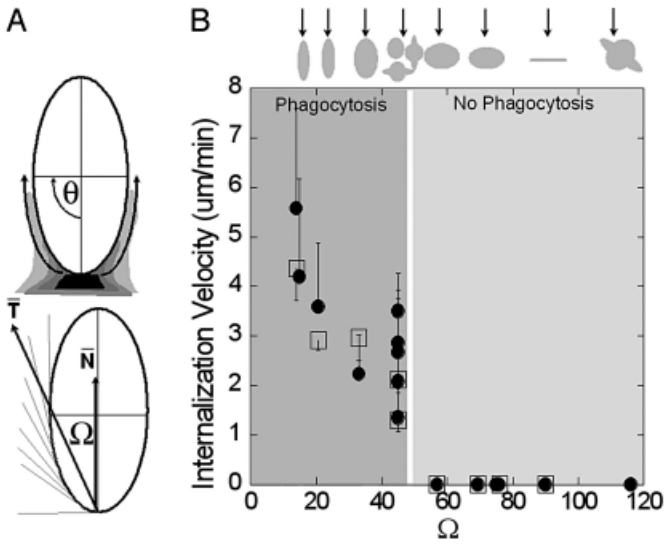

Figure 2.2. A. Schematic of contact angle. B. Representation of internalization velocity with changing contact angles. Reprinted from Champion and Mitragotri (2006). Copyright 2006 the National Academy of Sciences.

Phagocytosis was not initiated at $\Omega > 45^{o}$ for non-spherical particles. Opsonized and non-opsonized particles had the same Ω dependence (Champion and Mitragotri, 2006). This essentially means that particle internalization is primarily dictated by the shape of thesurface at the point of initial contact. For example, in a rod shaped particle internalization is initiated only if the tip/end of the rod comes in contact with the cell membrane of the macrophage and no internalization happens if the point of contact is the sidewall. Therefore orientation of the rod prior to interacting with macrophage will play a great role in determining if internalization proceeds or not. Spherical particles are not faced with this complication and therefore will more readily undergo internalization.

This is pertinent to our study because we are employing SWNT which are rod shaped and have high aspect ratio. The shape of SWNT clearly affords it an advantage in

comparison to spherical and ovoid particles as extraneous and additional factors such as orientation does not have any role in their internalization.

Hydrophilicity:

As Allen (1994) aptly put it “If you want to be invisible, look like water”. Opsonins, IgG and complement factors and plasma proteins in general adsorb readily on hydrophobic surfaces more than hydrophilic surfaces (Illum et al., 1986; Jeon et al., 1991; Allen, 1981). In vitro and in vivo studies have also demonstrated higher degree of phagocytosis and increased sequestration to hepatic tissue of hydrophobic particles in comparison to hydrophilic particles (Tabata and Ikada, 1990; Illum et al., 1986; Gabizon and Papahadjopoulos, 1992; Tabata and Ikada, 1988). In order to counteract the attractive hydrophobic forces between the hydrophobic particle and proteins, polymers such as polyethylene glycol (PEG) are conjugated to hydrophobic surfaces (Otsuka et al., 2003). PEG along with other similar polymers are hydrophilic, inert (no net charge), biocompatible and elicit no response from plasma proteins (Otsuka et al., 2003). The presence of polymer coating on hydrophobic surfaces creates a water cloud which serves as a potential barrier against plasma proteins by preventing any binding from occurring and denying any attachment sites (Coleman et al., 1982).

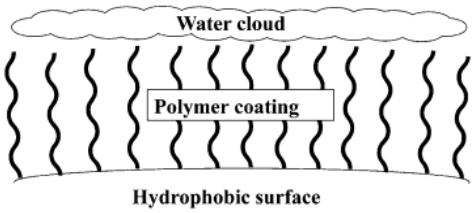

Figure 2.3. Schematic of water cloud on hydrophobic surface induced by polymer. Reprinted from Vonarbourg et al. (2006). Copyright 2006 Elsevier Ltd.

The water cloud is formed due to the high affinity and linking of two to three water molecules by each polymer chain (Antonsen and Hoffman, 1992). The low attractive forces between the surface and proteins are due to the creation of minimum interfacial free energy by the water cloud (Coleman et al., 1982). Besides polymers such as PEG, polysaccharides are also used mainly due to their biodegradability (Romberg et al., 2008).

As coating materials for CNT we have carefully selected only hydrophilic, biocompatible and biodegradable materials such as polysaccharides and proteins. PEG was also employed as a standard.

Surface Charge and Functional groups:

Most functional groups have a net charge and even though they can independently contribute to the interaction dynamics with plasma proteins and macrophages, we will analyze them together in this section. Recent investigation using nanoshells have shown that positively charged particles have a higher rate of uptake by phagocytic cells in

comparison to negatively charged and neutral particles (Yamamoto et al., 2001). Highly charged surfaces in comparison to neutral particles attract complement factors. However, Liu and Liu (1996) demonstrated that complement factors are not activated in the presence of neutral and negatively charged particles. Patel and Moghimi (1998) on the other hand demonstrated that positively charged particles became negatively charged in serum after the opsonization process.

Experiments on polystyrene particles functionalized with amine, hydroxyl, carboxyl and sulfate groups have demonstrated that amine groups along with hydroxyl groups activate complement proteins C3 and C4 (Alexis et al., 2008). Also experiments on thiolated nanoparticles have revealed their plasma half-lives to be ~3hrs and are preferentially up taken by the spleen (Kommareddy and Amiji, 2007). It can then be concluded that amine, hydroxyl and thiol groups are detrimental to the design of any 'stealth' nanoparticle.

Our choice of materials to render stealth property to CNT have been heavily influenced by these studies and we have made sure the surface charge on the different types of stealth CNT we have manufactured possess either neutral charge or negative charge. We also made sure that the materials possessed only carboxyl and sulfate groups for maximal compliance.

CHAPTER 3

Interfacing natural polymers with carbon nanotubes: Coating and characterization of carbon nanotubes by dextran sulfate

Opsonins, such as complement factors, immunoglobulins, and serum proteins, are known to more readily adsorb on hydrophobic particles (Jeon et al., 1991). Single Walled Carbon Nanotubes (SWNT) being essentially hydrophobic in nature, even after chemical oxidation, require to be shielded against opsonins; in lieu of the promise shown towards biomedical therapeutics and diagnostics (Kim et al., 2007; Zharov et al., 2007). Shielded SWNTs will supposedly repel the opsonins in the blood and be immune to ingestion by macrophages (Owens and Peppas, 2006; Carstensen et al., 1992; Muller et al., 1992). Macrophages are cells of the innate immune system and form the first line of defense against any foreign material introduced via the bloodstream (Adams and Hamilton, 1984). Till now, the most reliable and commonly used shielding agents were polymers hat are hydrophilic and inert. Polyethylene glycol (PEG), polysaccharides and phospholipids are amongst the most popular agents that control protein adsorption (Otsuka et al., 2003; Yamamoto et al., 2001).

---

*Reprinted with kind permission from “Carbon Nanotubes Fed on "Carbs": Coating of Single-Walled Carbon Nanotubes by Dextran Sulfate” by N. Kotagiri, J. –W. Kim, Macromolecular Bioscience, 2010, vol. 10, pp. 231-238. Copyright 2010 Wiley-VCH Verlag GmbH & Co. KGaA (see Appendix)

For convenience, we can classify anti-opsonin agents into four categories: Synthetic polymers, modified synthetic polymers, natural polymers and modified natural polymers. Our goal was to utilize an agent belonging to each single class and sheath SWNT to prevent opsonin adsorption. The agents representing the modified natural polymers and natural polymers are Dextran sulfate (DSS) and Protein A - Factor H (PrA-FH) conjugate, respectively. At the same time we also want to conjugate antibodies, as specific recognition moieties, on these hybrids for downstream applications where a specific cell type is targeted for therapy or sensing. Interfacing of DSS with SWNT will be discussed in this chapter followed by interfacing of PrA-FH to SWNT along with antibody conjugation to DSS-SWNT in the next chapter. The synthetic and modified synthetic polymers will be discussed in the subsequent chapter.

Dextran sulfate has the potential for being a good anti-opsonin agent and has been employed extensively on a variety of nanoparticles (Kotagiri and Kim, 2010; Abir et al., 2004). However, there are no conclusive studies utilizing DSS-SWNT for preventing opsonin attachment. Besides preventing CNT from triggering foreign-body response, there is also a need to render CNTs biocompatible and enhance their solubility in biologically relevant aqueous solutions.

Introduction:

Carbon nanotubes (CNTs) have eluded absolute control over its solubility, dispersity, and other solution properties that are paramount for its applicability in device and system integration. CNT's dispersity in aqueous solutions is fundamental to the efficient utilization of CNTs for biological and biomedical applications (Hirsch, 2002; Wong et al., 1998). CNTs' potential cytotoxicity is also considered to be a bottleneck despite the differences in opinions among investigators (Maynard et al., 2004; Huczko and Lange, 2001; Huczko et al., 2005; Lam et al. 2004; Warheit et al., 2004; Shvedova et al., 2005; Yokoyama et al. 2005; Sato et al. 2005; Poland et al., 2008; Schipper et al., 2008; Lewinski et al., 2008). Furthermore, to render their intended functions in vivo, they should be biocompatible without triggering foreign-body responses, i.e., the sequestration into the organs, such as liver and spleen, by the cells of the reticuloendothelial system (RES). Therefore, there is a great need for efficient and effective interfacing with molecules and materials that can not only render CNTs biocompatible, but also enhance their solubility in biologically relevant aqueous solutions. Mild and simple processing strategies for aqueous solubility of CNTs are desired when their role as a molecular transporter and drug vector is envisaged.

DNA, proteins, and carbohydrates have been recently employed to disperse CNTs in aqueous solutions on the basis of the amphiphilic nature of proteins and carbohydrates and the ability of DNA toπ-stack (Zheng et al., 2003; Balavoine et al., 2002; Star et al., 2002).Considering the dimension and robust characteristics of polysaccharides, they could have an advantage with respect to DNA and proteins. Polysaccharides exist as highly flexible, extended polymeric coils, which assume their conformity to

accommodate the particle that they are interacting with (Star et al., 2002).CNT, in particular single-walled carbon nanotube (SWNT), with a high surface volume ratio would serve as an ideal platform for helical wrapping of the polysaccharide. The wrapping generally occurs by the hydrophobic interaction between the amphiphilic polysaccharide and the hydrophobic CNT sidewall (Star et al., 2002). Due to their high molecular weight and molecular dimensions, polysaccharides would offer more uniform coverage of CNTs per unit length and hence impart higher hydrophilic character to CNTs. In addition, polysaccharides have a higher threshold for denaturation compared to DNA and proteins, hence simplifying the processing and post-processing phase of CNT-polysaccharide interaction (Fure et al., 1975).DSS is a polyanionic derivative of dextran, a polymer of anhydroglucose, and extremely water soluble, biocompatible, and readily biodegradable. It is composed of repeating unitsofα-D-1,6-glucose-linked glucan (95%) and 1,3-glucose residues as branches (5%) (Rees and Scott, 1971). Amphiphilic nature of DSS attributes to the hydrophobicα-D-1,6-glucose residues, which constitute the inner lining of the helical polymeric chain, and the hydrophilic sulfate (SO_3^-) groups, which constitute its external backbone. It is the highly negatively charged sulfate backbone that is responsible for most of the intermolecular attraction and repulsion dynamics of DSS in solution. Recently, Star et al. (2002) and Ikeda et al. (2007) have demonstrated wrapping of starch-iodine complex and polysaccharide Curdlan with ammonium cationic groups around SWNTs, respectively. However, there was no evidence of complete coating of SWNT and the reaction steps also involve converting the water insoluble polysaccharide to water soluble form after conjugation with iodine or ammonium ions. Also, Goodwin et al. (2009) have used phospholipid-dextran to functionalize SWNT, where the

hydrophobic phospholipid was used to stack on the SWNT sidewall and the dextran moiety to impart hydrophilicity.More recently, Cathcart et al. (2008) demonstrated complete coating of SWNT using double stranded DNA. However, complete coating only happened in a controlled atmosphere after 35 days of incubation.The goal of this research is to use readymade DSS without any chemical conjugation/modification steps, to completely wrap SWNT in a facile and easily reproducible procedure.

Experimental Part

General Procedure:

All experiments were performed under ambient conditions. All water used was purified with an EASYpure® RF system (Barnstead, Dubuque, IA; 18.2 Ω). SWNTs were purchased from Carbon Nanotechnologies Inc. (Houston, TX). All other reagents (ACS grade) were purchased from Sigma-Aldrich (Milwaukee, WI).

DSS Interaction with Pristine SWNTs:

The reaction mixture consisted of 1 mg of pristine SWNTs and an appropriate amount of DSS in 1 mL of water. The reaction mixture was subjected to sonication in a bath sonicator (VWR, West Chester, PA). The vial containing the reaction mixture was placed in a beaker and then inserted in the bath to dampen the sonic waves. This was done to reduce the disruptive effect of the strong sonic waves on the integrity of the DSS

structure. After 12-h sonication, the DSS-coated SWNTs were harvested and washed three times with water after mild centrifugation at 4,000 × g for 5 min.

DSS Interaction with Processed SWNTs:

The pristine SWNTs were oxidized, dispersed, shortened, and rendered hydrophilic as described previously (Kim et al., 2006), with the initial concentration of 1 mg-SWNT/mL. The processed SWNTs were reconstituted in water. The reaction medium for the DSS binding consisted of 1 mg of DSS in 1 mL of the processed SWNT solution. The reaction mixture was incubated at room temperature with mixing (1,000 rpm) in an Eppendorf Thermomixer (Eppendorf North America, Westbury, NY). After 1-h incubation, the DSS-associated SWNTs were used for further analyses.

Physicochemical Characterization:

The absorption spectra of samples were obtained using a DU-800 ultraviolet/visible/near-infrared (UV/Vis/NIR) spectrophotometer (Beckman Coulter Inc., Fullerton, CA).

The physical characteristics of the DSS bound SWNTs were assessed using atomic force microscopy (AFM). AFM imaging is a preferable technique for high resolution analysis of bio-abio hybrids, in particular under aqueous environments, as the differences in materials become apparent regardless of surface topography in phase images. Also, rapid and simple sample preparation steps along with availability of various analytical

software tools for subsequent characterization and representation in 2D and 3D make it an attractive alternative as compared to other wet-mode high resolution imaging techniques such as environmental scanning electron microscopy (ESEM) and cryo-transmission electron microscopy (Cryo-TEM). Moreover, electron microscopies may not be particularly effective to image polysaccharides due to their poor electron density.

The AFM imaging was implemented with a Veeco Multimode Scanning Probe Microscope with Nanoscope IIIa Controller (Veeco Instruments, Woodbury, NY). Samples were scanned in tapping mode either in air or in fluid. For example, the AFM analysis in tapping mode in air was started with loading 5 µL of each sample solution on a mica substrate (Novascan, Ames, IA). The mixture with 5 µL of water was used as a control. The loaded sample was treated with gentle N_2 blow to minimize watermarks after drying, which may cause unwanted noises in the AFM imaging. The AFM tip used was a NanoWorld Pointprobe® NCSTR AFM probe (NanoWorld AG, Neuchâtel, Switzerland), which is designed for soft tapping mode imaging and enables stable and accurate measurements with reduced tip-sample interaction, in order to obtain high-resolution AFM images with minimal sample damage. The sample scan rate was 1.0 Hz with an aspect ratio of 1:1. The force constant of the tip for scanning was 7.4 N/m. The free resonance frequency of the cantilever was automatically tuned by the Nanoscope Software (version v5.30r3sr3; Veeco Instruments). For AFM analysis in fluid mode, 5 µL of each sample solution was loaded on a freshly cleaved mica substrate and was immediately followed by addition of 5 µL of 0.125 M Magnesium acetate. Magnesium ions in solution act as a bridge between the negatively charged mica and sulfate groups on DSS. The AFM tip used was the narrow 100-µm Silicon Nitride probe (Veeco

Instruments, Woodbury, NY) with spring constant 0.32 N/m, which is ideal for imaging soft samples in tapping mode in fluids. After loading the tip on the Fluid cell (Veeco Instruments, Woodbury, NY), which comprises the glass cantilever holder and the silicon O-ring, 30 μl of distilled water was added on top of the tip. To ensure that the tip is constantly in a fluid environment, the fluid cell is connected to a syringe pump (KD Scientific Inc., Holliston, MA) via its inlet at a setting of 100 μL/min flow rate and the outlet is connected to a drain. The cantilever was manually tuned by setting a frequency of 7 kHz for the probe and drive frequency to 20 Hz. Once peaks started to appear in the sweep plot, they were maximized by increasing the drive amplitude. The sample scan rate was 0.5 Hz with an aspect ratio of 1:1.

Particle Size Analysis:

The 'Section' and 'Particle Analysis' parameters in the Nanoscope software were used for the estimation of the dimensions of particles, including DSS, SWNTs, and DSS-SWNTs. The numbers of particles used for analyses were at least 10.

Results and Discussion

Interaction of DSS with SWNT:

In order to understand the dynamics of DSS-SWNT interaction, the starting materials, SWNT and DSS, should be well characterized. SWNT's physicochemical properties, including its dimension and hydrophobic nature, are well

documented(Dresselhaus et al., 1996).However, high resolution imaging characterization of DSS for its dimension is lacking, although its chemical properties are well known. AFM analyses with tapping mode in air and liquid were performed for the structural assessments of DSS with three different molecular weights: 5 kilodalton (kD), 100 kD, and 500 kD. The 100-kD and 500-kD DSS were observed to be in coil conformation (Figure 3.1A and Figure 3.2) and were henceforth used for furtheranalysis.

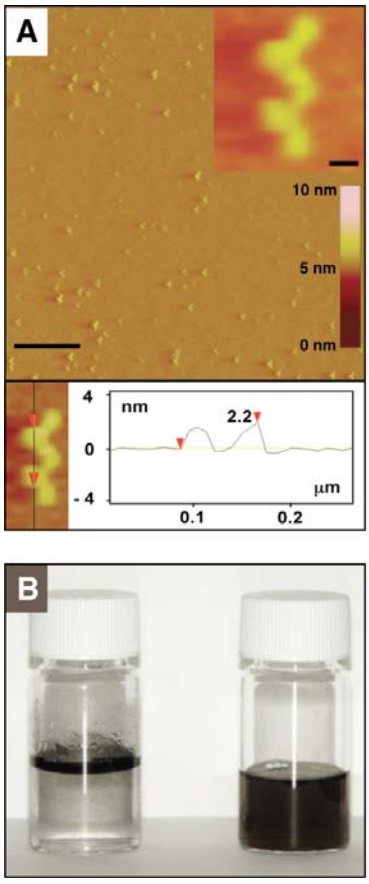

Figure 3.1. (A) Phase AFM image in tapping air mode (top) and its section analysis result (bottom) of DSS (500 kD). The inset (top) is the DSS's magnified phase image. Scale bars represent 500 nm for the main image and 50 nm for the inset. (B) Photographs of pristine SWNTs in water (left) and SWNTs after 12-h sonication with DSS in water (right).

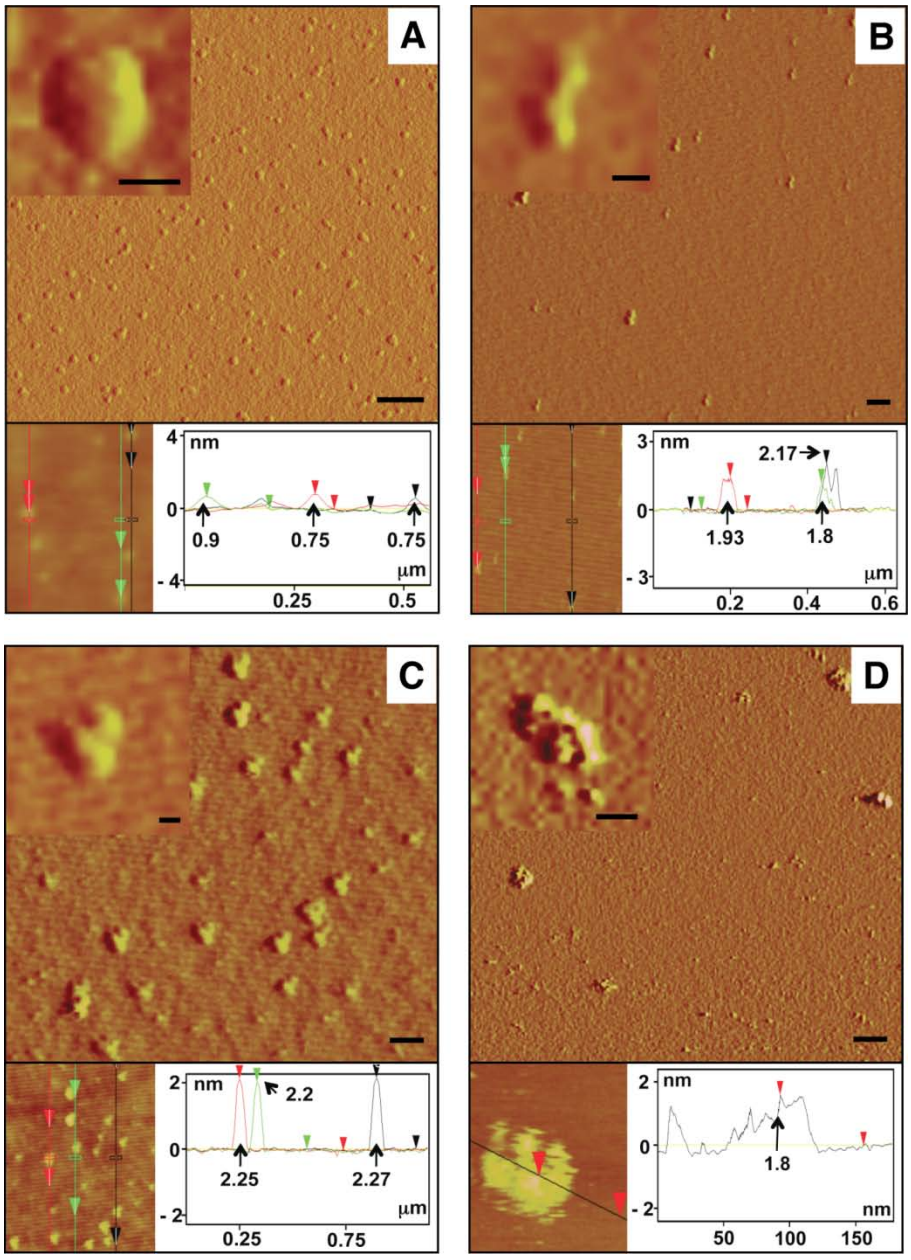

Figure 3.2. Phase AFM images in tapping air mode (top) and their section analysis results (bottom) of DSS with molecular weights of (A) 5 kD, (B) 100 kD, and (C) 500 kD. (D) Phase AFM image in tapping fluid mode (top) and its section analysis result (lower right) of DSS with molecular weight of 500 kD. The insets (upper left) are the magnified phase images. Scale bars represent 200 nm for the main images and 10 nm (A) and 50 nm (B,C,D) for the insets.

For effective DSS coating, the SWNT/DSS concentration ratio was first evaluated using various initial concentrations of DSS with the two different sizes at a fixed SWNT concentration (i.e., SWNT/DSS concentration ratios (w/w) of 1:1, 1:10, 1:50, and 1:100). The effectiveness of the binding here refers to the complete coverage of SWNTs by DSS molecules without any gaps of SWNTs on the basis of AFM analysis. DSS coating was performed by mixing appropriate amounts of pristine SWNT powder and DSS in distilled water, followed by 12-h sonication in a sonic bath. While pristine SWNTs are hydrophobic, it was observed that the SWNTs were readily dispersed in the DSS solution after 12-h sonication as evident by the dark color of the solution with minimal aggregates and precipitates (Figure 3.1B). This indicates the association of DSS with SWNTs, making them hydrophilic and affording the aqueous solutions that are stable for more than a month. Also noticeable is the fact that no buffers to balance neither pH nor temperature regulation of the reaction were used, which is otherwise typical of reactions involving DNA and protein. The reaction solution can tolerate temperatures in excess of 70^{o}C, as was recorded from the bath sonicator after the 12-h cycle. The AFM analyses with tapping mode in air revealed that, at all the concentration ratios tested, clear associations between SWNTs and DSS could be detected, along with the observation that the DSS-SWNT are dispersed and shortened in the process (Figure 3.3A-B and Figure 3.4). However, multiple AFM scans of the samples revealed that the most effective binding of DSS to SWNTs took place at the concentration ratio of 1:10 (Figure 3.3B). All the dispersed SWNT in solution were uniformly covered with DSS molecules, barely leaving any raw SWNT areas exposed. Also noticeable is the relative absence of un-reacted or free DSS in solution, suggesting that the majority of the DSS molecules have

reacted with SWNTs. On the contrary, lesser degrees of binding took place at 1:50 and 1:100, and very minimal binding was observed at 1:1 (Figure 3.3A and Figure 3.4A). The most probable explanation for this phenomenon is that, at the high concentration ratios (*i.e.*, 1:50 and 1:100), the excess DSS in solution experience steric hindrance, due to its large size and net negative charge, inhibiting any chance for them to come in contact on the SWNT surface and much of DSS remaining unbound. At 1:1, the concentration of DSS is not high enough to bind around the SWNTs, and more so make the complete coverage of SWNTs possible.

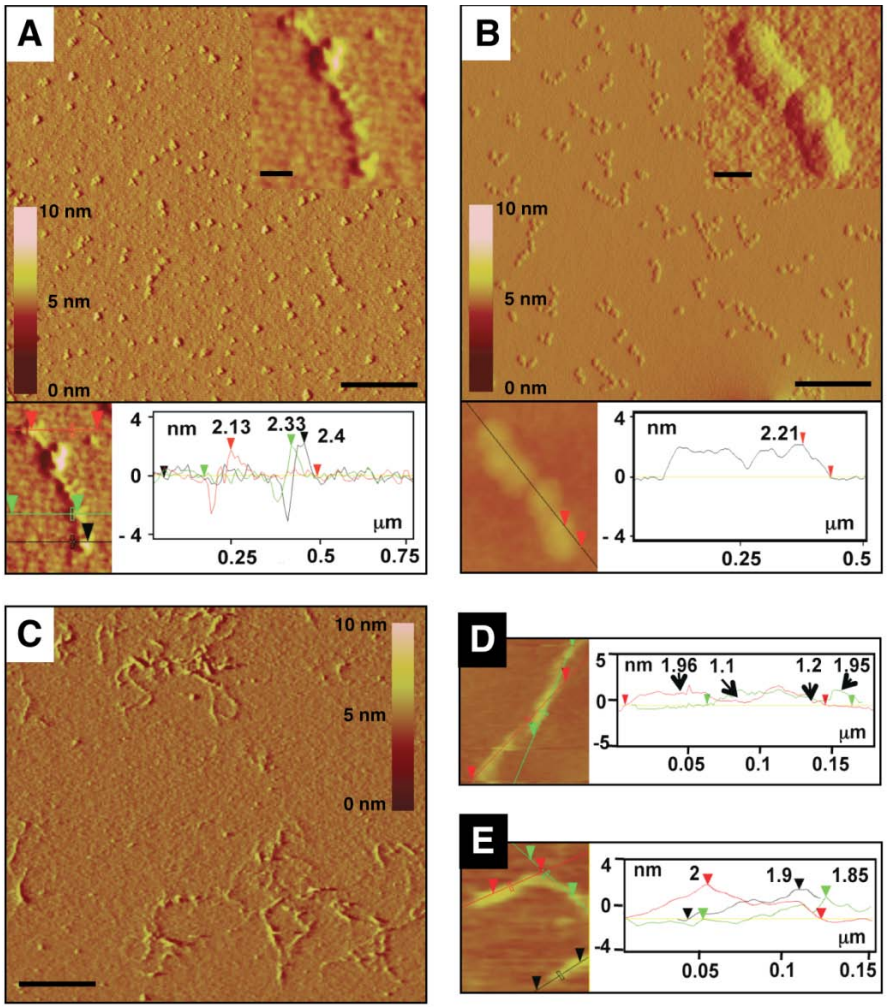

Figure 3.3. Tapping air-mode phase AFM images (top) and their section analysis results (bottom) of (A) DSS-grafted SWNTs at a SWNT/DSS concentration ratio (w/w) of 1:50 and (B) DSS-grafted SWNTs at a SWNT/DSS concentration ratio of 1:10. (C) Tapping liquid-mode AFM image of DSS-grafted SWNTs at a SWNT/DSS concentration ratio of 1:10. (D) A representative tapping liquid-mode image and section analysis result of partially coated DSS-grafted SWNTs. (E) A representative tapping liquid-mode image and section analysis result of completely coated DSS-grafted SWNTs. The molecular weight of DSS is 500 kD. The insets in A,B (top) are the magnified phase images. Scale bars represent 500 nm for the main images and 100 nm for the insets.

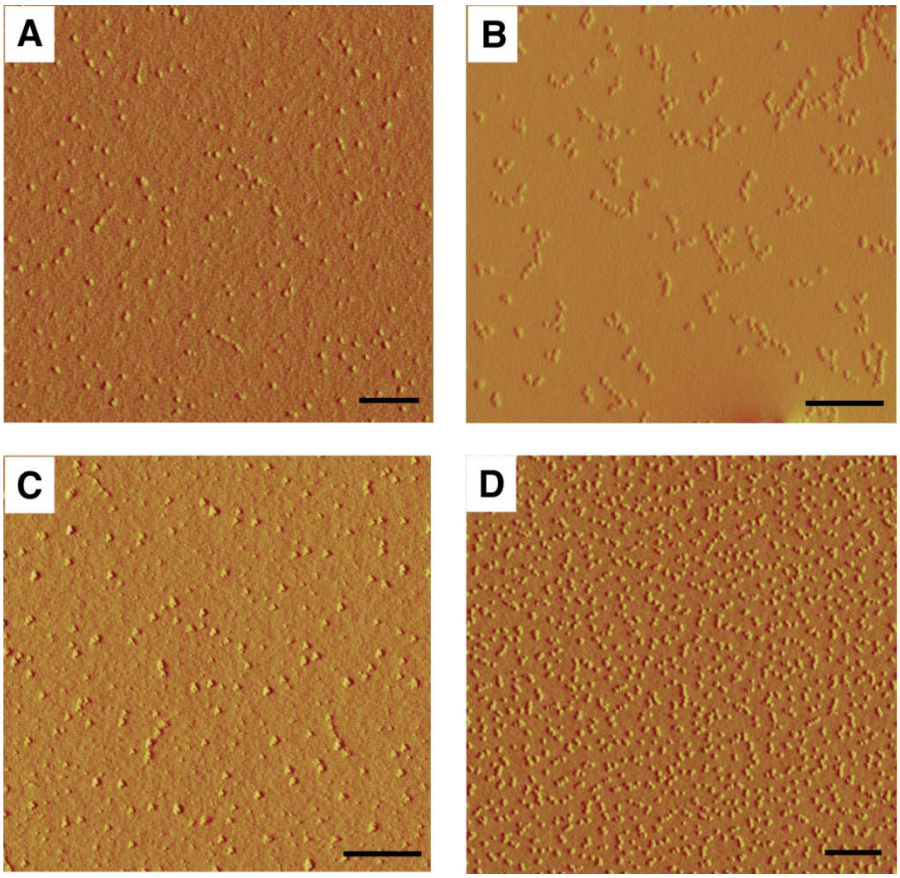

Figure 3.4. Phase AFM images in tapping air mode of DSS-grafted SWNT at SWNT/DSS concentration ratios (w/w) of (A) 1:1, (B) 1:10, (C) 1:50, and (D) 1:100. The molecular weight of DSS is 500 kD. Scale bars = 500 nm.

As it was noticed in liquid mode AFM scans of DSS only, there was an observed decrease in the lateral dimension. We contemplated the cause of swelling in dry mode to be associated with deformation of the rather flexible DSS during the drying process. Deformation is relevant in polymers that are physically adsorbed to mica substrate. Deformation, due to van der Walls and capillary forces, is especially significant in the areas where DSS is not in contact with the mica surface (Moreno-Herrero et al., 2004).We assumed that the increase in the lateral dimension of DSS in dry-mode AFM scans could also give a false impression of complete coverage of underlying SWNT.

Therefore, liquid-mode AFM scans were performed on the SWNT-DSS hybrid sample,produced at the 1:10 concentration ratios, to eliminate the associated error with drying and also to observe the hybrid in its natural state in aqueous solution. Figure 3.3C shows a representative liquid-mode scan of the SWNT-DSS hybrids. Here, magnesium ions were used to bridge the negatively charged mica surface and the negatively charged sulfate layer on the SWNT-DSS hybrids. On comparing the images in dry mode and liquid mode, it is clear that SWNT-DSS hybrids imaged in dry mode appear uniformly distributed and those imaged in liquid mode appear to be in a clustered arrangement. This could falsely give the impression of SWNT-DSS hybrids existing as aggregates in solution. Theoretical modelling and experimental validation done in the past provide us with enough evidences of the phenomena occuring in both dry and liquid environments (Kralchevsky and Nagayama, 1994; Johnson and Lenhoff, 1996). Due to the presence of the divalent cation, the film of liquid over the mica substrate has high ionic strength, which greatly weakens the interparticle repulsions between the SWNT-DSS hybrids. This leads to the particles being arranged tightly on the surface as they diffuse through the film. The capillary attractive forces betweeen the particles is inversely proportional to the distance between the particles, thereby causing further clustering and reordering of the particles on the mica surface. On the contrary, in dry mode where the ionic strength of the evaporating liquid (i.e., distilled water) is low, more uniform deposition and adsorption on mica occur. Also, since the particles are widely spaced, the capillary forces presumably cannot overcome the van der Waals forces holding the particles in position. Another apparent difference between the dry and liquid mode scans is the relative decrease in the lateral dimension of DSS on the SWNT-DSS hybrids. This gives a beaded

and conjoint appearance to the SWNT-DSS hybrids in dry mode and makes them look thicker and continuous in comparison to the hybrids imaged in liquid mode. The DSS on the hybrids in liquid mode are only distinguishable due to their relative height signatures apparent in the phase images. This can be attributed to the relative absence of deformative forces in liquid media as compared to the dry state, as discussed previously. On the basis of the section analyses, it was revealed that there were a significant number of SWNT that were not completely coated with DSS. Figure 3.3D is a representative section analysis of an image in liquid mode showing incomplete coating of SWNT by DSS, where pockets of sub 1.2 nm height signatures were found. However, a good majority of the SWNT was also noticed to be completely coated as shown by the representative analyses of a liquid-mode image (Figure 3.3E).

To investigate if the DSS particles indeed coiled around SWNTs and did not stack on them, we analyzed the DSS-SWNT conjugates by AFM section analysis and conducted experiments using shortened and relatively well-disperse SWNTs processed according to Kim et al. (2006). The rationale behind using the processed SWNTs was to render them hydrophilic. The process apparently introduces sulphonic acid (SO_3H) and carboxyl (COOH) groups on the sidewall of CNTs, imparting hydrophilic character to the CNTs (Musso et al., 2007). As proposed earlier and demonstrated (Star et al., 2002), the binding of amphiphilic polysaccharides to SWNTs is through hydrophobic interaction. By rendering the SWNT sidewall hydrophilic, it can be presumed that the hydrophilic outer surface of DSS, *i.e.*, the negatively charged sulfate groups, will interact with the negatively charged SWNT sidewall with the help of sodium ion (Na^+) bridge as DSS is a sodium salt, thus stacking on the SWNT surface but not coiling around it. Figure 3.5A

shows the AFM image and section analysis results of the processed SWNTs after treating with DSS. The AFM scans indicate the associations of DSS with SWNT (Figure 3.5A, top); however, the section analysis (Figure 3.5A, bottom) revealed the width of the processed SWNT-DSS complex to be between 3.4 – 4 nm, which corresponds to the combined diameter of SWNT (1.5 – 1.9 nm) (Cathcart et al., 2008) and DSS (2.2 – 2.4 nm for 500 kD). This suggests that the DSS is stacking on the processed SWNT through the hydrophilic interaction between the hydrophilic outer surfaces of DSS and the processed SWNT sidewall. If the DSS were coiled around SWNTs, the effective diameter of the DSS-SWNT complex should show little change. The estimated diameter of the DSS- unprocessed SWNT complex was ~2.2 nm (Figure 3.3B, bottom), indicating that DSS is coiling around the pristine SWNTs. This hints the significance of SWNT surface hydrophobicity for the coiling of DSS.

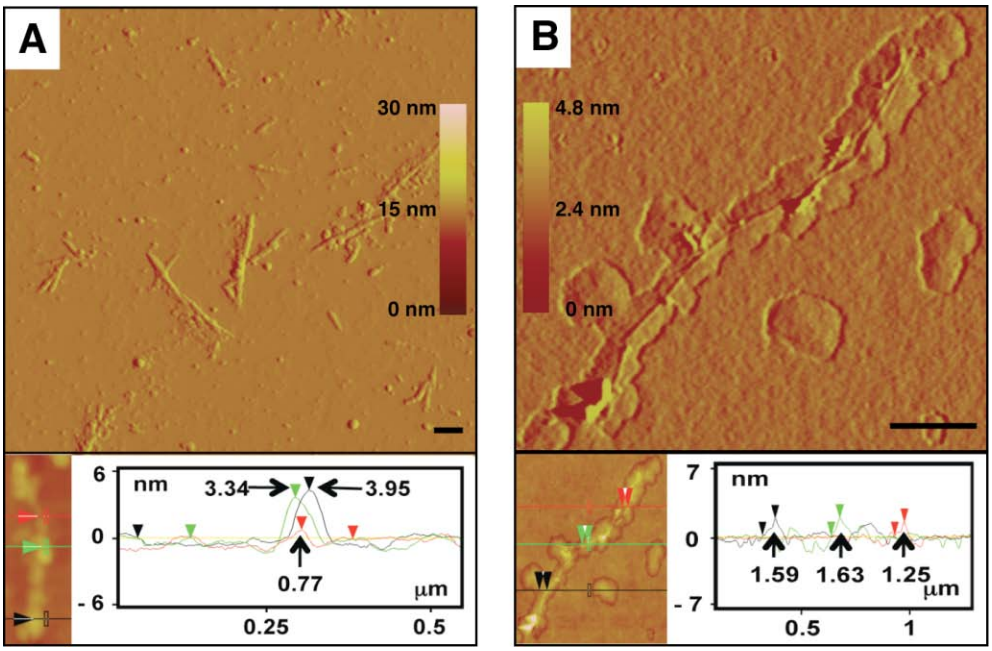

Figure 3.5. Phase AFM images in tapping air mode (top) and their section analysis results (bottom) of (A) the processed SWNTs (i.e., oxidized, dispersed, and shortened as described previously)[21] after 1-h incubation with DSS at a SWNT/DSS concentration ratio of 1:10 and (B) SWNTs on partially degraded DSS after 4 days at ambient conditions to hydrolyze and degrade DSS molecules from DSS-grafted SWNTs. The molecular weight of DSS is 500 kD. Scale bars represent 500 nm (C) and 200 nm (D).

However, the evidence that SWNTs are indeed present within the linear DSS formations is still indirect and therefore needs direct corroboration. It is known that DSS particles hydrolyze when exposed to moisture and air and is subject to natural degradation by microorganisms and other enzymes. An AFM grid deposited with DSS-SWNT mixture was allowed to stand for 4 days at ambient conditions to hydrolyze and degrade DSS molecules. The AFM scan after 4-d incubation showed the exposure of SWNT, which became apparent as the result of the hydrolysis and degradation of the overlying layer of DSS (Figure 3.5B, top). Remnants of the underlying DSS were still visible in the image. The placing of SWNT over the partially digested DSS after allowing

for the hydrolysis of DSS to occur serves as direct evidence that the DSS molecules do indeed coil around SWNTs as proposed and do not stack on them. AFM section analysis confirmed the diameter of the embedded SWNT to be 1 – 1.6 nm (Figure 3.5B, bottom), thus also proving that SWNTs are not only well dispersed and shortened but also unbundled to the very basic dimension.

Sequential AFM image analyses conveyed the mechanism of the DSS-SWNT interaction. On analyzing the AFM images, we hypothesized that the angle and side of approach of DSS towards SWNTs determine the outcome of the binding and eventual wrapping action. We assumed that the DSS molecules exist as pre-determined coils in solution and very much resemble a semi rigid spring in shape, as our AFM images of DSS imply (e.g.,Figure 3.1A, inset). Notice that the DSS molecule approaches the SWNT from the right side and forms an acute angle with respect to the proximal part of SWNT axis, the upper end, in Figure 3.6A. This may attribute to the hydrophilic-hydrophobic repulsion between the hydrophilic tips of SWNT, which were cut and oxidized during sonication process, and the hydrophobic interacting face of DSS. Also notice that, in Figure 3.6B, the DSS molecule approaches the SWNT from the left side forming an acute angle with respect to the proximal part of SWNT axis, in this case the lower end. It can be deduced that the acuity of angle along with the sidedness of approach is mainly because the DSS molecule is aligning itself with respect to the SWNT, to avoid any possible hydrophilic-hydrophobic repulsion.

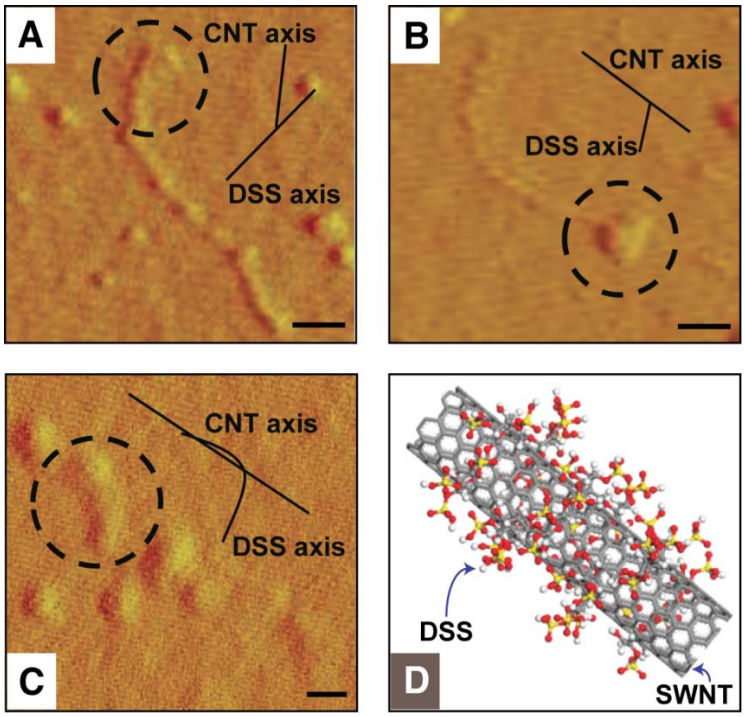

Figure 3.6. Phase AFM images in tapping air mode that indicate (A,B) DSS winding around SWNT by approaching from the tip side and (C) DSS winding around SWNT by approaching from the sidewall. Scale bars represent 100 nm. (D) Schematic of DSS coiling around SWNT by hydrophobic interaction. The schematic was generated using ChemBio3D (CambridgeSoft, Cambridge, MA) and Materials Studio (Accelrys, San Diego, CA) software packages. Grey, white, red, and yellow colors stand for carbon, hydrogen, oxygen, and sulfur, respectively.

Using this approach (i.e., acuity and correct sidedness), DSS may ensure that the maximal part of its hydrophobic surface comes in contact with the maximal part of the hydrophobic surface area of SWNT sidewall. Thus, a DSS molecule prefers to be oriented in such a way that its long axis forms an acute angle with the SWNT axis, which is closest to, for the initial binding to occur and for the helical winding to be initiated. Figure 3.6C shows a DSS molecule occupying a central position on the SWNT sidewall since either ends have already been occupied by other DSS molecules. Notice that the

angulation and flexibility of the molecule as the helical wrapping is taking place. This hints that the positioning of the DSS molecule on the SWNT sidewall is random and no gliding of DSS molecules, to accommodate other DSS molecules, occur. The gaps, if exist, on SWNTs are filled by additional DSS wrapping. Once complete wrapping of the individual DSS molecule has concluded, it is permanently stationed. These observations through the AFM scans strongly relate to the Random Sequence Adsorption (RSA) model, which is defined as random placement of particles one by one on a one dimensional surface. The placement of particles is considered successful when the particles are immobile after adsorption and no overlapping of particles occur (Feder, 1980).Therefore, it can be deduced from our findings that the DSS molecules are helically wrapped around the SWNT sidewall as illustrated in Figure 3.6D. This can be attributed to the hydrophobic-hydrophobic interaction between the α-D-1,6-glucose residues in the inner lining of DSS and the hydrophobic character of the pristine SWNT sidewall. The hydrophilic outer surface of DSS renders a strong hydrophilic character with subsequent dispersity and solubilization.

Finally, the optical spectral analysis of the DSS-SWNT showed that the DSS coating did not affect the CNT's inherent NIR responsiveness, but significantly improved (> 2 fold) their NIR responses (Figure 3.7). This demonstrates high promise of DSS-CNT conjugates as NIR contrast agents.Recently, CNTs have shown unique capabilities as NIR-responsive photothermal (PT) and photoacoustic (PA) contrast agents for medical diagnosis and therapy of tumors and infections (Kim et al., 2009; Kim et al., 2007; Zharov et al., 2007; Zerda et al., 2008). However, CNTs' clinical relevance is still in question due to concerns over their potential toxicity. Our unique combination of DSS

and CNTs should greatly improve upon the biocompatibility of CNTs, thereby obviating the CNTs' limitations for such biomedical applications.

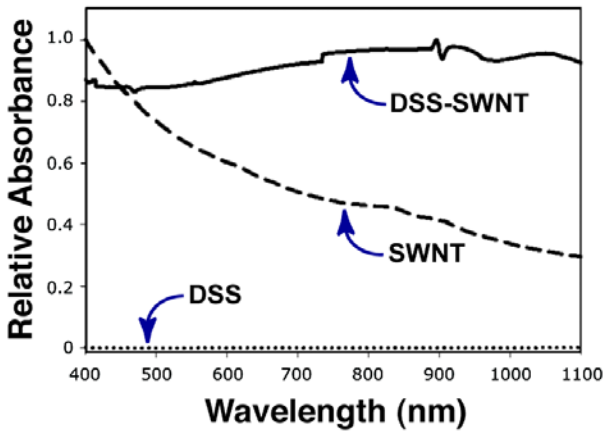

Figure 3.7. UV/vis/NIR plasmon-derived optical resonances of DSS, SWNT, and DSS grafted SWNT in water. Each datum point was normalized on the maximal absorption in the wavelength range of 400 to 1100 nm of the plasmon responses of each product.

Conclusion:

We have demonstrated a simple and efficient strategy toprocess SWNTs using de xtran sulfate to mitigate SWNTs toxicity and enhance their solubility and compatability in biologically relevant aqueous solutions, and have outline a possible mechanism of the binding interaction between the two moieties. This process offers a highly effective and inexpensive way of completely wrapping SWNTs using a biomaterial considering the cost effectiveness and robustness of DSS in relation to other biopolymers such as DNA and proteins. This hybrid nanoparticle holds tremendous promise for biomedical

applications, such as PT and PA diagnosis and therapy, due to the synergistic uniqueproperties of SWNT and dextran sulfate, including enhanced NIR contrast, aqueous solubility, and biocompatibility, and reduced toxicity. Also, the presence of hydroxyl and negatively charged sulfate groups on the hydrophilic surface of DSS molecules along with the reducing end of sugar moiety should facilitate the functionalization of the hybrid SWNTs with bio-ligands such as antibodies and DNA. This opens up a wide array of possibilities for using DSS-grafted SWNTs to target different tissue types for molecular diagnostics and nanotherapeutics.

CHAPTER 4

Interfacing natural polymers with carbon nanotubes: Purification and antibody functionalization to the DSS-SWNT hybrid and attaching immunological disguising proteins, Protein A and Factor H to SWNT

Introduction:

The major obstacle for successful application of DSS-SWNT as *in vivo* and *in vitro* agents is the lack of a well-defined separation technique to exclude the unreacted DSS from the hybrid DSS-SWNT. Carbohydrates in general present a major challenge to researchers on account of their heterogeneity in branching, linkages, molecular weight and lack of any active functional groups (Linhardt and Pervin, 1996). We were faced with the task of separating DSS that had wrapped on SWNT from the DSS that had not. Basically, it means the DSS-SWNT and free DSS had intact sulfate groups on the exterior and were similar in charge characteristics. This made us safely rule out charge based separation techniques. Due to the size variation of unbound DSS and DSS-SWNT hybrids, we attempted ultracentrifugation, dialysis and membrane filter based centrifugation techniques. Despite some encouraging results, the resolution of these separation techniques was not appreciable as DSS-SWNT hybrids needed to be completely devoid of free DSS for downstream antibody functionalization. In the presence of free DSS in solution the antibodies would get conjugated to them and yield false positive results when specific attachment to target cells are attempted. High purity and high yield of DSS-SWNT is the eventual goal of the post characterization step described in the previous section. We attempt to address the purity issue in this section.

Another key difference between DSS wrapped on SWNT and free DSS is the availability of the hydrophobic internal lining in the free DSS, which is occupied on the SWNT in DSS-SWNT hybrids. Our next task was to identify a process/agent that will selectively bind to the hydrophobic inner lining of DSS (free DSS) and not to the hydrophilic sulfated external backbone of DSS (DSS-SWNT). If the process/agent can selectively bind to the hydrophobic region of DSS then only free DSS can be affinity separated from the DSS-SWNT hybrids, which are not expected to bind.

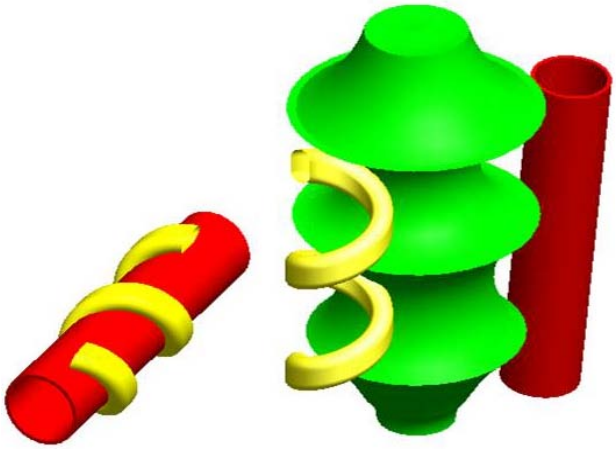

Figure 4.1. Schematic of free DSS binding to Con A and not the DSS-SWNT hybrid.

There is one such protein that specifically interacts with the hydrophobic lining and minimally with the hydrophilic lining of polysaccharides (Poretz and Goldstein, 1970). Lectins are a family of proteins known to have high affinity to bind polysaccharides (Goldstein et al., 1980). They bind to a wide variety of oligosaccharides such as mannose, glucose, galactose and fucose that are present in various

polysaccharides, thus imparting specificity to the lectin towards a sugar. Concanavalin A (Con A) is one such lectin that has affinity towards mannose and glucose residues in sugars (Sumner, 1919). DSS is a complex of glucose moieties, therefore Con A is the obvious choice to differentiate between the free DSS and complexed DSS. Lectin affinity chromatography is a separation process which uses Con A as one of the ligands to separate macromolecules namely glycosylated proteins in a sample (Freeze, 2001). It has been used in the past preferentially over other separation techniques due to the high specificity of the biological interaction and its simplicity, often culminating in a one-step purification system (Freeze, 2001). We propose a novel lectin affinity purification system that employs Multiwalled Carbon Nanotubes (MWNT) as support that is embedded on polypropylene microcentrifuge tubes, serving as the cartridge. Some of the characteristics required for good affinity supports are high surface area and volume (high aspect ratio) and good mechanical and chemical stability (Porath, 1974). MWNT has over the years proven to be an ideal material for applications where such traits were highly desired. However, besides the above mentioned traits an ideal support also should have minimal nonspecific binding properties and it is pretty obvious MWNT and carbon nanotubes in general have high nonspecific binding affinity towards a variety of materials (Chen et al., 2003). Nevertheless, we will be demonstrating how nonspecific binding is not a concern, because the lectin Con A was shown to bind to the MWNT surface nonspecifically and almost complete coverage of the MWNT was observed. Even if there were areas of uncovered MWNT, the incoming ligand, DSS and DSS-SWNT, will be unlikely to nonspecifically attach to MWNT as shown in the previous section. Polypropylene microcentrifuge disposable tubes as cartridges provide the flexible, low cost, convenient

and speedy module that is ideally suited for our needs as it eliminates potential cleaning and cross-contamination issues. The most intriguing and important finding was the ability to embed the MWNT in the polypropylene inner wall using a rather commonly known chelator, Ethylenediaminetetraacetic acid (EDTA). With EDTA enabling the attachment of MWNT to Polypropylene and other similar polymers, we have found a new functionalization scheme that would afford a simple and effective means to enable CNT to functionalize polymers such as Polyethylene glycol (PEG). More of CNT-PEG interaction will be explored in the next chapter.

The oriented conjugation of antibody to DSS-SWNT hybrids will be discussed using 3,3´-N-[ε-Maleimidocaproic acid] hydrazide (EMCH), a crosslinker.

Staphylococcus aureus, a pathogenic gram positive bacterium secretes a surface protein, Protein A, which prevents attachment of anti-bacterial antibodies in right orientation thereby preventing recognition and eventual engulfment by macrophages (Goding, 1978; Surolia et al., 1982). Protein A has binding sites for the F_c region of Immunoglobulin G (IgG), so do macrophages, and by not binding to the F_{ab} region of IgG it disrupts the ability of macrophages to recognize the pathogen thus enabling its escape from the host defenses (Surolia et al., 1982; Patel and Moghimi, 1998). Factor H is a plasma protein that regulates the complement system by preventing the complement factors from acting against host cells and directs it towards foreign substances and pathogens (Pangburn, 2000; Wu et al., 2009). Factor H shares the same binding region as the complement receptor 1 (CR1) on the macrophage, for the opsonin C3b. By competitively binding to C3b, Factor H essentially prevents macrophage recognition of the host. Peculiarly some pathogens have developed mechanisms to recruit Factor H to

prevent phagocytes from binding to the bacteria (Pandiripally et al., 2003). We assumed that by taking a clue from nature and using Protein A and Factor H we could address the issue of CNT recognition by macrophages, even though opsonins are deliberately made to attach to the CNT. This allows a convenient method to attach antibodies to the PrA-FH-SWNT hybrid for downstream applications where specific attachment to a target cell is desired.

Materials and Methods:

General Procedure:

All experiments were performed under ambient conditions. All water used was purified with an EASYpure® RF system (Barnstead, Dubuque, IA; 18.2 Ω). SWNTs were purchased from Carbon Nanotechnologies Inc. (Houston, TX) and MWNTs from NanoLab Inc. (Waltham, MA). Dibromobimane (DBrB), Sodium periodate, Dextran sulfate, Protein A and Factor H were purchased from Sigma-Aldrich (Milwaukee, WI), 3,3´-N-[ε-Maleimidocaproic acid] hydrazide (EMCH), 1-Ethyl-3-[3-dimethylaminopropyl] carbodiimide Hydrochloride (EDC), *N*-hydroxysulfosuccinimide (Sulfo-NHS), FITC-IgG and 1-pyrenebutanoic acid, succinimidyl ester (PSE) from Pierce Biotechnology (Rockford, IL),

Depositing MWNT on Polypropylene tubes:

To 190µl of dsMWNT in PP tube, 10µl of EDTA is added and shaken for 2 hrs at RT at 1400rpm. For experiments with Magnetic particles, comparable concentration to MWNT is used.

Reaction of Con A with dsSWNT:

For solution phase, 5 µl of 0.25mg/ml of Con A is added to 95µl of 0.1mg/ml dsSWNT and shaken at RT for 2 hrs at 800rpm. For solid phase 5µl of 0.25mg/ml Con A is added to Tris buffer pH 7.4 and shaken in the PP tube for 2 hrs at 1400rpm.

Reaction of DSS-SWNT, DSS mixture with ConA-attached to tube:

100µl of 0.5mg/ml of DSS-SWNT solution is mixed with Tris buffer with 10 mM Mn^{2+} and Ca^{2+} ions and shaken at 1400rpm for 2 hrs at RT. The process is repeated 3 times till all the free DSS is bound to the Con A matrix.

Antibody attachment to DS-SWNT:

For confirming the presence of thiol groups on IgG, 0.25mg/ml of FITC-IgG was dissolved in PBS solution pH 7.4 to ensure all the thiol groups are completely nucleophilic. DBrB was dissolved in dimethylformamide (DMF) and appropriate dilutions of 0.25X, 0.5X, 1X and 20X to that of IgG were prepared. IgG and DBrB were

allowed to react at room temperature (RT) for 2 hours and protected from light all through the reaction and analysis stages.

DS-SWNT was prepared as shown previously (Kotagiri and Kim, 2010). 1mg of Sodium periodate was dissolved in 100mM Sodium acetate buffer pH 5.5 and reacted with 1mg/ml of DS-SWNT in a 1:1 ratio for 2 hours at RT. The sample is then dialyzed overnight using a 30kDa Cellulose acetate membrane to get rid of excess periodate. Separately, 2.5mg of EMCH is dissolved in 1ml of PBS solution pH 7.2 and mixed with 0.25mg/ml of FITC-IgG at RT for 2 hours in the dark. The two solutions, sodium periodate treated DS-SWNT and EMCH treated FITC-IgG are then mixed at RT for 2 hours in the dark.

Attachment of Protein A and Factor H to SWNT:

PSE was attached to SWNT as described previously (Kim et al., 2006). Protein A was covalently linked to of Factor H using Sulfo-NHS and EDC according to the manufacturer's instructions. Briefly, to 0.25mg/ml of Protein in 100mM MES buffer pH 6, 1mg of EDC was added and 2mg of Sulfo-NHS was added and allowed to stand for 15 min at room temperature. Excess EDC and Sulfo-NHS was removed by filtering the solution in a 30kDa microcentrifuge filter at 5000rpm for 5 min and washed three times. Subsequently, 0.25mg/ml Factor H in 100mM PBS pH 7.4 is added to Protein A and allowed to react at RT for 2 hrs. Then 100ul of PrA-FH conjugate in 100mM PBS is then mixed with 100ul of SWNT-PSE and allowed to react at RT for 2 hrs. The pH is checked

to make sure it is above 7.2 to allow spontaneous attachment of amine groups on protein to the NHS group on PSE.

UV-vis spectra and AFM evaluation:

The absorption spectra of samples were obtained using a DU-800 ultraviolet/visible/near-infrared (UV/Vis/NIR) spectrophotometer (Beckman Coulter Inc., Fullerton, CA).

The AFM imaging was implemented with a Veeco Multimode Scanning Probe Microscope with Nanoscope IIIa Controller (Veeco Instruments, Woodbury, NY). Samples were scanned in tapping air mode. AFM analysis in tapping mode in air was started with loading 5 μL of each sample solution on a mica substrate (Novascan, Ames, IA). The AFM tip used was a NanoWorld Pointprobe NCSTR AFM probe (NanoWorld AG, Neuchatel, Switzerland), which is designed for soft tapping mode imaging. The sample scan rate was 1.0 Hz with an aspect ratio of 1:1. The force constant of the tip for scanning was 7.4 Nm^{-1}. The free resonance frequency of the cantilever was automatically tuned by the Nanoscope Software (version v5.30r3sr3; Veeco Instruments).

Fluorescence Microscopy:

Fluorescence microscopy for the samples was performed using a light microscope Axioskop 2 Plus (Carl Zeiss, Inc.,Germany) equipped with a filter set DAPI (Carl Zeiss) consisting of a band-pass filter covering 350–370 nm for an exciter and an absorbance filter covering wavelength of 400 nm, as well as a QICAM 12 bit

Monochrome Fast 1394 Cooled charge coupled device CCD camera (QImaging, Burnaby, Canada) with a resolution of $1.4X10^6$ pixels. The 100X oil immersion objectives were used to visualize and acquire the fluorescence images.

Results and Discussion:

In order to create a reliable purification module, the support-cartridge system needs to be robust, in that the MWNT should be firmly embedded in the polypropylene and should not show any signs of detachment over a period of time. We have come up with a novel way to do so using EDTA, which helps in the attachment of dsMWNT to polypropylene only when shaken at 1400rpm. The reason the speed of 1400rpm was chosen was because at this speed the solution in the tube would revolve and be in contact with the top half of the tube, where we would ideally be performing the affinity based separation. This enables the dsMWNT in the solution to embed in the polypropylene during the course of 2hrs. In order to determine the type of CNT (SWNT vs. MWNT) and surface activity of CNT (carboxyl group functionalized vs. non functionalized) most suited as support, the respective CNT were prepared and series of control experiments performed. Pristine SWNT and MWNT along with dsSWNT and dsMWNT were added individually to polypropylene tubes containing EDTA and shaken at 1400rpm at room temperature.

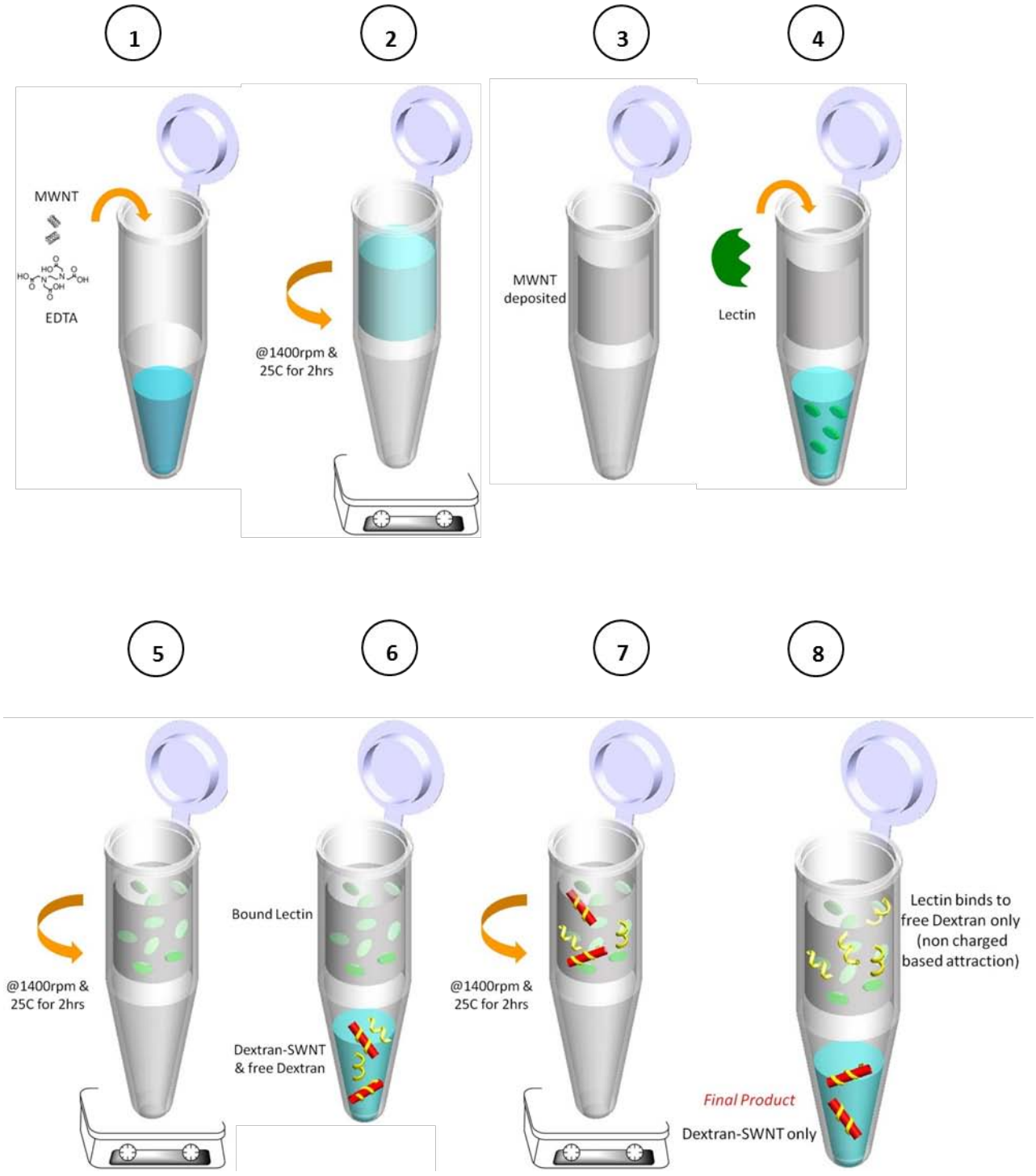

Figure 4.2. Schematic overview of the MWNT polypropylene tube based lectin affinity chromatography system.

It was observed visually that only dsSWNT and dsMWNT embedded on the upper half of the tube and not the pristine CNTs, as apparent by the dark coloration of the tube (Fig.4.3).

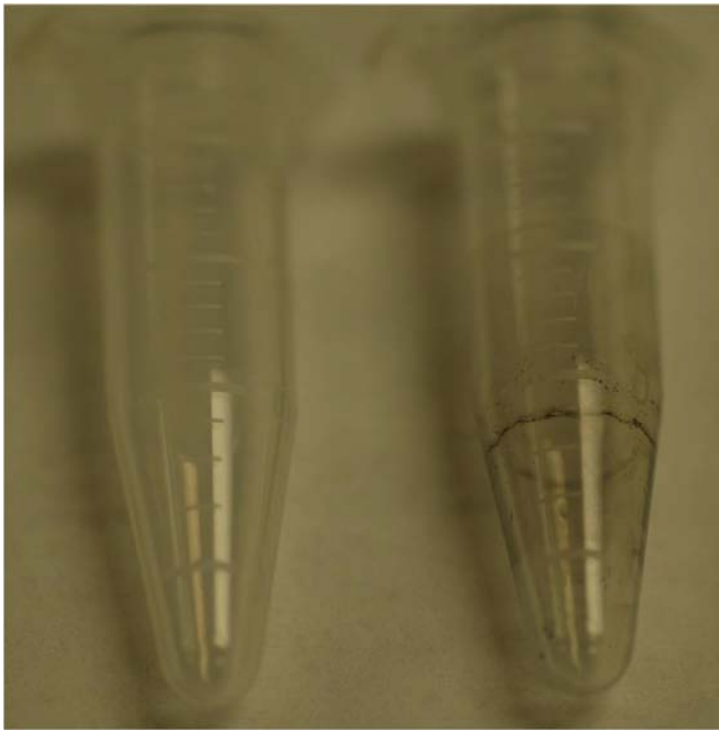

Figure 4.3. The right tube shows dsMWNT deposited in the walls of the tube after shaking at 1400rpm for 2hrs. Left tube is the control.

It was also apparent that dsMWNT achieved a much higher degree of attachment in comparison to dsSWNT, which was confirmed by UV-Vis spectrophotometry (Fig. 4.4). We believe dsSWNT, which has been chemically oxidized and suspended in water, without any dispersant is more likely to reaggregate in an ionic solution such as EDTA, in comparison to similarly treated dsMWNT. MWNT has been the preferred CNT of

choice to manufacture bacterial and viral flow filters which seek a homogeneous filter matrix that lacks preferential flow paths (Srivastava et al., 2004; Moon and Kim, 2010). Also, MWNT being relatively inexpensive and easier to handle and process, will be an attractive choice for scaling up and batch production.

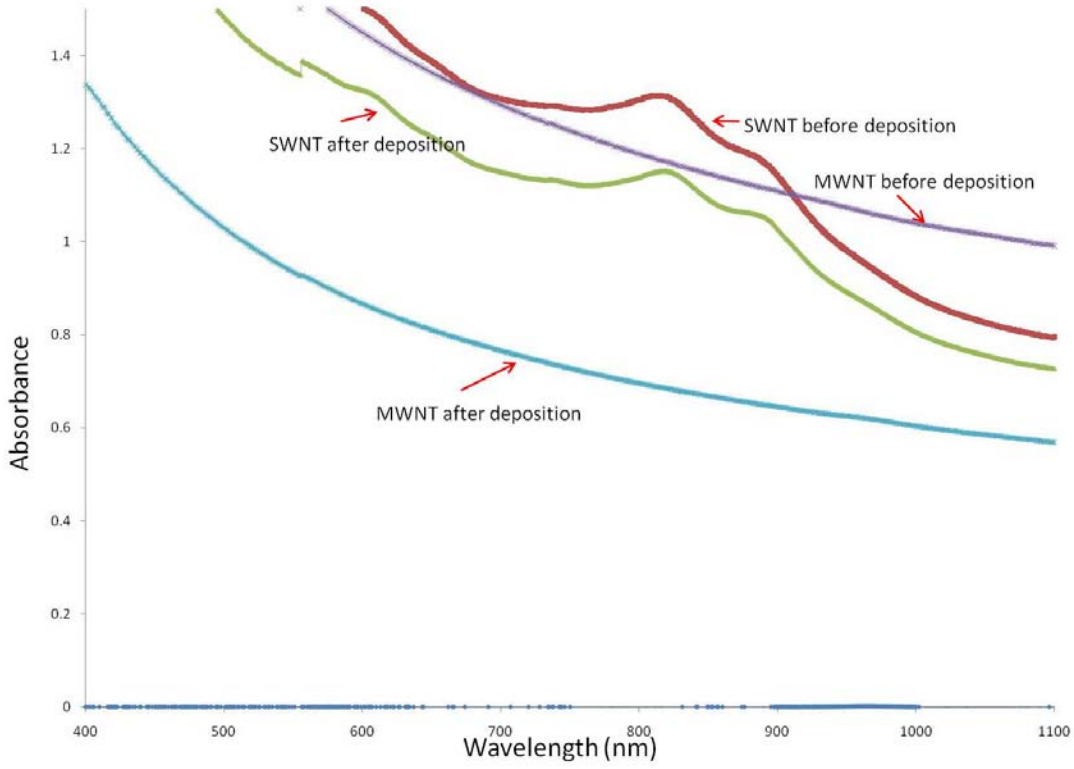

Figure 4.4. UV-Vis spectra showing the marked decrease in MWNT concentration in comparison to SWNT after deposition.

To reemphasize, attachment of dsMWNT to the polypropylene only occurred when EDTA was added to the solution and when the solution was shaken. Therefore, in

order for a support-cartridge module to be established all three variables need to be satisfied, namely oxidized and dispersed MWNT, presence of EDTA and shaking at 1400rpm. In order to decipher the mechanism behind the attachment of dsMWNT to the tube it is imperative that each variable be closely examined by performing a series of experiments that could give a clue as to whether the interaction is charge based or simple adsorption. Magnetic Nanoparticles (MP), amine and carboxyl group modified, were chosen to support the data obtained using dsMWNT and also understand the overall mechanism. Solution of MP-Amine with EDTA, MP-Amine alone was shaken at 1400rpm and another solution of MP-Amine with EDTA was just allowed to stand. Likewise, a solution of MP-Carboxyl with EDTA, MP-Carboxyl alone was shaken and MP-Carboxyl with EDTA allowed to stand. Only MP-Carboxyl with EDTA that was shaken showed dark coloration of the tube walls. This clearly suggests that only negatively charged particles bind to polypropylene and that too in the presence of EDTA while shaken. Therefore, the interaction has to be charge based i.e. positive charge is generated on the plastic surface otherwise if it were simple adsorption MP-Amine should have also attached.

In order to appreciate the fact that concurrent action of EDTA and shaking is essential for binding to occur, EDTA solution was shaken in the tube for 2hrs and washed to remove any excess EDTA. MP-Amine and MP-Carboxyl were added in separate tubes without EDTA and shaken. No binding of either MP-Amine or MP-Carboxyl to the tube was observed. Apparently neither negative nor positive charge was generated on the tube lining by the initial action of EDTA alone. Hence, it can be concluded that binding takes place concomitantly in the presence of EDTA and shaking, in real time. If the attachment

of dsMWNT is indeed occurring in real time as EDTA is twirling on the polypropylene surface, how is it possibly happening on a most inert material that is supposedly used to manufacture laboratory grade 'test tubes'? 95% of microcentrifuge tube has polypropylene as its major component and it's logical to assume the changes are on polypropylene and not the other 5% of the tube constituents. We assume the negatively charged EDTA and the twirling of the solution across the tube wall could be converting the inert methyl groups of Polypropylene to a positively charged moiety that attract the negatively charged MWNT and MP.

It is not uncommon for proteins to adsorb on hydrophobic surfaces and there are many reports where this is the preferred type of attachment as it circumvents the need for further modifying the surface which could lead to changes in the properties of the surface (Chen et al., 2003). Especially in the case of CNTs, nonspecific binding in the form of π-π stacking and hydrophobic attraction is preferred, as any modification to enable covalent attachment will not only disrupt the electronic properties of CNT but also could lead to destruction of the carbon framework due to the harsh chemical processing steps. AFM was used to demonstrate binding of Con A to dsSWNT in solution phase. dsSWNT was used instead of dsMWNT because of the similar solution properties and relative ease of characterization using AFM. Fig. 4.5 clearly shows 'beading' of dsSWNT surface which can be attributed to the adsorption of ConA on the sidewalls. Section analysis revealed the height of the ConA-dsSWNT hybrid to be the combined height of dsSWNT and ConA, thus confirming the attachment process to be simple adsorption.

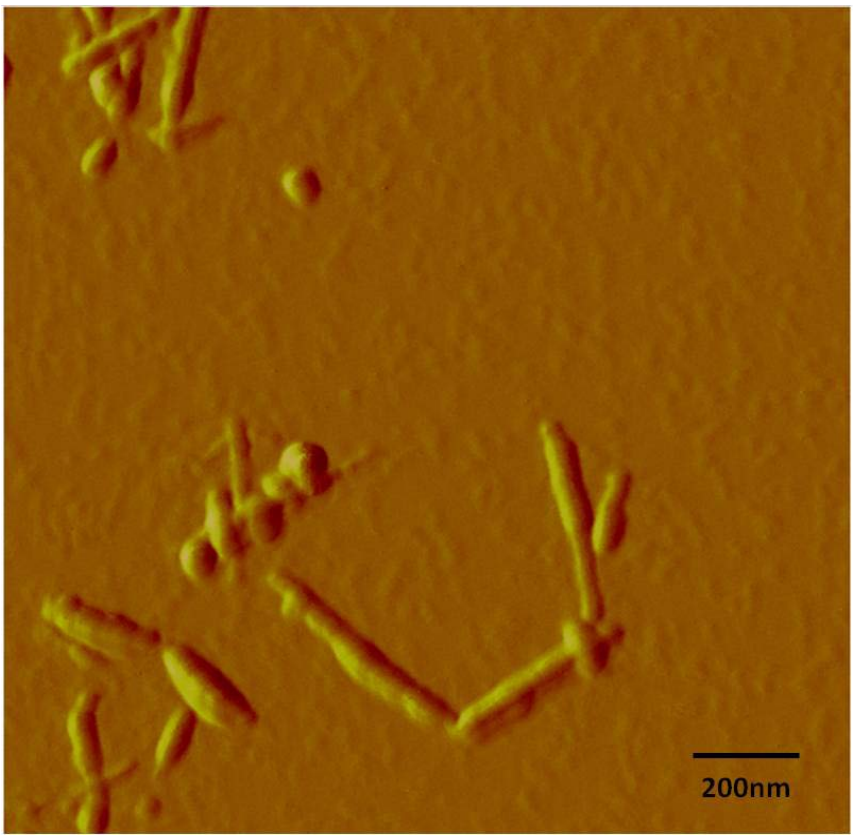

Figure 4.5. Phase AFM image of Con A adsorbing on dsSWNT.

The same process was repeated, except this time Con A was to adsorb on dsMWNT that were already embedded on the Polypropylene tubes. Con A in Tris buffer pH 7.2 containing CaCl2 and MnSO4 was shaken at 1400rpm for 2hrs to allow adsorption on the dsMWNT support. Con A is a metalloprotein and a tetramer having four identical subunits each with a molecular weight of 25,500. Each monomer has binding sites for the metal cations, calcium and manganese, without which carbohydrate binding ability is abolished (Kalb and Levitzky, 1968). Therefore it is imperative to have calcium and manganese ions in solution to enable free DSS attachment to Con A. The carbohydrate binding site of the Con A monomer has two subsites deep within, one is a

large hydrophobic site and the other a small hydrophilic site (Linhardt and Pervin, 1996). Due to the size disparity of the two subsites it is speculated that if there are carbohydrates with hydrophobic domains and also hydrophilic domains, Con A will preferentially bind to the hydrophobic domain (Linhardt and Pervin, 1996). Since there is only one carbohydrate binding site per monomer it is unlikely that the hydrophilic domains will be occupied unless there are no more hydrophobic domains or excess Con A is present in solution. Before we proceeded with adding the DSS-SWNT solution to the tube we wanted to revisit and confirm the interaction and binding of Con A to DSS. Con A in Tris buffer was mixed with 100kDa DSS and results analyzed using AFM. The lateral dimension of Con A only was measured to be in the range of 45nm-50nm and that of free DSS was in the range of 75nm-85nm. Large aggregates were observed in the Con A-DSS sample which measured 150nm-200nm in diameter (Fig. 4.6c). These aggregates could contain more than one Con A-DSS conjugates. Nevertheless, it can be concluded with confidence that Con A does precipitate DSS in the conditions provided.

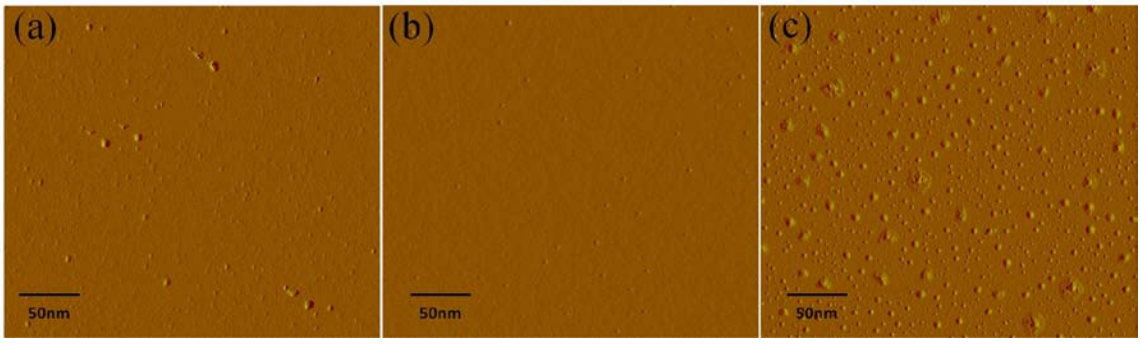

Figure 4.6. Phase AFM image of a) Con A, b) DSS, c) Con A-DSS precipitate

The next control was to add the DSS only solution in the tube with Con A already adsorbed to the surface to test if the retentate obtained after shaking for 2 hrs contains any DSS. Ideally, as envisaged all the DSS must have formed associations with the Con A and minimal to none of the DSS must be found in the retantate. AFM scans taken of the DSS solution showed a count of ~250 DSS particles in a field of 2 microns. After shaking for 2 hrs at 1400rpm, not more than 2-3 DSS articles were found in the same field size (data not shown). At this stage we believe the tube is ready to separate out any free polysaccharides that have affinity towards Con A and provide a sugar free retentate. We finally tested DSS-SWNT with free DSS by adding the solution to the tube and shaking for 2 hrs. AFM images show the linear DSS-SWNT particles without any free DSS in the field. (Fig. 4.7)

Figure 4.7. Phase AFM image of DSS-SWNT that separated from the free DSS. Notice the minimal free DSS in the field.

This clearly demonstrates that the interaction of Con A is with the hydrophobic inner lining of free DSS, as that of DSS wrapped on SWNT has its hydrophobic domains occupied. It next logical step would be to elute the free DSS from Con A and make the tube reusable. It is conceivable to do so using glucose to displace the DSS from the biding site. However, given the low cost of the materials it would be safer, faster and cleaner to make this a disposable separation system. In principle this concept and process can be applied to separate antibodies in solution by attaching Protein A to the dsMWNT on the walls and can also be extended to all affinity based purification systems.

Attachment of Antibody to DSS-SWNT:

The area of antibody attachment to DSS is still unexplored partly due to the reason DSS acts as an IgG repellant, hence its use as an anti-opsonin agent (Ma et al., 2008). In order to achieve oriented conjugation of antibody we needed to introduce aldehyde groups on the DSS. The reducing end of any polysaccharide can be converted to an aldehyde using Sodium periodate. The carbonyl groups generated at the ends of each DSS moiety is unlikely to interfere with the sulfate backbone of DSS and effect the solubility of DSS-SWNT in solution. Subsequently 3,3´-N-[ε-Maleimidocaproic acid] hydrazide (EMCH), a crosslinker with a maleimide groups that reacts with thiol groups on IgG and a hydrazide group which reacts with the carbonyl group on the DS-SWNT complex (Fig. 4.8a).

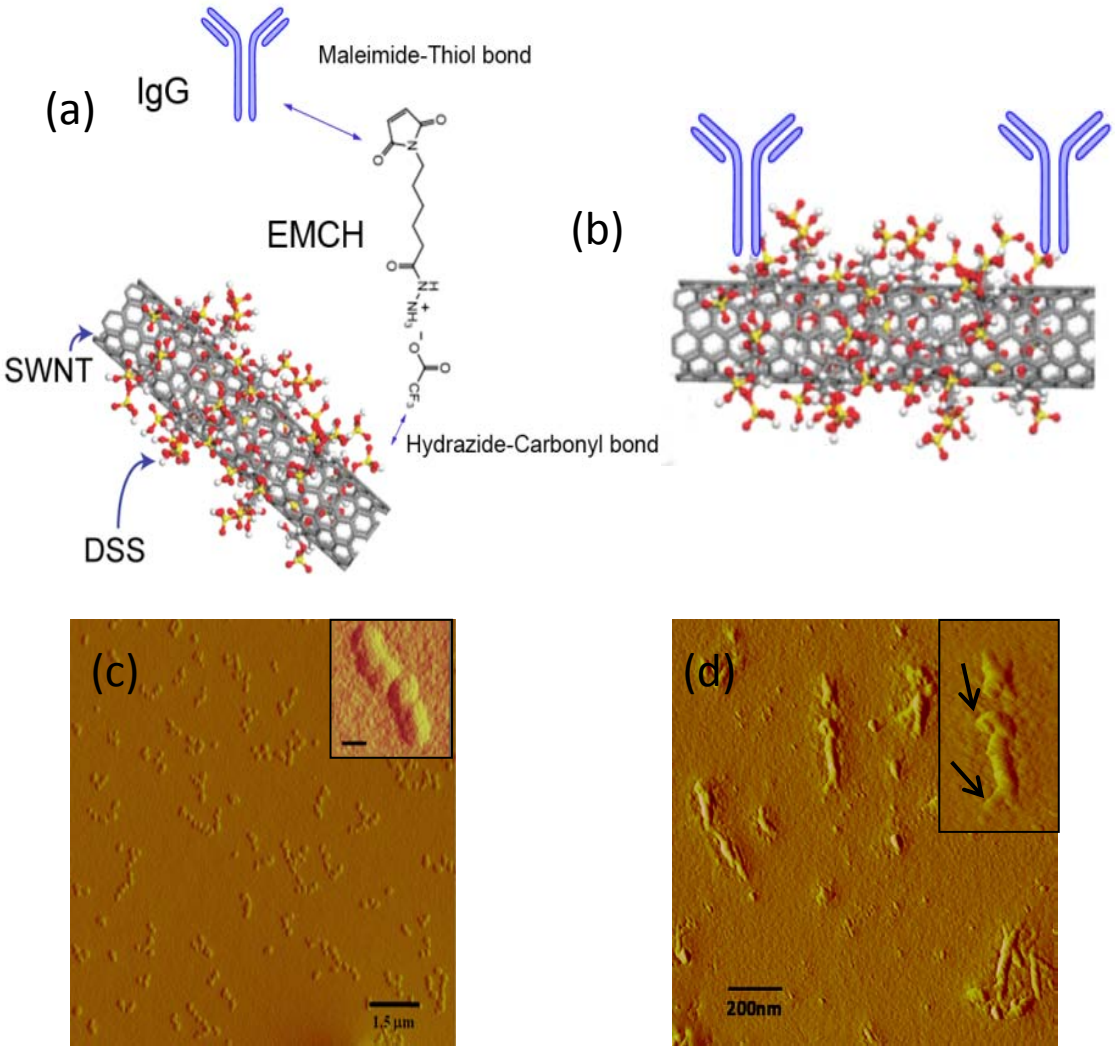

Figure 4.8. (a) Schematic of DS-SWNT conjugation with IgG using EMCH. (b) Schematic of IgG covalently conjugated to DS-SWNT. (c) Phase AFM image of DS-SWNT. Inset showing a magnified image. (d) Phase AFM image of IgG conjugated to DS-SWNT. Inset showing a magnified image. Arrows pointing the IgG aligned away from the SWNT axis.

We were skeptical about the intact whole IgG possessing free thiol groups for reaction with the maleimide group on EMCH; it is common practice to cleave the antibody to obtain free thiol groups. Dibromobimane is a thiol specific reagent and is

commonly used as a fluorescent crosslinking agent as it possesses two identical bromomethyl groups that react spontaneously with thiol groups at pH 7.4. The efficacy of Dibromobimane as a thiol detector comes from the fact that it becomes fluorescent only when both the bromomethyl groups are occupied by thiol groups (Kim and Raines, 1995).

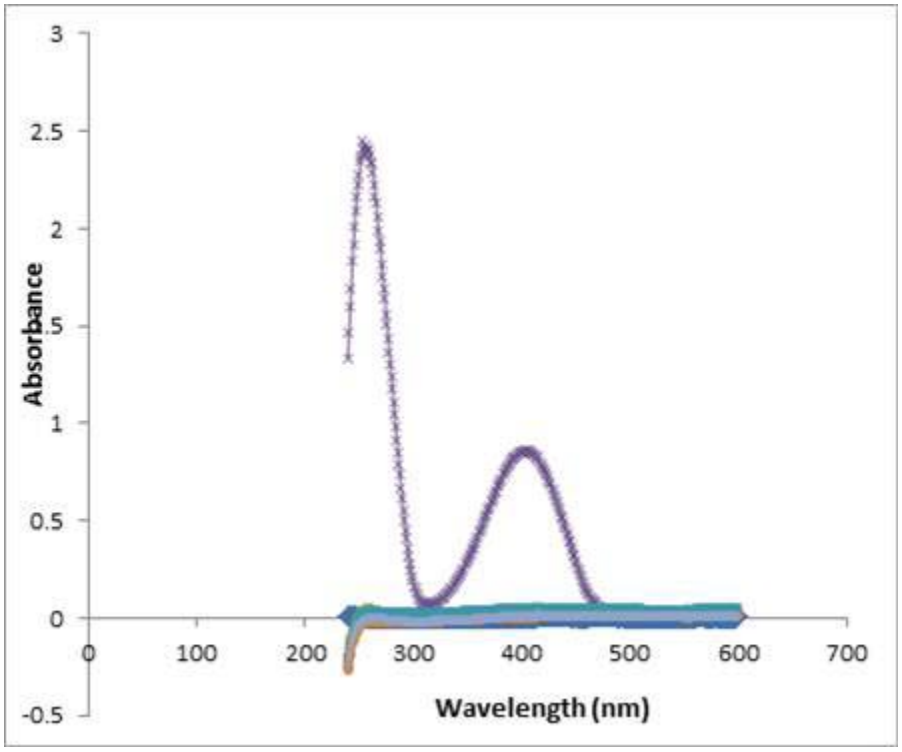

Figure 4.9. UV-vis plot of IgG reacted with Dibromobimane. The only peak is that of 0.5X DBrB:IgG.

To test this we used 0.25, 0.5, 1 and 20 times the concentration of Dibromobimane to that of antibody. Since every Dibromobimane molecule will require two antibodies we assumed the test samples 0.25, 1 and 20X will not yield any fluorescence and only 0.5X will. UV-vis spectra show a distinct fluorescent peak at

400nm only for the 0.5X sample and not the other three (Fig. 4.9). This proves the existence of free thiol groups on IgG which can be used for conjugation with maleimide group on EMCH. This makes sure that oriented attachment of antibody on the DSS-SWNT surface is taking place by utilizing the thiol groups for covalent linkage (Fig. 4.8b). AFM images showed the presence of IgG aligned away from the DSS-SWNT axis (Fig. 4.8d). This is in stark contrast to the DSS-SWNT images that showed no such protrusions away from its axis (Fig. 4.8c). Also noticeable in the image is the relatively similar size of IgG and DSS given the MW is 150kDa and 100kDa respectively. The z-axis dimension, height, of Immunoglobulins is approximately 3.8nm as confirmed by our AFM scans and section analysis. Section analysis of the IgG attached to DSS-SWNT showed the height to be 3.6nm. Fluorescent microscope imaging was used to image the IgG-FITC-DSS-dsSWNT hybrids as shown in Fig 4.10.

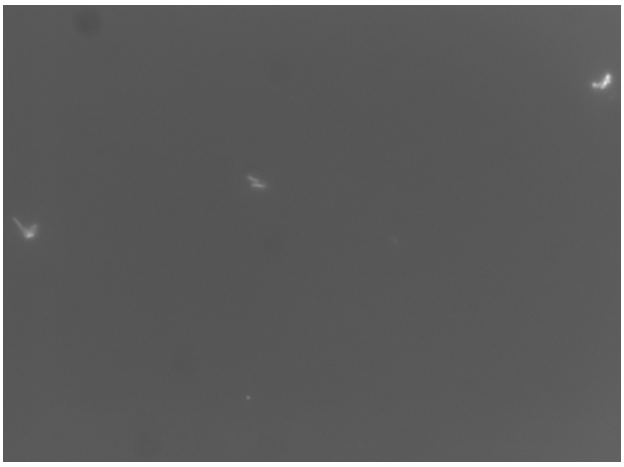

Figure 4.10. Fluorescent image of FITC tagged IgG on DSS-SWNT. Magification is 100X under an FITC filter.

These results however only demonstrate attachment of IgG to DSS-SWNT and in no way prove the orientational attachment favoring the antigen binding site to be exposed, except for the theory and mechanism used. The IgG-DSS-SWNT will be put in practice in the later chapter on *Staphylococcus aureus* to precisely test and confirm this.

Attachment of Protein A and Factor H to SWNT:

Protein attachment to CNTs in general or for that matter attachment of any ligand to CNTs has so far been attempted and practiced on a one ligand-one CNT paradigm. Even though CNTs offer excellent framework for attachment of ligands due to its varied and versatile surface characteristics that can be modified as per the needs of the coupling chemistry, in the aspect of precise, location specific and controllable functionalization it is still a difficult material to work with. As demonstrated in an earlier publication 1-pyrenebutanoic acid, succinimidyl ester (PSE) was used to conjugate proteins where the ester group would be covalently linked to free amino groups on proteins (Chen et al., 2001). This is a very effective way to attach proteins on CNTs as the π-stacking of pyrene on CNT does not disturb its structural integrity and the ester groups provides for covalent attachment which ensures there is no disassociation of protein in varied solutions with different ionic strengths.

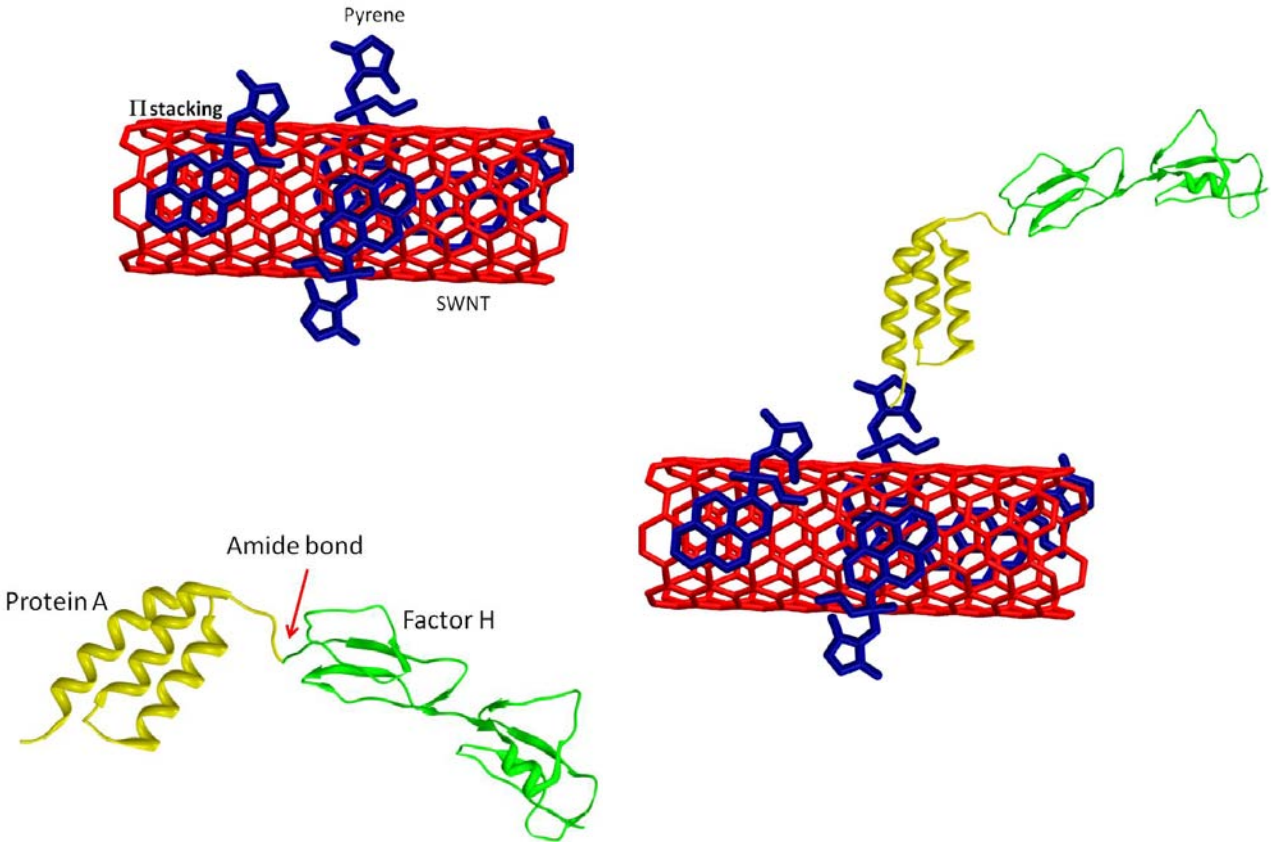

Figure 4.11. Schematic of step wise reaction, first of PSE with dsSWNT, then Protein A with Factor H. Finally attaching the dual protein complex to the SWNT-PSE.

However, it is still a homogeneous coating on CNT with a single group type which means only a single protein can be attached on any single CNT unless molar ratios of a mixture of proteins is finely tuned to allow attachment of all types of proteins to the same CNT. This was not very encouraging as it could yield myriad combinations of protein-CNT complexes. We had to attach both Protein A and Factor H on the same SWNT, two protein-one CNT, to derive the benefit of both the proteins in protecting the SWNT from opsonins. This unique challenge was addressed by attaching the protein

separately first and then coupling one of the protein to the ester group on SWNT covalently.

Protein A, not having any free thiol groups due to lack of amino acid cysteine allows for only carbodiimide based coupling to Factor H. The classic EDC-sulfo NHS reaction mechanism was used to couple the carboxyl groups on Protein A to the amino groups on Factor H. AFM image analysis of Protein A revealed the lateral dimension to be 55nm (Fig 4.12a). Lateral dimension of Factor H was 82nm (Fig. 4.12b). The difference in the lateral dimension is due to the larger size of Factor H that has a MW of 155kDa than Protein A with a MW of 60kDa. After conjugation AFM image reveals the size variance between the two proteins. The cleft in the image shows the point of attachment of the two proteins (Fig. 4.12c). The lateral dimension of the PrA-FH conjugate is 135nm, which coincides with the combined lateral dimensions of the individual proteins.

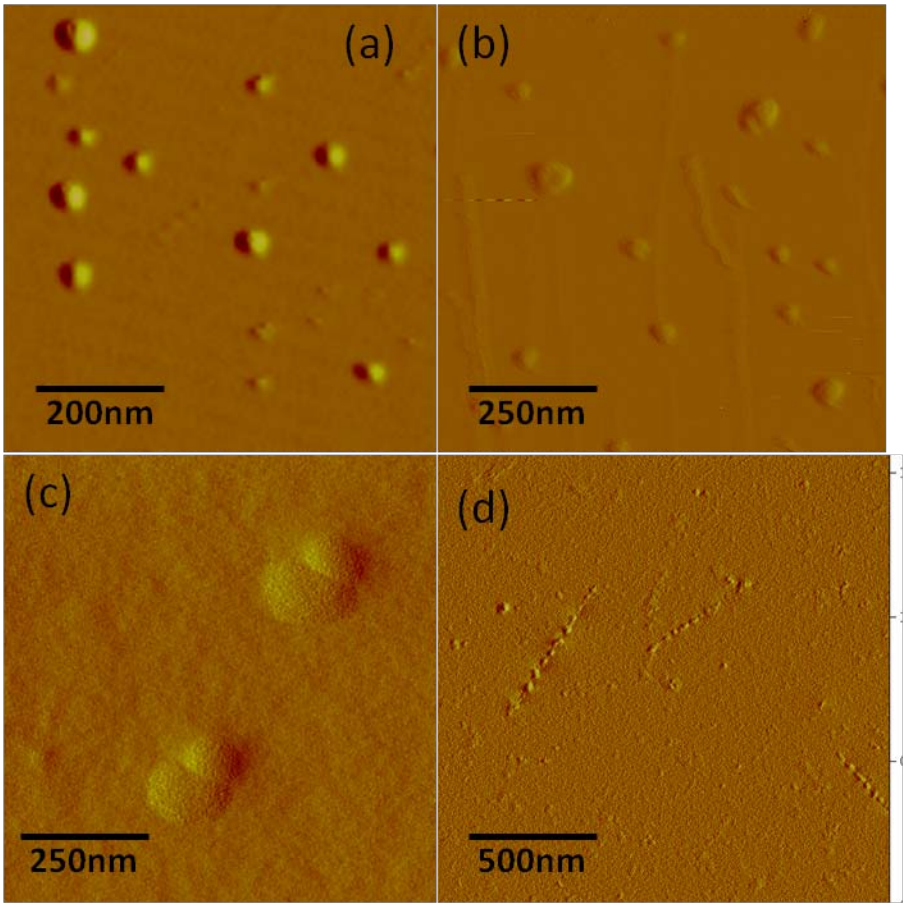

Figure 4.12. Phase AFM images of a) Protein A. b) Factor H. c) PrA-FH conjugate. d) PrA-FH on PSE-SWNT.

PSE on dsSWNT (dispersed and shortened SWNT) was confirmed using fluorescence microscopy imaging as shown previously. Attachment of PrA-FH to PSE-dsWNT spontaneously under the conditions used and was confirmed by AFM imaging. The beaded appearance of the SWNT is due to the proteins and the continuity of the 'beads' all along the length of the SWNT show uniform and complete coverage (Fig. 4.12d). On section analysis the height of the protein conjugate alone was 2.6nm and that of PrA-FH-dsSSWNT adduct was 3.5nm. Taking into consideration the average diameter of well dispersed SWNT being 0.8-1.2nm, this agrees well with the findings above. The

attachment of IgG-FITC to PrA is spontaneous and will be tested in a later chapter where it will be targeted against *Staphylococcus aureus*.

CHAPTER 5

Interfacing synthetic compounds with carbon nanotubes: Fluorescent byproduct of Ampicillin heralds new possibilities for carbon nanotubes

Introduction:

Carbon nanotubes (CNT) holds tremendous promise in a multitude of applications like sensors, circuits, scaffolds for bone growth, *in vivo* tumor targeting agents and many others. Even though we are focused on developing efficient tumor targeting vectors out of CNTs, the basic groundwork of fine tuning the raw material to its finished product is mostly the same for most applications. The burden lies on the researcher to develop methods and processes that will convert the raw material to its final form, based on the technology available. More often than not a laboratory comes up with its own unique protocol to custom prepare the materials that serves their need best. However, there are some universal procedures employed that are popular with almost all laboratories dealing with that particular material. One that easily comes to mind is the usage of ionic and nonionic surfactants such as Sodium dodecyl sulfate (SDS) and Triton X to disperse stubborn hydrophobic materials. SDS and its aromatic substitute SDBS are the most common surfactants used to disperse CNT in aqueous solutions (Niyogi et al., 2002). Solubility in aqueous solution is a prerequisite for any intended biomedical application. In such a scenario, it is but natural to employ surfactants to do the job of dispersing and rendering the hydrophobic CNTs water soluble. In hindsight, ever since CNTs were being processed either by chemical oxidation or simple sonication, addition of surfactants was the final step to make them hydrophilic; and the most readily available surfactants were

used just because it was convenient and nothing better existed. We have identified a new chemical that we hope will challenge the old ways of dealing with hydrophobic materials. The impetus for finding a new way to disperse CNTs mainly came from our experience in dealing with the surfactants. To list some of the issues: reaggregation of oxidized and shortened CNTs (dsCNT) in buffer solutions, difficulty in preparing grids for AFM and transmission electron microscope (TEM) as it leads to conspicuous water marks and bubble formation in the scanning field and eventually in the images, quenching of CNT fluorescence in the presence of salts and above all surfactants do not instill any new traits or advantages by coating CNTs, besides just dispersing them; more like dead weight. Hence the need for better ways to disperse CNTs that will not only address the issues listed above but also contribute actively towards the potential application of the CNT by coating it and imparting new traits. We identified a new chemical that is a derivative and modification of the beta lactam antibiotic, Ampicillin.

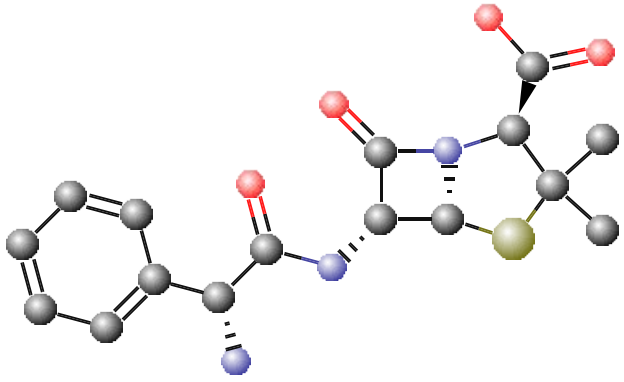

Figure 5.1. Structure of Ampicillin.

This modified Ampicillin (mAmp) has demonstrated high fluorescence and provides a high degree of dispersability to SWNTs on simple sonication. Besides being fluorescent and acting as a surfactant it is also a 'smart' chemical in that it responds to changes in pH values apparent through its changing fluorescent profile. Here, it is shown how it can be used as a superior alternative to the traditional surfactants and more so aid CNT in easy visualization using fluorescent microscopy and AFM imaging, by not forming any water marks or dense deposits on the mica surface. As we propose to use mAmp for biomedical applications mainly in mammalian tissue culture and bacterial studies, we also confirmed that the antibiotic nature of its parent compound, Ampicillin, was no longer present which augurs well for use *in vivo*. Most importantly, as will be discussed in the later chapters, it provides stealth character to SWNTs by making them transparent to opsonins in the blood and thereby preventing macrophages from engulfing them. After testing out most of the properties of this chemical, the biggest challenge was to decipher its structure which would help explain many of its traits. Noteworthy is the fact that only Ampicillin, in its class of beta lactam antibiotics, exhibits this type to behavior.

Also, due to the fact that we have identified a new method to functionalize synthetic polymers such as polyethylene and polypropylene to CNTs, the novel strategy will be employed to coat PEG on SWNT. Subsequently antibody attachment will also be discussed. Here PEG-SWNT is being developed to act as a standard to compare the novel stealth SWNT with.

Experimental Part:

Synthesis of mAmp:

15mg of Ampicillin (Sigma-Aldrich) was dissolved in 1 ml of distilled water and placed in a PCR machine. The temperature of the lid and thermocycler were set to 100^{o}C and 99^{o}C respectively. The solution was heated for 2 hrs after which they were kept at RT.

Estimation of Quantum Yield:

The first standard, Quinine sulfate (Sigma-Aldrich) was prepared by adding 2mg to 2ml of 0.1M Sulfuric acid. This served as the stock. Serial dilutions were made to determine the highest concentration to give an OD value of 0.1. 150X dilution yielded this value and thereafter five serial dilutions were prepared. Similarly, for 9, 10 Diphenylanthracene (9,10-DPA), the second standard, the same procedure was followed by dissolving the chemical in Dimethyformamide (DMF) and preparing serial dilutions which yield a maximum OD of 0.1. The first task was to crosscheck the two standards with each other to confirm if the method yielded the quantum yield (QY) of the standards as mentioned in literature. The QY of Quinine sulfate is 0.45 and that of 9,10-DPA is 0.9. The UV-vis absorbance spectrum of the first solvent was recorded and absorbance at the excitation wavelength noted. Next, the fluorescence spectrum of the same solution in the fluorometer was recorded. The integrated fluorescence intensity (that is, the area of the fluorescence spectrum) from the fully corrected fluorescence spectrum was then calculated. The steps above were repeated for all the five dilutions that were prepared. A

graph is then plotted with integrated fluorescence intensity vs absorbance and slope calculated. Using the equation:

$$\phi x = \phi st\left(\frac{Gradx}{Gradst}\right)\left(\frac{\eta x}{\eta st}\right)$$

the QY for each sample is calculated and averaged out. Finally, serial dilutions of mAmp are prepared and using Quinine sulfate as standard, the QY was calculated.

Agarose Gel to determine charge:

The mAmp and Ampicillin solutions were loaded onto a 5% Agarose gel. 1X TAE buffer was used as the electrophoresis buffer and was run for 30 mins at 110V. The gel was then imaged using a UV Gel-Doc (Biorad).

Dispersion of SWNT using mAmp:

The reaction mixture consisted of 1 mg of pristine SWNTs and in 1 mL of water to which 50µl of mAmp was added. Likewise another reaction mixture consisting of 1mg/ml of oxidized and shortened SWNT (dsSWNT) was also prepared. The reaction mixture was subjected to sonication in a bath sonicator (VWR, West Chester, PA) for 20 mins.

^{1}H NMR on mAmp:

^{1}H NMR spectrum was measured on a Bruker micro-bay Avance 300MHz NMR spectrometer at ambient temperature using a Broadband observed probe with Z-Gradient. The sample was dissolved in D_2O and placed in a 5mm tube.

FTIR:

mAmp and Ampicillin solutions were dried in a Rotovap (Labconco) before FTIR analysis. The spectrum was recorded on a Bruker Tensor 27 Spectrometer at the resolution of 2 cm^{-1} in wavenumber.

HPLC-MS:

HPLC experiments were carried out on a Bruker Esquire (Bellerica MA) ion trap LC/ESI MS. The HPLC column was a Supelco (St. Louis MO) reverse Phase C8 packing with a dimension of 4.6 x 150 mm and 5 micron particles. The flow rate was set to 0.8 ml/min. For the gradient the solvents were: A- 0.1% FA in water and B- 0.1% FA in Acetynitrile. After a 5 min hold at 5%B the gradient was programed linearly to 100% B at 50 min. Mass spectra were collected in the default full scan mode using standard conditions for the instrument in the electrospray ionization mode.

Ammonia Assay:

Ammonia assay was done according to the manufacturer's instructions. Briefly, to three tubes with 1 ml of water marked as Blank, Test and Standard is added 100µl of water, 100µl of sample and 50µl of ammonia standard, respectively. After incubation at RT for 5 mins the absorbance is recorded at 340nm. 10ml of L-Glutamate Dehydrogenase is added to each cuvette and then absorbance recorded again after 5 mins. The equations used to derive the final value are:

$$\Delta A_{340} = A_{Initial} - A_{Final} \quad (1)$$

$$\Delta(\Delta A_{340})\text{Test or Standard} = \Delta A_{340}\text{ (Test or Standard)} - \Delta A_{340}\text{ (Blank)} \quad (2)$$

$$\text{Mg of Ammonia/ml} = (A)\,(TV)\,(F) \times 0.00273/(SV) \quad (3)$$

Where $A = \Delta(\Delta A_{340})$Test or Standard

TV = Total Assay Volume in ml

SV = Sample Volume in ml

F = Dilution Factor from Sample Preparation

Antibiotic sensitivity test:

Two LB Agar plates, one with 50µg/ml Ampicillin and other with 50µg/ml mAmp were streaked with *Escherichia coli K12* strain obtained from the American Type Culture Collection (Rockville, MD). The plates were then incubated at 37^{o}C for 14 hrs.

Attachment of PEG to SWNT and IgG to PEG-SWNT:

dsSWNT were prepared as shown previously (Kim et al., 2006). 1mg of PEG-COOH (Laysan Bio., Arab, AL) was dissolved in 0.5ml of SWNT in water containing to which 50 µl of 100mM EDTA is added. The solution is shaken at 1000rpm for 4 hours at RT. The sample is dialysed overnight using a 100nm PTFE membrane to remove excess PEG and EDTA. 10µl of 0.25mg/ml FITC-IgG is added 200µl of the PEG-SWNT solution and incubated for 2 hours at RT in the dark.

Physicochemical characterization:

The absorption spectra of samples were obtained using a DU-800 ultraviolet/visible/near-infrared (UV/Vis/NIR) spectrophotometer (Beckman Coulter Inc., Fullerton, CA). The fluorescent spectrum was obtained from the Nanodrop 3300 fluorospectrometer (Thermo Scientific Inc., Fremont , CA)

The physical characteristics of the DSS bound SWNTs were assessed using AFM. The AFM imaging was implemented with a Veeco Multimode Scanning Probe Microscope with Nanoscope IIIa Controller (Veeco Instruments, Woodbury, NY). Samples were scanned in tapping mode either in air or in fluid. For AFM analysis in tapping mode in air**,** 5 µL of each sample solution was loaded on a mica substrate (Novascan, Ames, IA). The mixture with 5 µL of water was used as a control. The sample after loaded on the mica was treated with gentle N_2 blow to minimize watermarks after drying, which may cause unwanted noises in the AFM imaging. The AFM tip used was a NanoWorld Pointprobe® NCSTR AFM probe (NanoWorld AG, Neuchâtel,

Switzerland), which is designed for soft tapping mode imaging and enables stable and accurate measurements with reduced tip-sample interaction, in order to obtain high-resolution AFM images with minimal sample damage. The sample scan rate was 1.0 Hz with an aspect ratio of 1:1. The force constant of the tip for scanning was 7.4 N/m. The free resonance frequency of the cantilever was automatically tuned by the Nanoscope Software (version v5.30r3sr3; Veeco Instruments).

Phase-contrast and transmittance microscopy was performed using a light microscope (Axioskop 2 Plus, Carl Zeiss, Inc., Germany) equipped with a 12-bit Color MicroImager II Cooled digital camera (QImaging, Burnaby,Canada) with a resolution of 1.3 million pixels. The 100 or 63 oil immersion objectives (Carl Zeiss) were used tovisualize and acquire the images. The light microscopysystem was additionally equipped with a FITC filter set(Carl Zeiss) consisting of a band-pass filter covering 450–490 nm for an exciter and an absorbance filter-coveringwavelength of 515 nm.

Fluorescence Microscopy:

Fluorescence microscopy for the samples was performed using a light microscope Axioskop 2 Plus (Carl Zeiss, Inc.,Germany) equipped with a filter set DAPI (Carl Zeiss) consisting of a band-pass filter covering 350–370 nm for an exciter and an absorbance filter covering wavelength of 400 nm, as well as a QICAM 12 bit Monochrome Fast 1394 Cooled charge coupled device CCD camera (QImaging, Burnaby, Canada) with a resolution of $1.4X10^6$ pixels. The 100X oil immersion objectives were used to visualize and acquire the fluorescence images.

Results and Discussion:

mAmp was synthesized by heating a fresh solution of Ampicillin in a PCR machine for 2 hrs at 99^{o}C. PCR machine was chosen because the temperature of the incubation chamber can be kept constant and to prevent any evaporation the lid was set to a temperature of 100^{o}C. The clear solution turned amber after the reaction was complete (Fig. 5.2a). In the past fluorescent derivatives of Ampicillin have been reported where they were synthesized using aldehydes (Formaldehyde) and alkali (NaOH) along with heat (Uno et al., 1981). However, the derivatives hypothesized to have formed cannot be matched to mAmp unless its structure is deciphered. More will be discussed later on in this section. The mAmp solution emits light blue light when examined under a UV lamp (Fig. 5.2b). The solution when dried leaves a yellow colored precipitate unlike its parent compound which is white (Fig. 5.2c).

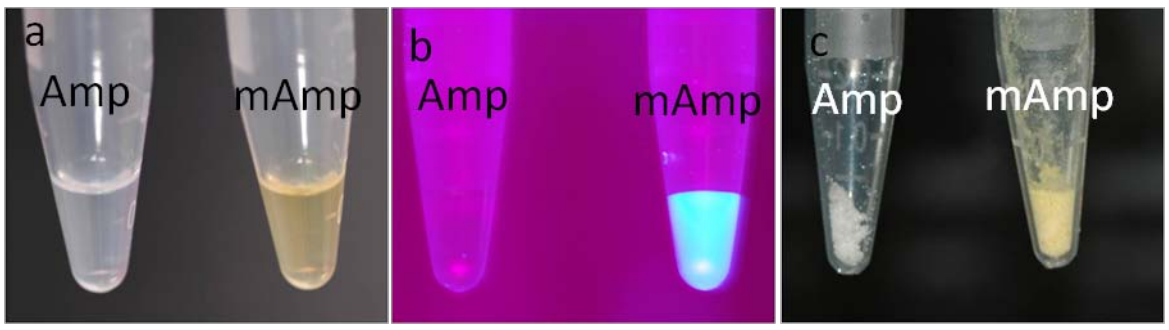

Figure 5.2. a) Amber coloration of mAmp after heat treatment. b) Fluoresence of mAmp after heat treatment, on UV exposure. c) mAmp Yellow powder after drying.

UV spectra (Fig. 5.3) and fluorescence spectrum (Fig. 5.4) show absorbance and emission at 340nm and 420nm respectively. The parent compound on the other hand shows no peak at 340nm in the UV spectra. The excitation and emission peaks at 340nm and 420nm are characteristic of chemicals that are water soluble and show blue fluorescence.

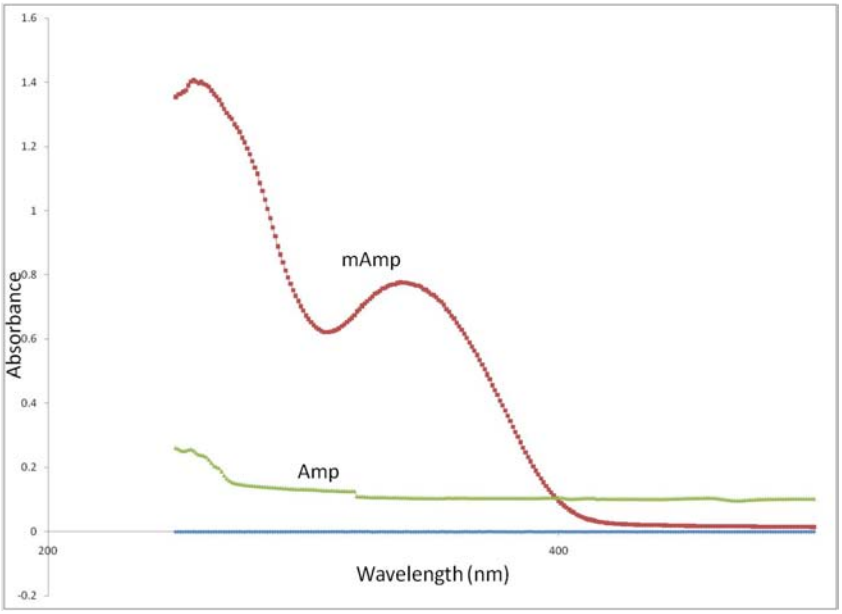

Figure 5.3. UV-vis spectra of Amp and mAmp.

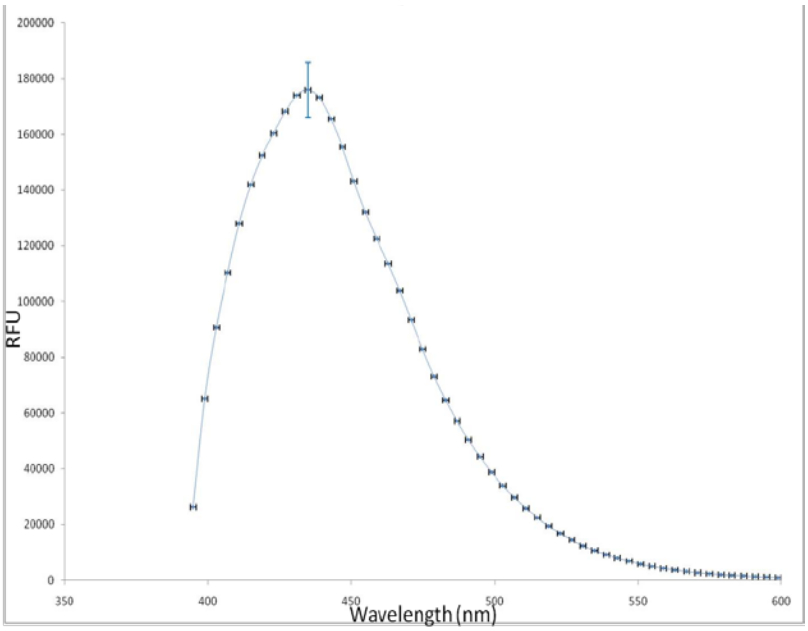

Figure 5.4. Fluorescence spectra of mAmp.

To calculate the quantum yield (QY) (ϕ) of mAmp was the next logical step given its high fluorescence. It gives the efficiency of the fluorescence process. It is defined as the ratio of the number of photons emitted to the number of photons absorbed.

ϕ = #of photons emitted/ # of photons absorbed

We use the comparative method of William et. al. (1983) to calculate the QY. Quinine sulfate and 9,10 Diphenylanthracene with QY of 0.45 and 0.9 were selected as standards. The choice of these standards was obvious because their emission profiles match that of mAmp. The two standards were cross-calibrated with each other to instill confidence in the method used. Five serial dilutions of each standard were selected and both UV-vis and fluorescence spectrometry recording were taken. After confirming the QY of each standard by this method, we proceeded with the calculation of QY of the sample, mAmp. We obtained a value of 0.11 on averaging the triplicates. A measure of the high QY of

mAmp can be had and appreciated by comparing it with two common fluorescent dyes that are widely used in biomedical imaging, cyanine dyes Cy3 with a QY of 0.04 and Cy5 with a QY of 0.28 (Mujumdar et al., 1993). It is apparent mAmp has a higher QY than Cy3, which by no means can be considered to be a push-over in dyes. Cy3 is known for its high photostability and brightness with minimal background fluorescence. We tested the photostability of mAmp over a period of one month by keeping the solution in a clear container under normal light. There was less than 5% decrease in the absorbance over this period.

It was unsure up to this point what would be the charge of mAmp. Is it amphiphilic like its parent compound Ampicillin having both amino and carboxyl group, or charged? 5% horizontal agarose gel was used with Ampicillin and mAmp as samples. mAmp could be readily visualized under the Gel-doc due to its bright fluorescence and was seen moving towards the anode, suggesting mAmp was actually negatively charged (Fig. 5.5). This meant the carboxyl group was intact and the amino group was lost in the process.

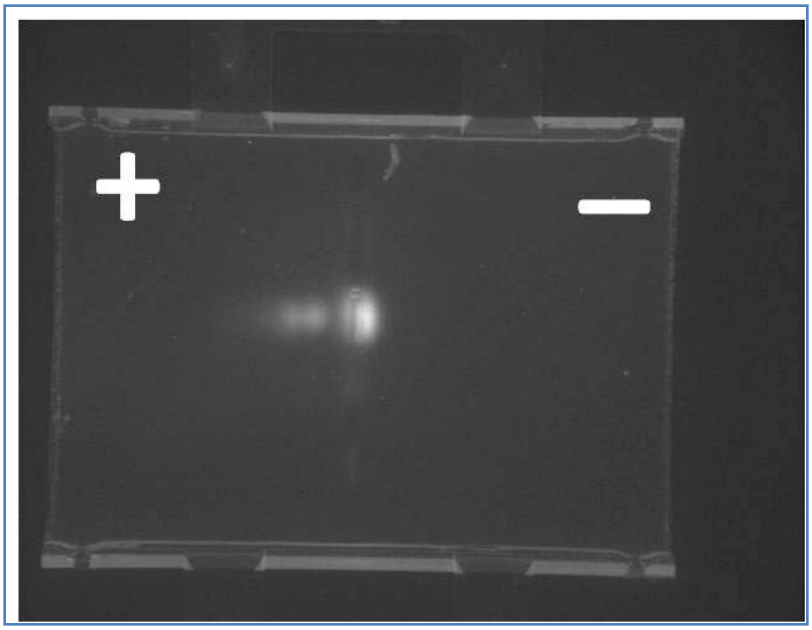

Figure 5.5. 5% Horizontal Agarose gel with mAmp moving towards the positive end.

Next, we wanted to test the bright fluorescence and photostability along with the ability to disperse hydrophobic materials, by mixing mAmp with both pristine SWNT and oxidized and shortened SWNT. After brief sonication for 20 mins in a bath sonicator, there was a profound increase in solubility of pristine SWNT apparent by the dark color of the solution. UV-Vis spectra displayed the characteristic Van Hove peaks of SWNT (Fig. 5.6), which is a significant result because we never witnessed Van Hove peaks of SWNT in any of our processes before, when we extensively used SDBS and other surfactants. More so, these peaks appeared on pristine SWNT without even subjecting them to chemical oxidation, which supposedly helps in dispersing the SWNT even further by breaking the van der Waals forces in the SWNT bundles.

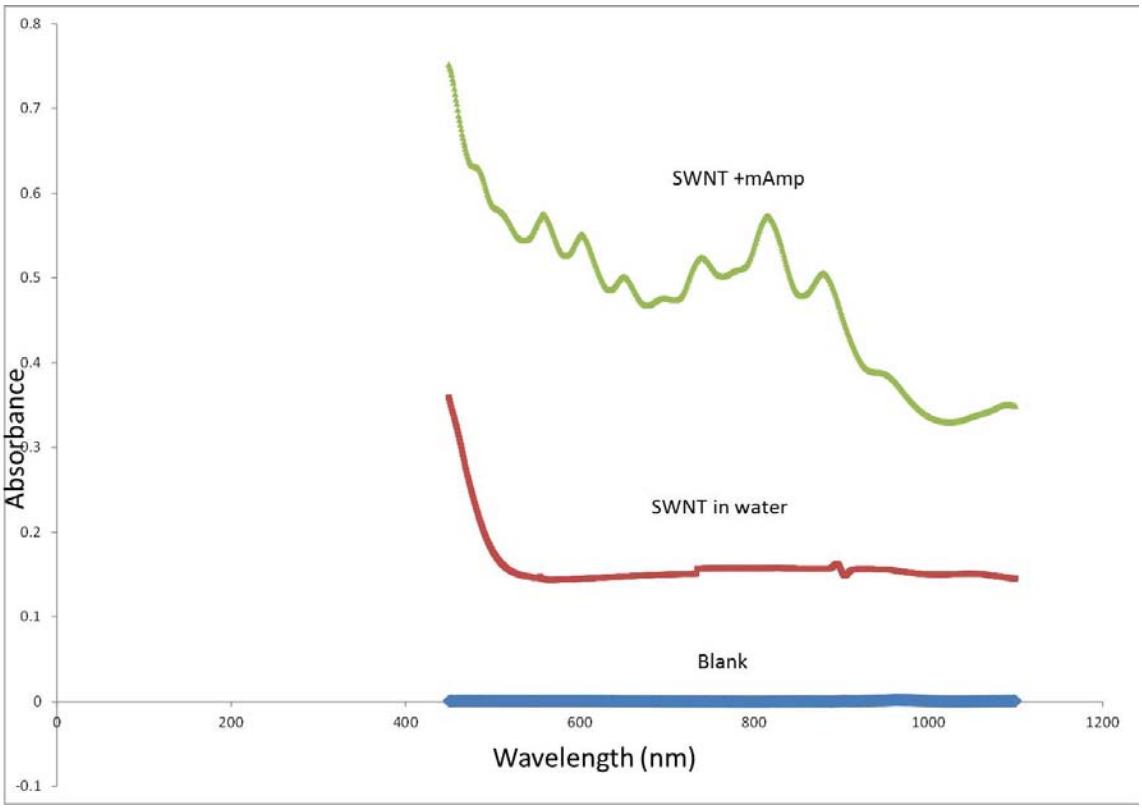

Figure 5.6. UV-Vis spectrum of mAmp-SWNT and SWNT alone. The Van Hove peaks characteristic of highly dispersed SWNT is conspicuous.

To confirm mAmp alone had this capability, we performed the SWNT dispersity test using Ampicillin, Amoxycillin, Penicillin G and Kanamycin. None yielded the same outcome. Atomic Force Microscopy (AFM) was used to confirm and analyze the high dispersity observed in the UV-vis spectra and on visual inspection. AFM scans of pristine SWNT in mAmp showed long SWNT uniformly distributed on the mica surface and section analysis revealed the diameter to be 1.1nm. Given that the diameter of individual SWNT is 0.8nm-1.2nm, this means the pristine SWNT were unbundled to its basic unit (Fig. 5.7b). AFM scans of dsSWNT in mAmp also yielded the same result except for the lengths, which were shorter than 500nm (Fig. 5.7a).

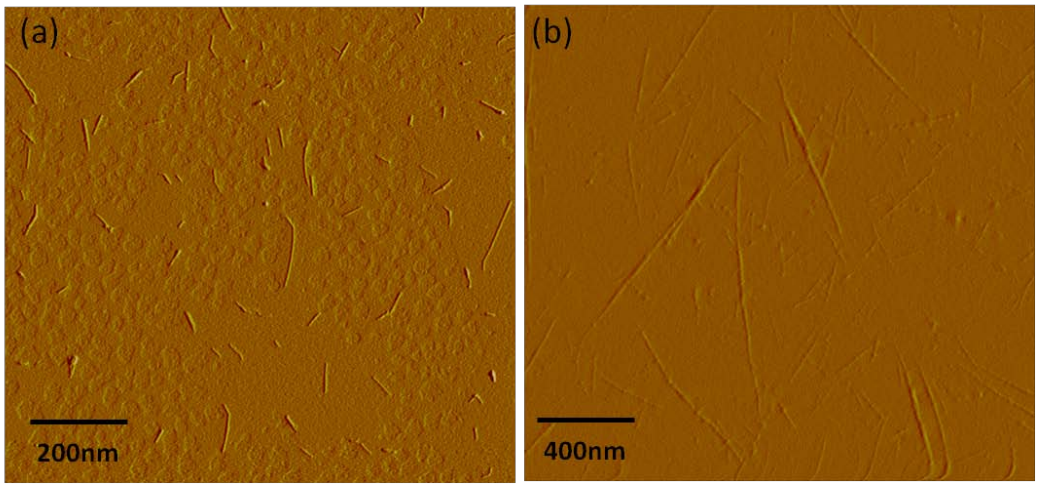

Figure 5.7. Phase AFM images of a) dsSWNT in mAmp and b) Pristine SWNT in mAmp

Fluorescence microscopy was used to evaluate the brightness of mAmp and test its photostability *in situ*. The SWNT were visualized at 100X magnification using the DAPI filter (scan range 320nm – 520nm). Bright rod shaped fluorescent particles were observed suggesting the intensity of fluorescence was in appreciable limits (Fig. 5.8). However, the particles started to fade away after continuous exposure to UV light, generated by a 100W halogen lamp, for 15 mins.

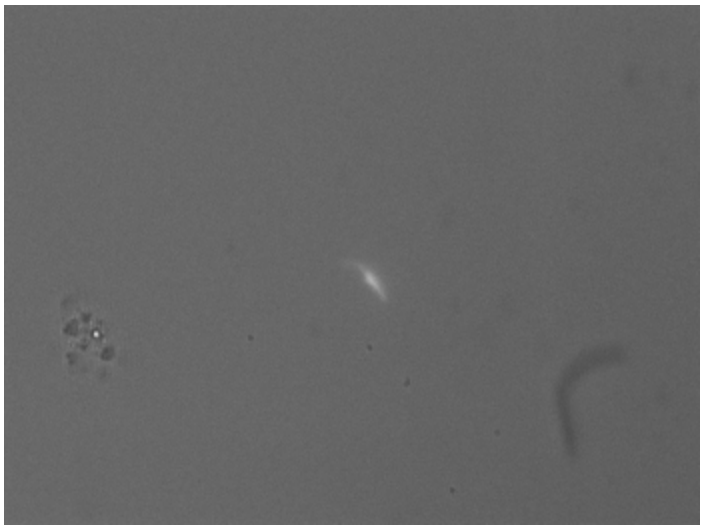

Figure 5.8. Fluorescence image of mAmp-SWNT at 100X magnification and under DAPI filter.

This is a significant advancement as a single compound is enabling both dispersion and fluorescent visualization of SWNT, a paradigm shift from our very own work reported previously that used SDBS to disperse the SWNT and a Pyrene derivative to visualize (Kim et al., 2006).

In order to completely understand the binding mechanism of mAmp to SWNT, its structure needs to be deciphered. However, contemplating the structure first and finding an acceptable explanation to the mechanism of binding might also work. We know that mAmp is amber colored, exhibits blue fluorescence and has a higher affinity for SWNT than its parent compound Ampicillin. Amber (yellow) colored compounds with blue fluorescence usually have a minimum of five conjugated bonds (C=C), a system of alternate double and single bonds connected by π orbitals with delocalized electrons (Riegel and Kent, 2007). Ampicillin, a colorless compound with no fluorescence has

three conjugated bonds, localized to the aromatic ring. Besides contributing to the development of fluorescence in compounds with a minimum of five conjugate bonds, the π- electrons also aid in forming bonds and associations with compounds having similar π- electrons; the association being known as π- stacking where the conjugate system of one compound aligns itself with the conjugate system of the other compound. If mAmp indeed has five conjugate bonds, amounting to 10 π-electrons, in comparison to Ampicillin that has three conjugate bonds, amounting to 6 π-electrons, mAmp is more likely to form a stronger association with SWNT. Therefore in order to have a continuous conjugate system with 5 C=C bonds, the amino group on the carbon adjacent to the aromatic ring has to be replaced by a ketone group. This can be supported by the gel experiment which suggests loss of amino group. The 3 C=C bonds of the aromatic ring and the successive 2 C=O bonds, amount to the desired arrangement and numbers. Having speculated the structure based on indirect experimental findings we can now perform definitive analytical studies on mAmp such as NMR, FTIR, HPLC and Mass Spectrometry to solve the puzzle.

^{1}H NMR was performed on mAmp dissolved in D_2O. As shown in Fig. 5.9 the shifts are labeled according to the corresponding hydrogen. On comparing the ^{1}H NMR shifts of Ampicillin and mAmp it is apparent that H-10 in mAmp has become nearly degenerate. All the other shifts are comparatively similar. This means that the structure of mAmp is identical to its parent compound, ampicillin, except for loss of H-10.

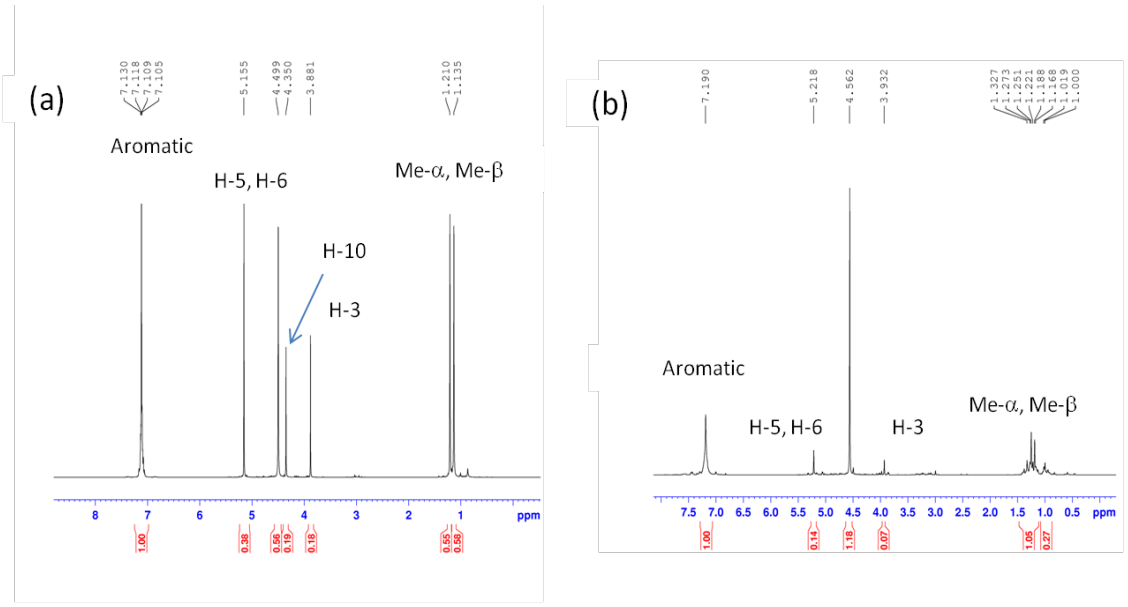

Figure 5.9 . ^{1}H NMR spectrum of a) Ampicillin and b) mAmp. Notice the spectrum is identical except for the loss of H-10 in mAmp.

FTIR was performed on a dry sample of mAmp. The mAmp solution was subjected to evaporation in a rotary evaporator for 4 hours to get rid of all the moisture. The FTIR signature of mAmp was compared to that of Ampicillin and turned out to be nearly identical, again suggesting that there were no major changes in the structure during the heating step (Fig. 5.10).

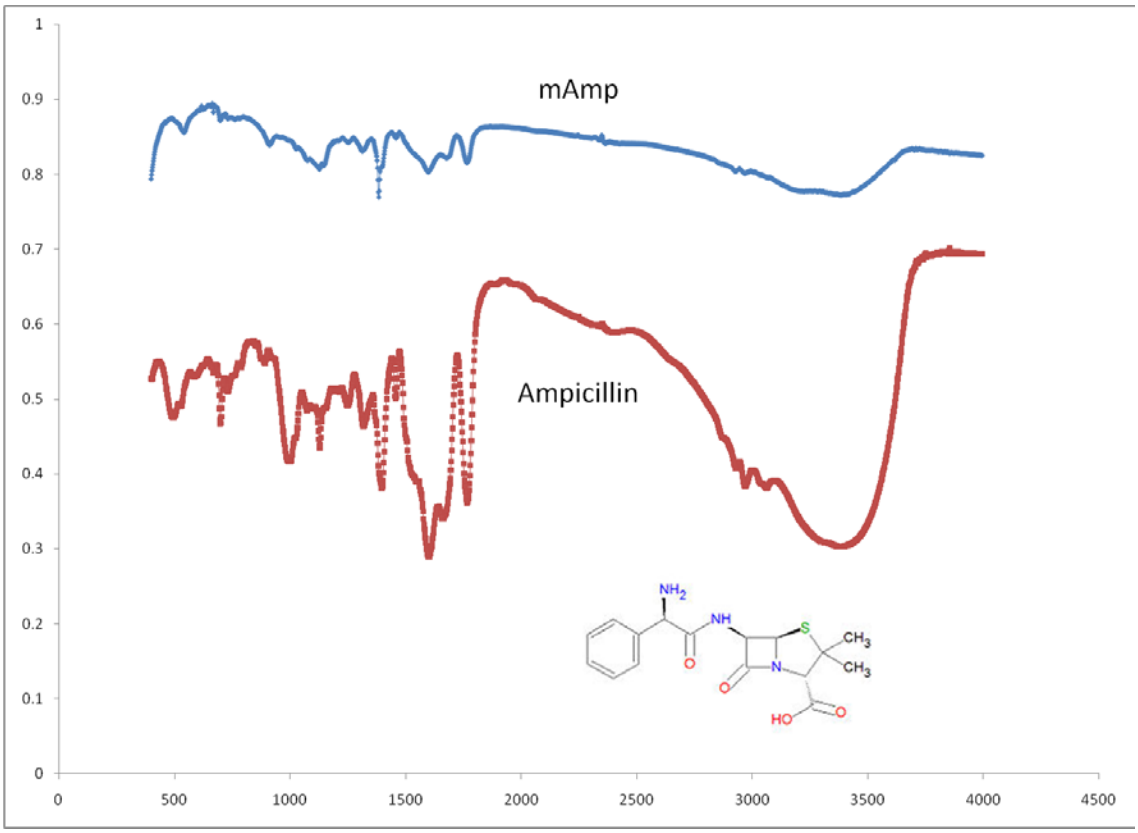

Figure 5.10. FTIR spectrum of mAmp (top) and Ampicillin (bottom)

We suspected, based on preliminary Electrospray ionization Mass spectrometry, that the mAmp solution could have many impurities that were the byproducts of the heating process (Fig. 5.11). It was thereby necessary to purify the sample to isolate the fluorescent derivative.

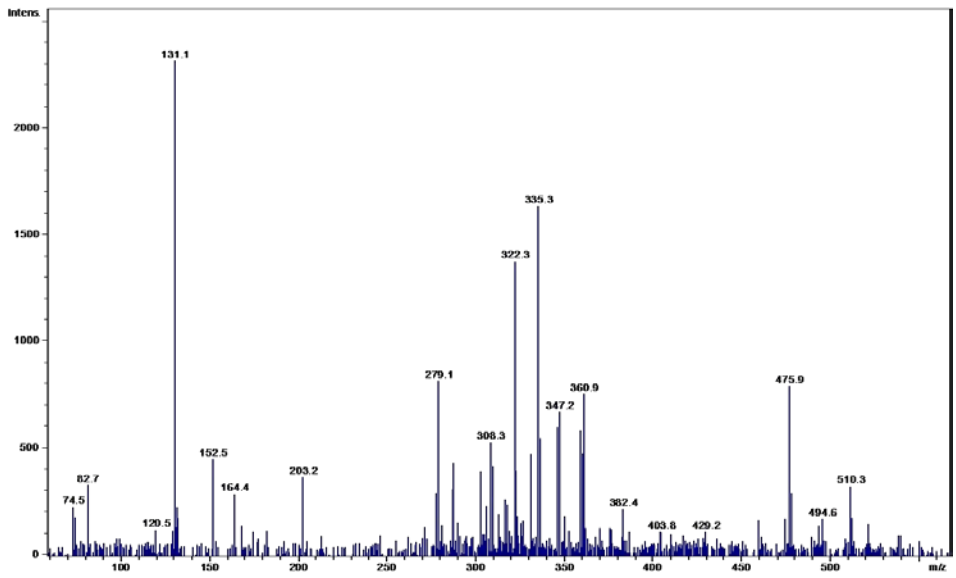

Figure 5.11. ESI MS of mAmp.

We performed HPLC on the sample using a C8 column and acetylnitrile/water (10%/90%) as mobile phase. The chromatograms of ampicillin and mAmp showed distinct peaks at 220nm and 340nm on using the PDA (Fig. 5.12). This agrees well with the UV–vis spectra obtained on the two compounds.

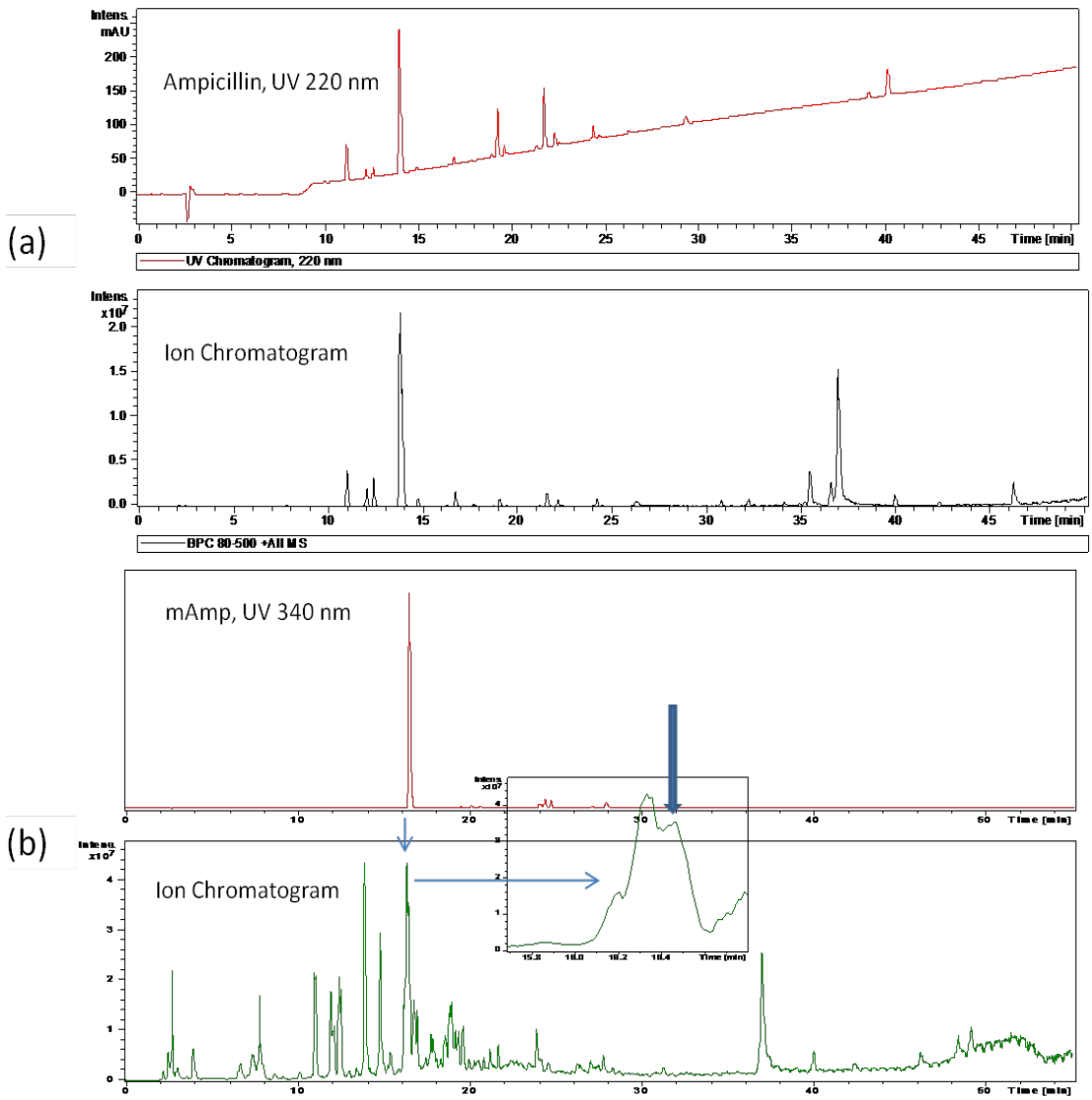

Figure 5.12. PDA data and Ion chromatogram of a) Ampicillin and b) mAmp

Using the same column HPLC-MS was then performed to obtain the molecular weight of the peaks at 220nm and 340nm. MS yielded a MW for Ampicillin at 349.7 which is very accurate and that for mAmp at 348.8 (Fig. 5.13). The MW of mAmp was 1Da less than Ampicillin.

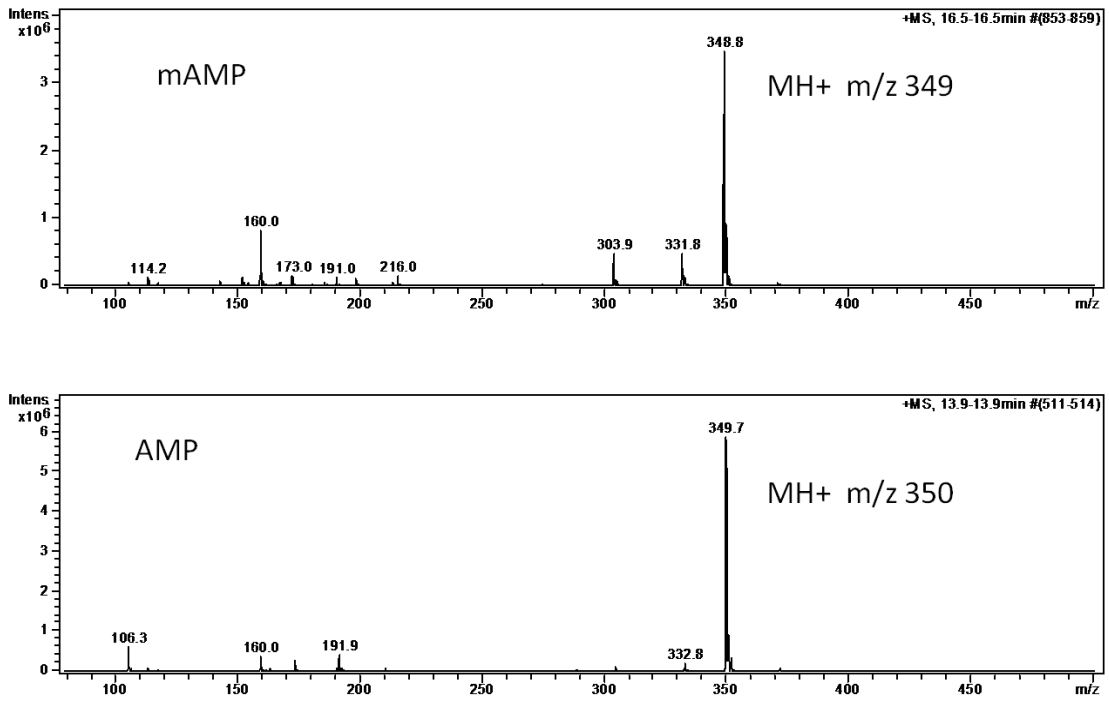

Figure 5.13. HPLC-MS data of mAmp (top) and Ampicillin (bottom).

This data agrees well with the NMR data that showed there was loss of 1 H atom, thus explaining the 1Da difference. However, there is a “Nitrogen rule” in MS which states that a compound with even numbered MW must contain either no Nitrogen or even number of Nitrogens and acompound with odd numbered MW must contain an odd number of Nitrogens. Ampicillin has 3 Nitrogens and has an odd MW. mAmp has an even MW therefore should have even number of Nitrogens. Since there is decrease in MW the only possibility left is loss of Nitrogen thus taking the number of Nitrogens in mAmp to 2. NMR data suggests there is loss of H-10, therefore it’s more likely for the amino group at that same location to have been replaced. Also we discussed previously that in order to exhibit fluorescence, there needs to be a ketone group replacing the amino

group adjacent to the aromatic ring. This hypothesis can now be supported by conclusive experimental data shown above. The MW of NH_2+H (H-10) is 17 and that of substituted O is 16, confirming the decrease in MW by 1Da. Our gel study to decipher the charge of mAmp showed that it was negatively charged, thus explaining the loss of amino group from the amphiphilic parent compound. If there is loss of amino group from the compound, it is likely to exist in solution as ammonium ion. In that case, ammonium being highly basic, the solution should become more basic. pH was recorded for both Ampicillin and mAmp and the reading for Ampicillin was 7.7 and that of mAmp was 8.75. This increase in pH can partly explain the fate of the amino group after dissociating from mAmp. We then performed an Ammonium assay to measure the precise amount of ammonia in solution. The sensitivity of the assay kit being 0.2 – 15μg/ml, ammonia is measured as a function of oxidation of NADPH. Decrease in absorbance of the sample at 340nm is an indicator of presence of ammonia in solution. We obtained a value of 0.744mg/ml for the amount of ammonia produced on modifying 14mg/ml of Ampicillin to mAmp. The reaction can be written as:

$$C_{16}H_{19}N_3O_4S + 2H_2O \xrightarrow{\Delta} C_{16}H_{17}N_2O_5S + NH_4^+ + H_20$$

We can hence say with confidence that the structure of mAmp is almost identical to Ampicillin except for a ketone group replacing the amino group adjacent to the aromatic ring thus forming 5 conjugated bonds (Fig. 5.14).

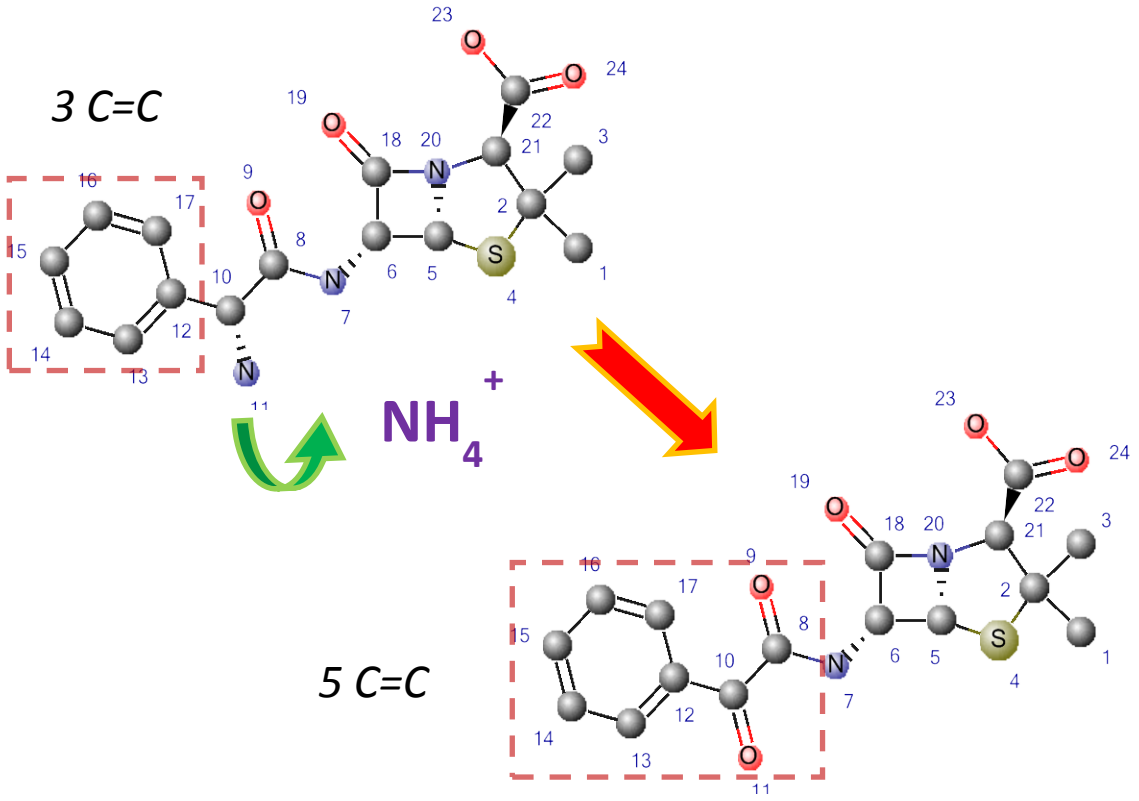

Figure 5.14. Schematic of Ampicillin transforming into mAmp.

We envisage the use of mAmp for biomedical applications and in order to do so must instill confidence in the research community about its safety and convenience. Ampicillin is an antibiotic and supposedly safe for human and animal consumption. However, there is always a risk that its antibiotic nature might harm the commensal flora that is considered beneficial. We performed bacterial susceptibility studies using a very common bacterium, E. coli K-12 strain that is sensitive to ampicillin. Two LB Agar plates, one containing mAmp and the other Ampicillin, were streaked with the K-12 strain and grown overnight at 37^{o}C. The plate with Ampicillin showed no growth and normal growth of colonies on the mAmp plates (Fig. 5.15). This indicates the loss of

antibiotic nature in mAmp. The beta lactam ring of Ampicillin is the one imparting antibiotic nature to this compound. Based on the structural studies there is no change in this part of the compound. Then how did mAmp lose its antibiotic nature when its beta lactam ring is still intact? We hope to address this issue at the earliest by creating silica derivatives of mAmp, essentially to convert the water soluble mAmp to a non polar compound, so that Gas chromatography Mass spectrometry can be performed (GC-MS) on it. GC-MS unlike LC-MS, which estimates only the MW of the compound, will yield a more definitive structure that can be compared to a library of already discovered compounds.

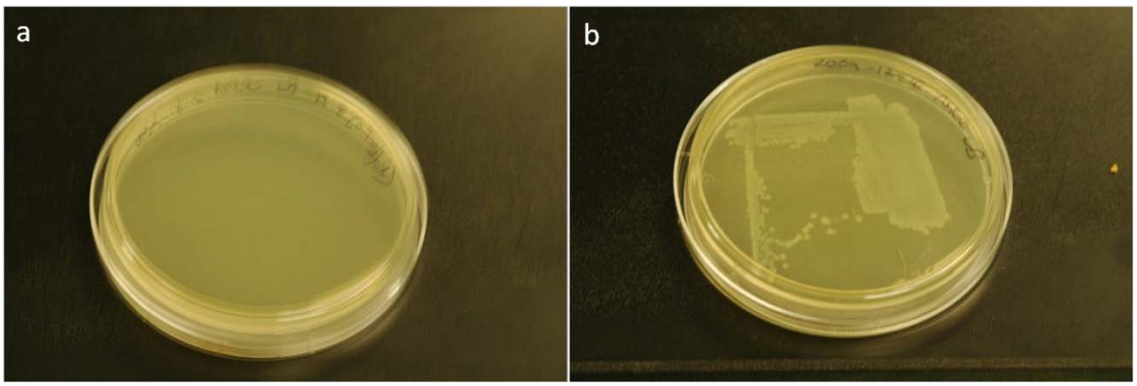

Figure 5.15. a) LB Agar with Ampicillin and *E. Coli* K12. b) LB Agar with mAmp and *E. Coli* K12

One of the promising traits of mAmp that we discovered is its ability to respond to changes in pH by lowering its fluorescence intensity. When attached to SWNT or any particle for *in vivo* or *in vitro* applications, in particular intracellular transport and sensing, it is assumed that the particle will be endocytosed by the cell and be contained

inside lysosomes in the cytoplasm. The pH of these endosomes can fall down to as much as 4.3 in the late stages of assimilation. We prepared acetic acid solutions with pH as low as 4.37 and tested how it altered the fluorescence profile of mAmp. There was ~50% decrease in the intensity of the fluorescence peak at that pH (Fig. 5.16). Triplicate readings were taken and the based on standard deviation there is significant loss of fluorescence on lowering the pH. The intensity slowly comes back to normal on increasing the pH.

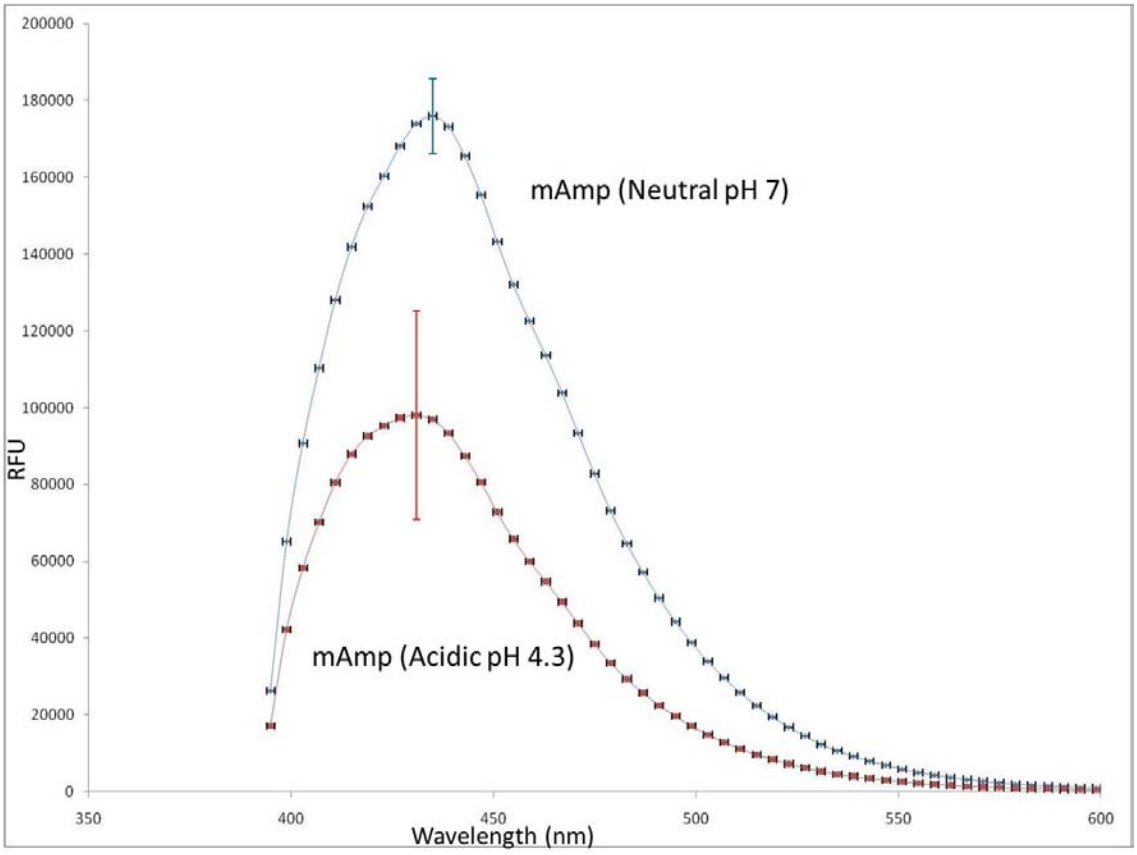

Figure 5.16. Fluorescence plot of mAmp in an acidic condition pH 4.3.

This has potential to act as a pH sensor, for example if the particle containing mAmp is endocytosed by a cell and when the fluorescence spectrum shows a significant decrease it could suggest that the particle is located inside the endosome. Real time monitoring of the fluorescence intensity will give a clue as to the location of the particle; if particle is released by endosome the fluorescence should raise back to normal.

Attachment of PEG-COOH to dsSWNT:

We did discuss previously how EDTA can mediate the attachment of dsMWNT to polypropylene. It is noteworthy to point out that EDTA enabled attachment of dsMWNT to most plastics (polymers) for e.g. Polydimethylsiloxane **(**PDMS**)** and polyethylene sheets. It however did not mediate binding of dsMWNT to glass. This is encouraging since glass can be used as a vessel where reaction between CNTs and plastics can be carried out in solution without the concern of losing CNTs to cross-reaction, as would be the case if commonly used polypropylene microcentrifuge tubes are used.

PEG-COOH was preferred over PEG and PEG-NH_2 because it is unlikely to bind to EDTA, which is predominantly carboxylic and negatively charged, thus leaving the carboxyl group free to either use for covalent modifications or electrostatic interactions. PEG-COOH attachment on dsSWNT using EDTA was performed by mixing the reaction mixture at 1400 rpm (Fig. 5.17a). AFM was used to characterize the PEG-dsSWNT hybrids. AFM images show increase in the lateral and vertical dimension of the dsSWNT suggesting coating by PEG (Fig. 5.17c). Also of importance is the uniformity of the

height profiles of all the PEG-dsSWNT in the AFM field. This will be significant when we compare the presence of antibody on the PEG-dsSWNT later on.

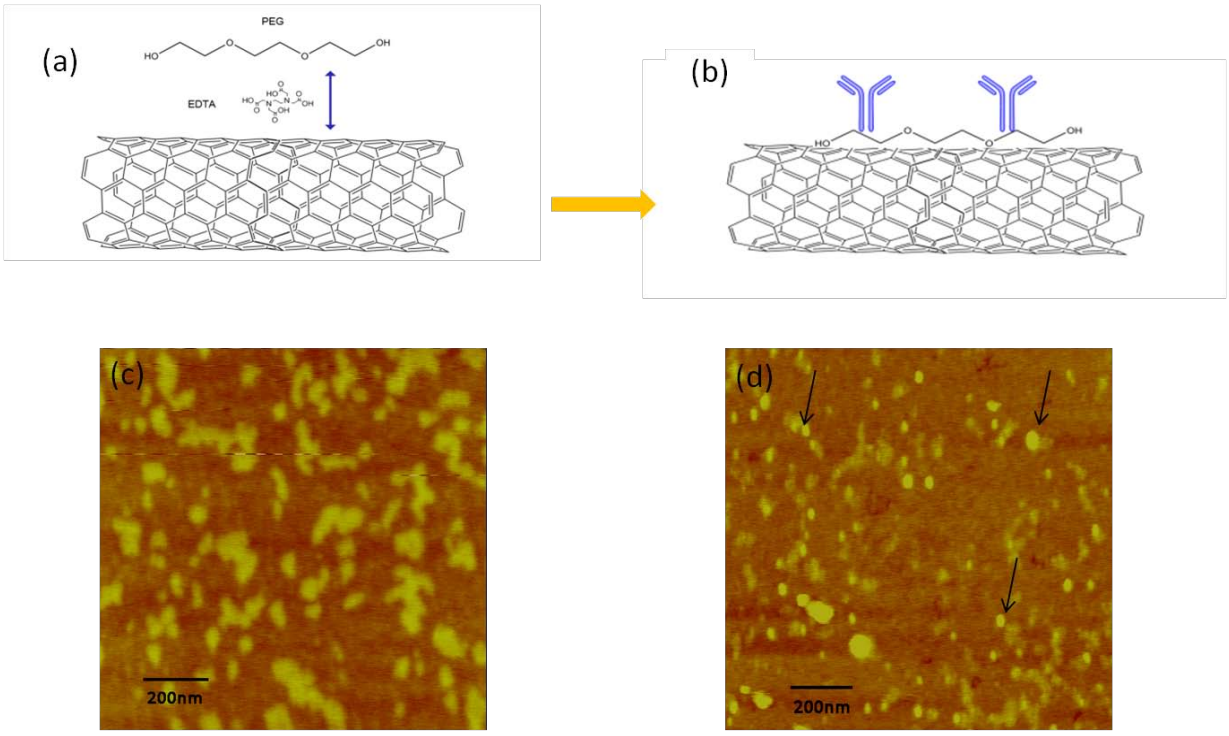

Figure 5.17. (a) Schematic of adsorption of PEG on SWNT using EDTA. (b) Schematic of IgG nonspecifically adsorbed on PEG-SWNT. (c) Height AFM image of PEG-SWNT. (d) Height AFM image of IgG adsorbed on PEG-SWNT. Arrows pointing the IgG, observed as bright spots.

For all our experiments we used fluorescent antibodies, IgG-FITC. Covalent coupling of IgG-FITC to the carboxyl group of PEG was attempted using the traditional carbodiimide based scheme. We noticed in spite of using water soluble sulfo-NHS, dsSWNT aggregated, which interfered with the subsequent characterization and application steps. We then attempted nonspecific binding between the positively charged

amine groups of IgG and the negatively charged carboxyl groups on PEG (Fig. 5.17b). The sample was dialyzed using a 100nm PTFE membrane for 48hrs before further analysis was undertaken. UV-Vis spectra showed the characteristic protein peak at 280nm post dialysis (data not shown). AFM images also confirm electrostatic binding of IgG to PEG-COOH. IgG are depicted by the bright spots in the image and are of higher contrast compared to PEG in the background (Fig. 5.17d). The variable height profile of the bright spots in comparison to the light colored areas of PEG also suggests presence of IgG on the grid. To state the obvious, there are two ways to attach antibodies which results in random orientation and the other more desirable oriented conjugation. Oriented conjugation through the F_c region of the antibody results in the F_{ab} portion directed outward from the surface therefore being available for targeting. This can be achieved very easily by using Protein A which preferentially binds to the F_c region. The other techniques are, to have a surface which has thiol and aldehyde groups that bind to the sulfhydryl groups and lysine rich regions of the antibody respectively. These methods have been used to conjugate antibodies to the DSS-SWNT and PrA-FH-SWNT hybrids and will be discussed in the next few sections. However, due to the unavailability of such groups on the PEG-dsSWNT, and there being no distinction between carbodiimide based covalent coupling and nonspecific adsorption as both result in random orientation, we employed simple adsorption based on electrostatic attraction to attach antibodies to PEG-dsSWNT. Due to the high absorbance of dsSWNT demonstrated in the UV-Vis-NIR spectra and the associated van hove peaks we do not expect to see the fluorescence spectra of the FITC linked to the IgG at 521nm. Instead we tried fluorescence imaging of the IgG-FITC-PEG-dsSWNT adducts expecting to see linear fluorescent profiles, in

consonance with the presence of IgG along the length of the SWNT. We have had remarkable success in the past imaging fluorescent labeled SWNT with high resolution which also opened up avenues for deriving complex trajectories of SWNT *in situ* and calculating the diffusion coefficient. Fig. 5.18 shows the fluorescent image of IgG-FITC-PEG-dsSWNT taken using a FITC filter.

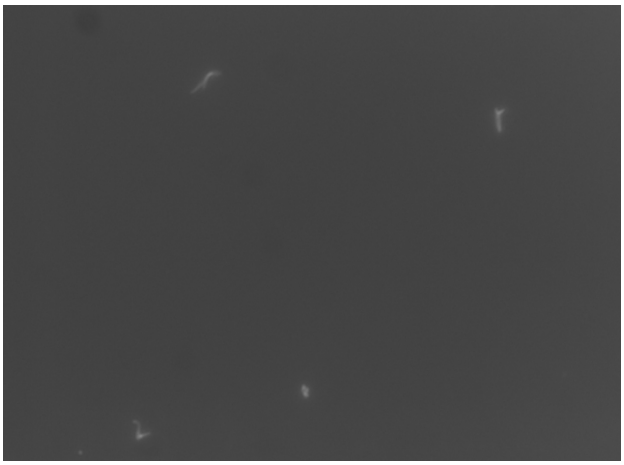

Figure 5.18. Fluorescent image of FITC tagged IgG on PEG-SWNT. Magnification is 100X under an FITC filter.

CHAPTER 6

Evaluation of Stealth character of 'Multivariate' Carbon Nanotubes on Human Macrophage

Introduction:

It is a matter of time before CNT will be used for the diagnosis, prevention and treatment of diseases and ailments. Its responsiveness to near infra-red (IR) radiation and ability to interact with biological moieties like proteins, carbohydrates and DNA and biocompatible materials like gold make them ideal for selective targeting of cells and tissues; and amenable to laser induced photothermolysis (PT). This versatility of CNT would impart a non-invasive and highly localized yet systemic approach to obliterating pathological lesions with minimal side effects. However, even before the CNT reach the target location they will have to encounter the cells of the reticuloendothelial system (RES), namely macrophages which form the first line of defense against foreign particles. Macrophages are part of the innate immune system where opsonins, plasma proteins such as complement factors and immunoglobulins, attach non-specifically to foreign objects and in turn are recognized by macrophages for phagocytosis and sequestration to liver and spleen. Therefore any particle that is introduced into the bloodstream will inadvertently be flooded with opsonins, which eventually control the fate of the particle. Recently many groups have published articles on selective targeting of tumors and other lesions using CNTs and also have performed systemic studies on the biodistribution of these particles. Most of these studies universally use the traditional coating materials such

as PEG to help the CNT evade the RES. What is ignored in this process is the microcosm where such particles can be attacked by opsonins flooding the site and rendering most of these particles useless. It is of utmost importance to study and develop particles with novel coatings that can survive these first few minutes in a hostile environment and come out unscathed. For achieving this, preparing materials in bulk and leaving them to their fate once injected is definitely not the step in the right direction. Precise control over the size of the starting material, selection of ideal coating material and uniform coverage of the coating on CNTs, are all vital priorities. We have developed and improved upon previous designs of stealth CNTs, which can potentially evade the macrophages by being transparent to the blood opsonins. The stealth CNTs are basically divided into four categories: synthetic – PEG-SWNT, semisynthetic – mAmp-SWNT, seminatural – DSS-SWNT and natural – PrA-FH-SWNT. They will be tested on both prokaryotic and eukaryotic cells, *Staphylococcus aureus* and human macrophages, for the ability to evade and in the case of the bacterium even selective attachment with the help of specific antibodies. *Staphylococcus aureus* is a facultative anaerobic gram positive coccus that causes a wide variety of illnesses due to its ubiquitous nature ranging from skin infections to infections of internal organs such as meningitis, pneumonia, endocarditis and toxic shock syndrome (Ryan and Ray, 2004). Staphylococcus is being used as a model prokaryote due to the presence of Protein A on its surface. Protein A confers immunological transparency to the bacterium and greatly helps the survival rate of the pathogen in a hostile environment.

Our goal was not to develop a stealth particle that would non-specifically attach to all types of pathogens in a given system; but to develop a highly specific targeting agent

that would attach only to a specific type of pathogen and evade all other pathogens, if present, including normal cells and predator cells. In other words our ‘grand design’ is to develop a semiautonomous particle that can reach its target location unguided and unobstructed and in the process avoid any type of nonspecific and random interaction that could remotely happen when such manufactured particles are sent *in vivo*. Firstly, we attempt to show how all the stealth SWNTs do not attach to *S. aureus* in lieu of their coating and when anti Protein A antibody is introduced to enable specific attachment, how the bacterium can be selectively lysed using laser induced photothermal ablation. The bacterium serves two purposes; one, the targeting modality is not exclusively developed to target mammalian tissues and can be extended to include pathogenic organisms and two, the bacterium serves as a good model to test the stealth characteristics of the developed particles early on before human macrophages are brought into play. We then move on to test the particles on human macrophages to examine their stealth behavior in the presence of opsonins, C3b and IgG (Fig. 6.1).

Finally, to our surprise we identified a new method that does not involve or require any form of coating to render SWNT transparent to macrophages. It is rather a noninvasive optical based technique which uses an external laser field to help SWNT escape macrophages.

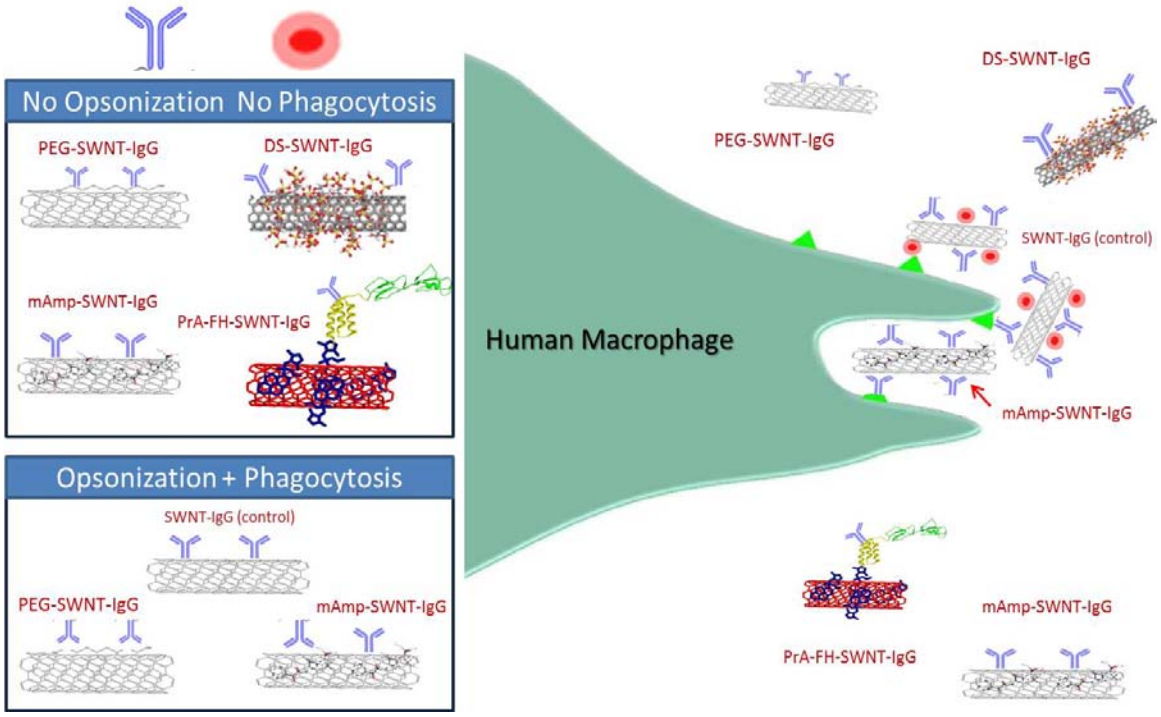

Figure 6.1. Schematic of proposed scheme of stealth character afforded by coating SWNT.

Experimental Part:

Interaction of S. aureus with the hybrid SWNT:

Staphylococcus aureus strain was obtained from the American Type Culture Collection (Rockville, MD) and maintained in Luria-Bertani (LB) medium (1% tryptone,0.5% yeast extract, 0.5% NaCl, pH 7). To prepare biomass for the study, bacteria culture was first streaked onto LB agar plate. After overnight incubation at 37^{o}C, an isolated colony was cultured in 5 ml of LB broth and transferred to 100 ml of LB broth. The culture was grown at 37^{o}C in a rotary shaker (200 rpm) for 14 hours. The resulting biomass was harvested by centrifugation at 2,200g (25^{o}C) for 30 minutes. The

pellet obtained from centrifugation waswashed three times with the phosphate buffer. Appropriateamounts of the resulting biomass were suspended withdispersed and shortened dsSWNT solution [1g-biomass (wet wt.)/L-dsSWNT] and the four particles PEG-SWNT, mAmp-SWNT, DSS-SWNT and PrA-FH-SWNT [1 g-biomass (wet wt.)/L-hybrid SWNT] in the phosphate buffer, and incubated for 0–2 hours (25^{o}C) at an incremental value of 0.5 hours to allow absorption and internalization of dispersed and shortened SWNTs (dsSWNTs)to the bacteria as well as bacteria absorption to the hybrid SWNT. For dsSWNT samples, after incubation, further centrifugation for 30 minutes at 2,200g (25^{o}C) and additional three-time washing with the phosphate buffer were done to remove unbound CNTs. Control samples were also prepared, including samples only containing dsSWNT, and those only containing *S. aureus*. Cells samples were evaluated using LIVE/DEAD BacLight Bacterial Viability Kit (Invitrogen, Carlsbad, CA) according to the manufacturer's specification.

Interaction of Macrophages and opsonins with Hybrid SWNT:

SC Human macrophages purchased from ATCC were cultured according to the vendor's specifications and kept in their original growth medium (Iscove's modified Dulbecco's medium) for the entirety of the experiment. The hybrid SWNT along with the dsSWNT control were preincubated with opsonins, IgG and C3b, at 37^{o}C for 2 hours and then added to the medium containing macrophages and mixed for 2 hours at 37^{o}C. The sample is then washed in the centrifuge at 3400rpm for 5 minutes three times to remove any unbound particles.

Laser Treatment:

The *S. aureus* samples with or without CNTs as well as CNT only samples were irradiated in an optical cuvette (Fisher Scientific, Pittsburg, PA) with quartz windows and adimension of 2 mm X 20 mm X 10 mm (light path of 10 mm,suspension height of 2 mm) using a He:Ne laser (Lasermate, Pomona, CA) operating at the wavelength 808nm in continuous mode. After exposure for 5 min to the laser at $0.6W/cm^2$ the cells were subjected to viability tests.

For the effect of laser on macrophages that has engulfed SWNT, continuous exposure to the laser radiation for 2 hrs was maintained.

Viability Tests:

Bacteria viability tests for the samples before and after PT treatment were performed using the LIVE/DEAD BacLight Bacterial Viability Kit (Invitrogen) accordingto the manufacturer's specification, which makes live cells green fluorescent and dead cells red fluorescent using epifluorescence microscopy.

Trypan blue (ATCC) based viability tests were performed on macrophages. 10μl of Trypan blue was incubated with an equal volume of cell suspension for 5 min and immediately analyzed using light microscopy.

Fluorescence and Light Microscopy:

Phase-contrast and transmittance microscopy was performed using a light microscope (Axioskop 2 Plus, Carl Zeiss, Inc., Germany) equipped with a 12-bit Color MicroImager

II Cooled digital camera (QImaging, Burnaby,Canada) with a resolution of 1.3 million pixels. The 100 or 63 oil immersion objectives (Carl Zeiss) were used tovisualize and acquire the images. The light microscopysystem was additionally equipped with a FITC filter set(Carl Zeiss) consisting of a band-pass filter covering 450–490 nm for an exciter and an absorbance filter-coveringwavelength of 515 nm.

Results and Discussion:

Hybrid SWNT and S. aureus:

We have successfully demonstrated in an earlier work how CNTs can act as photothermal (PT) contrast agents by adsorbing on bacterial surfaces and disintegrating them on laser irradiation (Kim et al., 2007). The same principle will be employed in our studies here to prove successful attachment of the stealth SWNTs after anti PrA IgG attachment. *S. aureus* exhibit characteristic grape-like cluster colony formation when viewed under an optical microscope (Ryan and Ray, 2004). This can be attributed to cell division in multiple planes and incomplete post-fissional movement due to cell walls remaining in close association to each other. *S. aureus* treated with dsSWNT, where dsSWNT nonspecifically adsorbs on the surface, did not show any signs of cell death using BacLight viability assay. The cells appear green (viable) and have intact grape-like clusters (Fig. 6.2a). However, on laser application the cells turned red (dead) and disaggregated demonstrating heat induced cell lysis and separation due to the effect of NIR radiation absorptivity and excitation of SWNT (Fig. 6.2b).

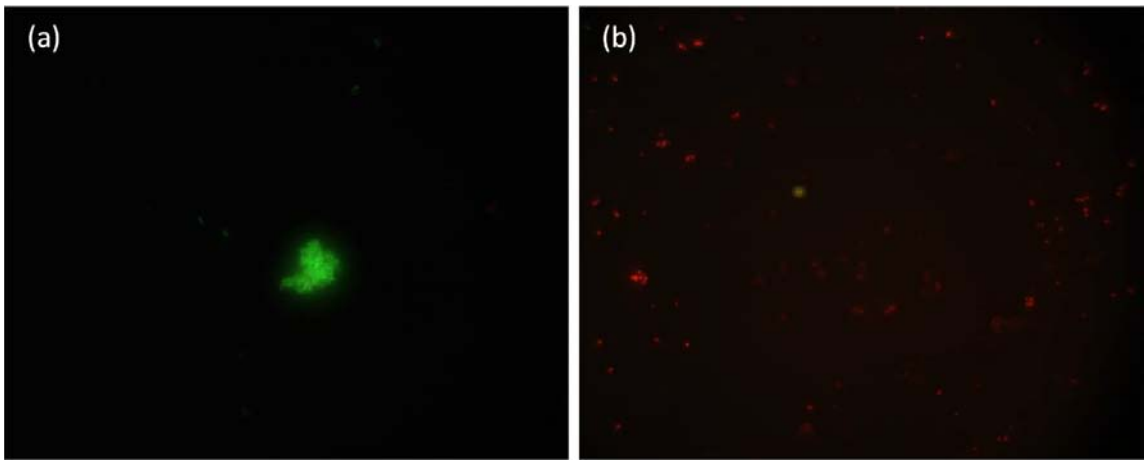

Figure 6.2. a) Fluorescent image of live *S. aureus* with dsSWNT without laser application. Notice the intact grape like aggregation. b) Fluorescent image of dead *S. aureus* with dsSWNT after laser application. The cells have disaggregated.

This control experiment proves that uncoated dsSWNT adsorbs on *S. aureus* and by itself is non-toxic to the bacterium. From our previous work we estimated the laser fluence required for bacterial lysis to be around 0.6W/cm^2 and used the same intensity throughout all the experiments. Previously we used dsSWNT that were suspended in surfactant. However in the experiments listed here we are using mAmp as a replacement for the surfactant as we want to avoid the use of surfactant completely due to toxicity issues. Also, it has been reported that surfactants could disrupt the enzymes responsible for the post-fissional separation of the cocci from each other thereby resulting in dense aggregates. This could give a false positive result when testing for evasion, if used unintentionally. We then went on compare the four particles, PEG-SWNT, mAmp-SWNT, DSS-SWNT and PrA-FH-SWNT in their capacity to evade *S. aureus* (Fig. 6.3). On laser ablation all four showed more than 80% cell viability, green on BacLight and intact grape-like clusters.

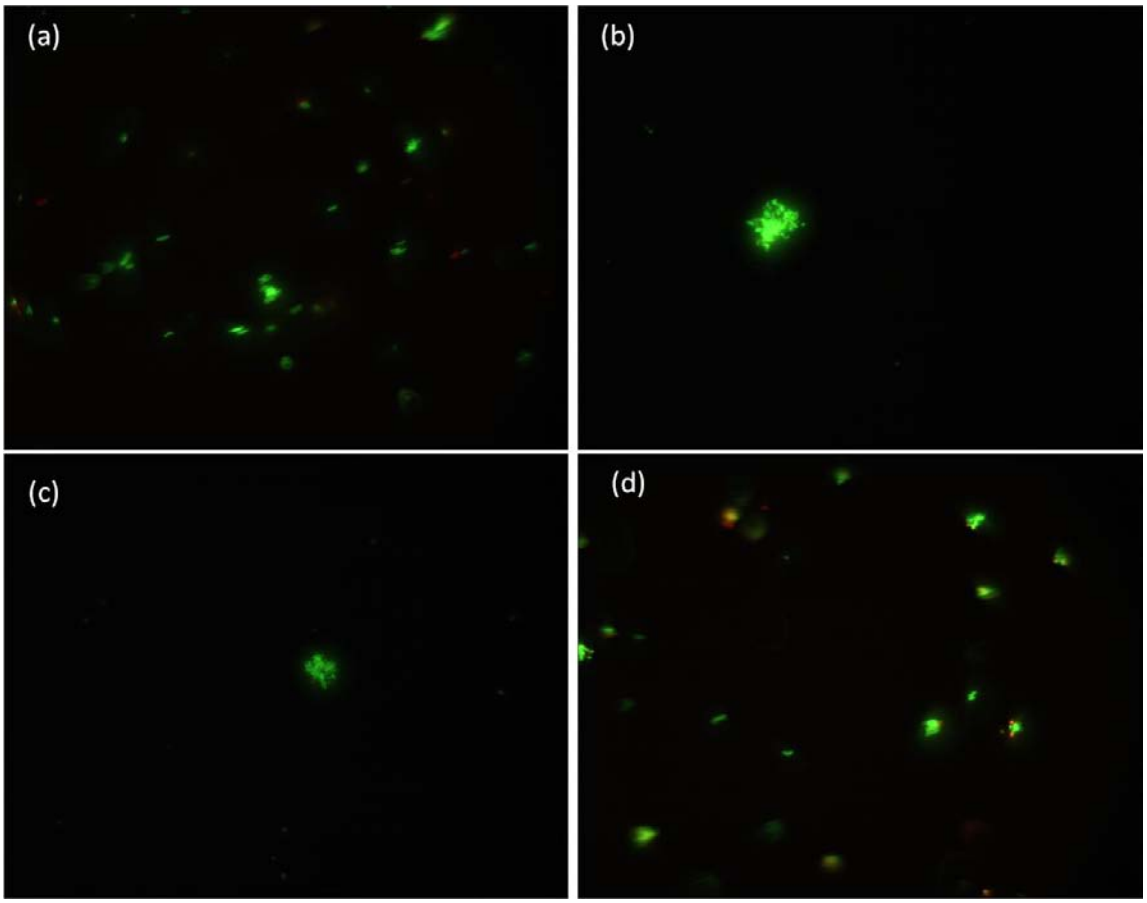

Figure 6.3. Fluorescent image of *S. aureus* with a) PEG-SWNT. b) mAmp-SWNT. c) DSS-SWNT d) PrA-FH-SWNT. The cluster formation is still intact in all four images.

S. aureus have a net negative charge on their surface due to the presence of Teichoic acid in their cell wall (Ryan and Ray, 2004). PEG-SWNT and PrA-FH-SWNT are neutral, PEG being inert and PrA-FH being amphiphilic and already being one of the constituents of the cell wall, and therefore will have minimal affinity for the cell surface. However, as found out previously, mAmp has a net negative charge as does DSS due to the presence of carboxyl and sulfate group respectively. mAmp-SWNT and DSS-SWNT could be experiencing electrostatic repulsion from the bacterial cell wall thus causing non

attachment and evasion. This result is an early indicator of the stealth nature of the four particles used.

The next goal was to selectively target *S. aureus* by using Anti Protein A antibody conjugated to the particles PEG-SWNT, mAmp-SWNT and DSS-SWNT and not to PrA-FH-SWNT. The monoclonal Anti Protein A IgG employed have F_{ab} binding sites specific for Protein A and has very low nonspecific F_c binding activity to Protein A. This essentially means that PrA-FH-SWNT cannot be used for this part of the study. The distribution of the surface protein of *S. aureus*, Protein A, is uniform in the bacterial inoculate obtained from the stationary phase of the growth cycle. To ensure this the inoculum was collected after 5 hrs of growth in LB medium. This is not a very important criterion for this phase of experiments as even an incomplete coating of bacterium by the particles conjugated to Anti Protein A IgG will lead to photothermal ablation due to the intense heat generated by absorption of NIR radiation by SWNTs. However, it will be important in the later sets of experiments where we would like to coat the organism completely so that there are potentially no attachment sites remaining for opsonins. After incubation for 1 hr at 37^o C, the samples were irradiated for 5 mins with $0.6W/cm^2$ laser energy and one half were used for fluorescent microscopy analysis and the other for AFM analysis. After staining with BacLight dye, fluorescence images showed samples containing all three particles, PEG-SWNT-IgG, mAmp-SWNT-IgG and DSS-SWNT-IgG have a high degree of dead cells (Fig. 6.4).

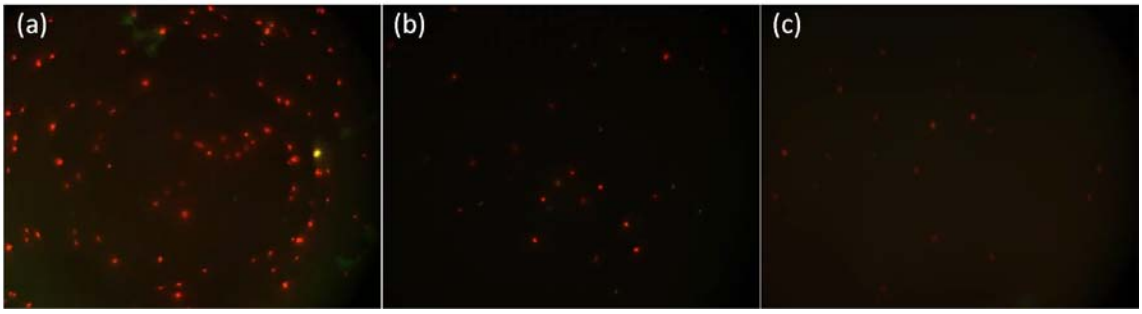

Figure 6.4. Fluorescent images of dead *S. aureus* with a) PEG-SWNT-AntiPrA Ab. b) mAmp-SWNT-AntiPrA Ab and c) DSS-SWNT-AntiPrA Ab.

AFM images taken of uncoated *S. aureus* showed a smooth surface which was markedly different from that of the coated *S. aureus* that displayed many 'blobs' on the surface (Fig. 6.5) . *S. aureus* has dimensions varying from 1 micron to 1.5 microns therefore the image was scanned at the highest possible scale, 15 microns, to image the bacterium in its entirety. At this magnification it was difficult to visualize the distribution of the particles on the surface. On magnifying the image to sub-micron scale the distribution and the original shape and dimensions of the particles could be appreciated. Only mAmp-SWNT-IgG seemed to cover the entire surface of the bacterium. The other two particles only appeared as large aggregates on the surface of the bacterium. The mAmp-SWNT particles looked to be evenly spaced on the surface of the bacterium and was an encouraging sign that most of the Protein A on the bacterial surface was occupied (Fig 6.5cii).

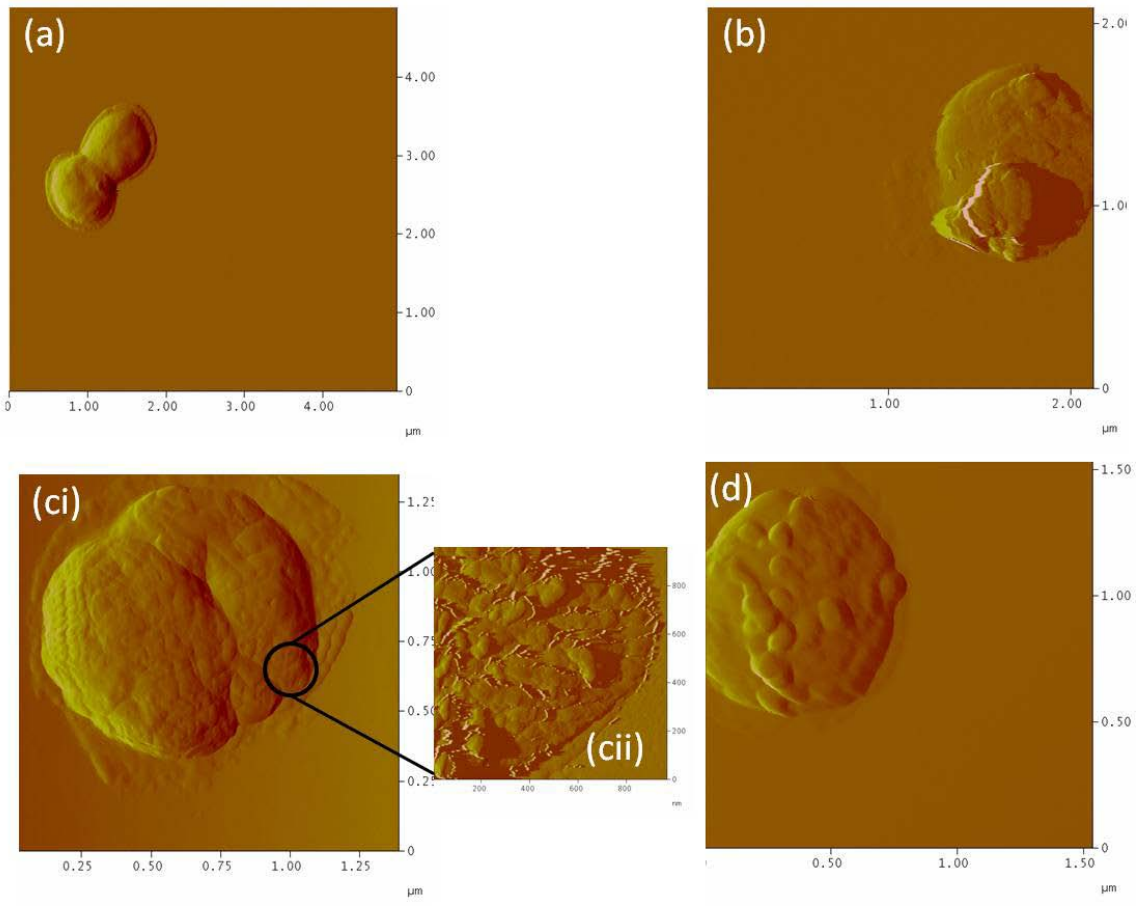

Figure 6.5. AFM phase images of a) *S. aureus* as control. b) PEG-SWNT-AntiPrA Ab on *S. aureus*. ci) mAmp-SWNT-AntiPrA Ab on *S. aureus*. cii) Magnified image showing damp-SWNT uniformly distributed on bacterial surface. d) DSS-SWNT-AntiPrA AB on *S. aureus*.

This result demonstrates that the four particles can be used to selectively target pathogens provided the antibody to the pathogen is conjugated to the particles. The ability of the particles to evade the pathogens completely when no antibody is conjugated and the high specificity of attachment after antibody conjugation essentially means that the particles could target selective pathogens present in a diverse population of microorganisms.

Hybrid SWNT with Macrophages:

For this set of experiments we used an additional particle, PrA-SWNT without the Factor H, to differentiate the particle from PrA-FH-SWNT, which is better suited as far as stealth is concerned. The concentration of opsonins, C3b and IgG, the most abundant in the blood with concentrations of 0.55mg/ml and 8mg/ml respectively (Greer and Wintrobe, 2008), will be adjusted to match the number of receptors on macrophages. A single macrophage has 2 million receptors for opsonins (Kronvall et al., 1970), therefore for realistic purposes the ratio of opsonin to macrophage will be fixed at 10^6:1. Based on AFM images and assuming there is uniform deposition of dsSWNT on the mica surface, we estimated the number of dsSWNT to be 2.5 x 10^5 per microliter of solution. We assumed a 4:1 opsonin:dsSWNT ratio would ensure tagging of all the SWNT in solution if they are non-transparent. The five particles along with a control particle, dsSWNT, were tested both with fluorescent (FITC) tagged antibodies attached to them. The particles were preincubated with the opsonins before introducing macrophages to prevent any nonspecific binding of particles to macrophages. We refrained from analyzing the attachment/non attachment of the particles to macrophages using the laser ablation method as used previously in the case of *S. aureus* due to a surprising and most exciting finding that will be revealed later in the section. Instead we used FITC tagged IgG to understand and study the location of the particles with respect to macrophages. Fluorescence microscopy was employed and the sample was evaluated under the FITC filter at 63X magnification. As shown in Fig 6.6 the control dsSWNT-IgG was readily taken up by macrophages suggesting that opsonins (especially C3b) would have adsorbed on the surface of dsSWNT and tagged it for phagocytosis. If the orientation of IgG that is

adsorbed on dsSWNT is unfavorable for macrophage recognition then C3b alone could lead to internalization.

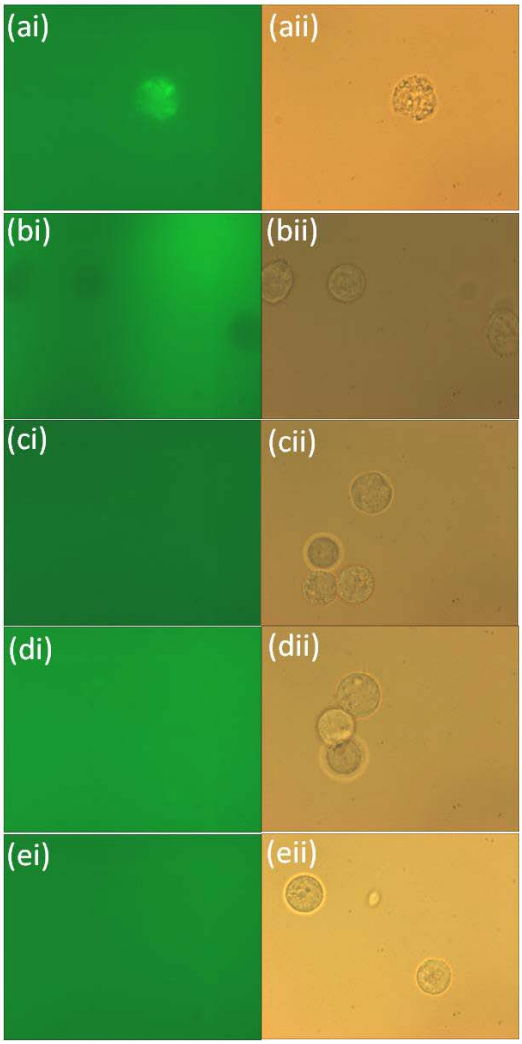

Figure 6.6. FITC Fluorescent (i) and Light microscopy (ii) images of macrophages with a) Control dsSWNT-IgG. b) PEG-SWNT-IgG. c) mAmp-SWNT-IgG. d) DSS-SWNT-IgG. e) PrA-FH-SWNT-IgG. The IgG is tagged with FITC. Notice the deformation and coarse nature of the cytoplasm in dsSWNT-IgG compared to others.

The high intensity fluorescence emanating from the macrophage is suggestive of presence of dsSWNT inside the cell and clearly shows and indicates the high degree of uptake by macrophage of any unprotected particle. The FITC fluorescence images of PEG-SWNT-IgG, mAmp-SWNT-IgG, DSS-SWNT-IgG, PrA-FH-SWNT-IgG and PrA-SWNT-IgG did not show any such signal from the cell interior. This is testament to the transparency afforded to SWNT by these coating materials.

However, we suspected that there should be some uptake of PrA-SWNT-IgG by macrophages because they were not rendered completely immune due to the lack of Factor H. It should still be susceptible to be tagged by C3b and engulfed by macrophage. We repeated the fluorescent microscopy analysis, this time using the DAPI filter; where the cells have a blue hue due to autofluorescence and the FITC tagged IgG appear green. This filter provides a very good contrast and can detect particles that previously went undetected in the FITC filter due to its high threshold for fluorescent light. This time the sample containing PrA-SWNT-IgG showed a handful of particles inside the macrophages suggesting that PrA-SWNT-IgG are susceptible to ingestion (Fig. 6.7). Given the concentration of C3b is 20X less than IgG in blood; it could explain why a high amount of PrA-SWNT-IgG were not phagocytized. The relatively low concentration of C3b might have prevented tagging of all the PrA-SWNT-IgG thereby resulting in a selected few to get engulfed and sparing the others.

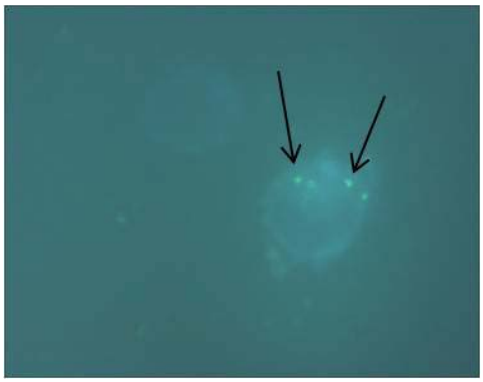

Figure 6.7. DAPI Fluorescent image of macrophage with PrA-SWNT-IgG. Arrows are pointing at the particle.

It would be interesting to study if IgG and C3b act exclusively in tagging foreign particles and exert their own dominion over a tagged particle on a first come first serve basis. In that case PrA-SWNT-IgG already has IgG attached to it artificially, which could lead to the assumption that C3b was not given access to the particle? The other four particles did not show up inside the macrophages under the DAPI filter. We can now confidently claim that PEG-SWNT, mAmp-SWNT, DSS-SWNT and PrA-FH-SWNT exhibit stealth behavior when encountered by opsonins and macrophages based on *S. aureus* and macrophage studies. Besides having all the essential traits to escape the cells of the innate immune system and the ability to wade through the microcosm of the injection site unscathed, the particles are also simultaneously ready to perform downstream targeting of tumors and disease sites in lieu of the antibodies attached.

Laser induced stealth to SWNT:

During the experiments with macrophage we tried to ablate the cells using He:Ne laser after the particles were mixed in the medium. To our surprise we found out that most of the macrophage survived with the control, SWNT, which was unusual and not what was expected. Since dsSWNT are too small to see under optical microscope we used pristine SWNT without any treatment and mixed them with macrophages. As expected SWNT bundles were seen internalized by macrophages. We observed the macrophages that had the phagocytized SWNT, in real time under light microscope for 2 hours. The macrophage rapidly showed signs of cell death such as thinning of cell membrane, increase in size, irregularities in the cell membrane and they eventually perished after 10 mins (Fig 6.8). However, the control macrophage with no SWNT continued to live up to 2 hrs and beyond.

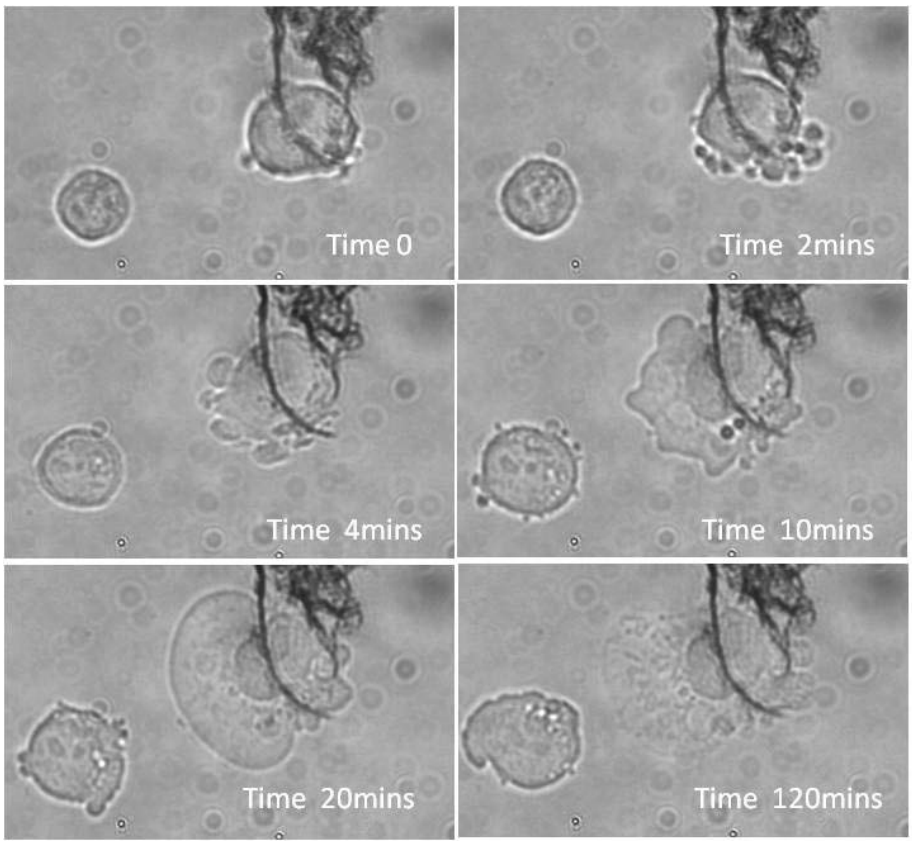

Figure 6.8. Real time light microscopy images. Macrophage on left has no SWNT in it and the one on right has internalized a SWNT bundle.

We used Trypan Blue to confirm that cell death had occurred and after 5 mins of incubation the macrophage associated with SWNT turned blue in color and the adjacent cells in the field not having SWNT remained viable and uncolored (Fig. 6.9).

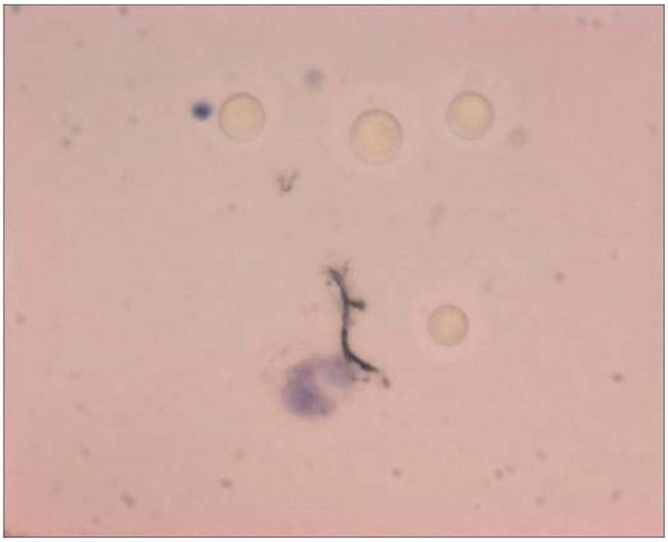

Figure 6.9. Light microscopy image of macrophage with pristine SWNT after Trypan Blue treatment.

We then positioned the He:Ne laser next to the microscope and aligned the beam on the sample to observe the real time changes to macrophages. Surprisingly, we observed the macrophage slowly disassociating with the SWNT bundle and moving away from it (Fig. 6.10). The cell disassociated at the 15 min mark and moved more than 3 microns away from the SWNT bundle it was associated with, in 2hrs.

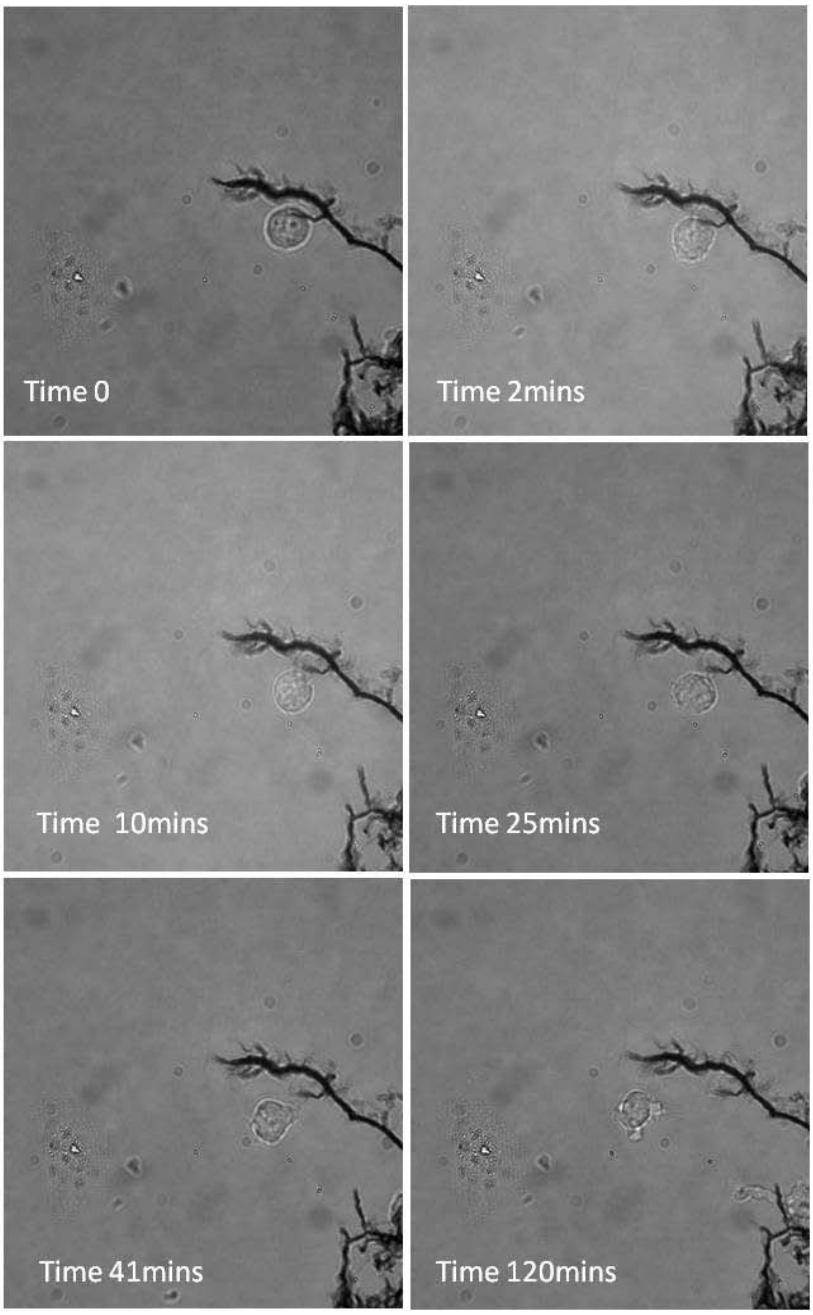

Figure 6.10. Real time Light microscopy images of laser treated macrophages that had internalized pristine SWNT.

Trypan Blue dye test showed the macrophage associated with SWNT was still viable and had no blue coloration (Fig. 6.11). After the heat stimulus is taken away there

is high possibility for the macrophage to re-internalize the SWNT as is evident in the image. However, the cell remains viable.

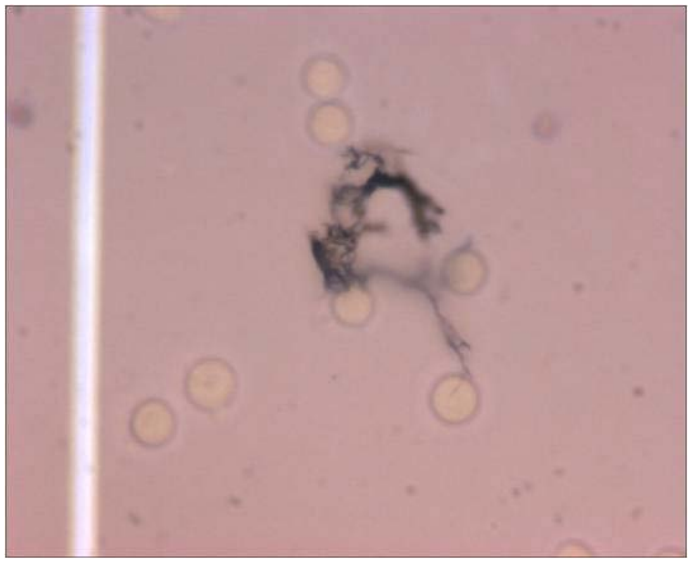

Figure 6.11. Light microscopy image of macrophage with pristine SWNT after laser and Trypan Blue treatment.

We wanted to see if this phenomenon was exclusive to macrophages and not other cell types, mammalian or prokaryotic. In our earlier study we showed prokaryotes are susceptible to laser induced ablation when SWNT are associated with it. We used human Breast cancer cell and colon cancer cell and mixed them with dsSWNT to facilitate nonspecific adsorption and then laser irradiation was performed followed by trypan blue treatment. It was observed that the cells exposed to SWNT had perished, as shown by the blue coloration, and was most likely due to the laser and SWNT induced ablation (Fig. 6.12 aii,bii). This means that the pristine SWNT did not disassociate with the tumor cells on laser application. Hence, we can conclude that this unique phenomenon is limited to

macrophages and most likely explanation being; macrophages being highly responsive cells, respond to heated SWNT (laser induced) as a reflex mechanism to save itself from being harmed.

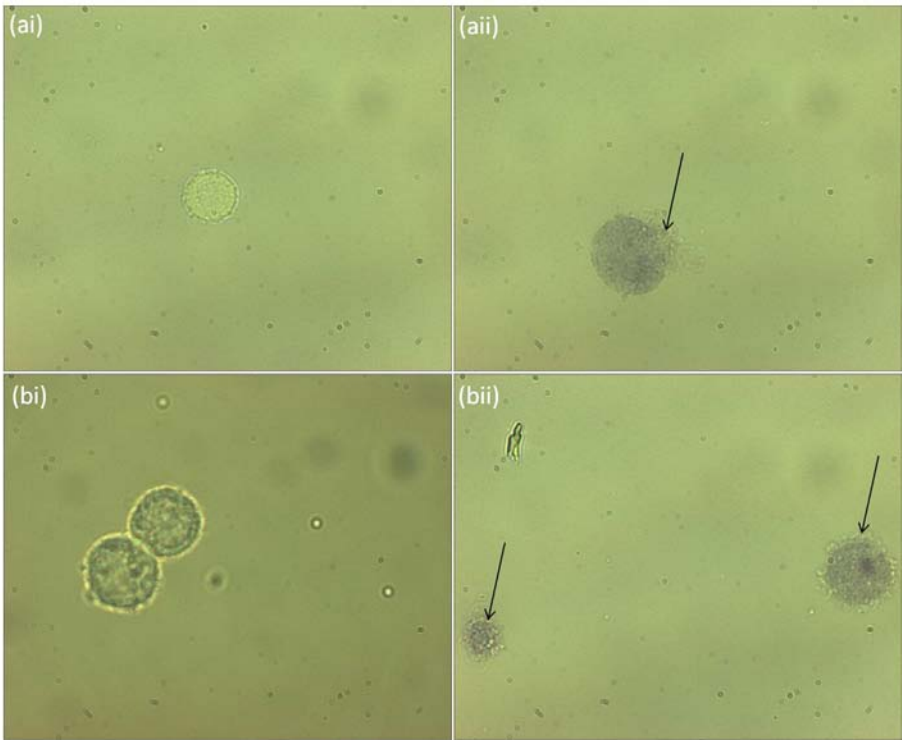

Figure 6.12. Light microscopy images of ai) Normal Breast cancer cell. aii) BC cell treated with pristine SWNT then subjected to laser and Trypan blue treatment. bi) Normal Colon cancer cell. bii) CC cell treated with pristine SWNT then subjected to laser and Trypan blue treatment. The arrows shot the bundled pristine SWNT on the surface of the cells.

This optical induced transparency afforded to SWNT against macrophages has potential in therapeutics due to its non-invasive nature and can be accomplished by irradiating the exterior of the body with harmless NIR radiation. It would perfectly complement the particles that we have developed and any other NIR responsive particle,

and aiding them to stay transparent to macrophages. By irradiating the body with NIR radiation we can but contemplate at this early stage, that targeting agents even if phagocytized by macrophages in small numbers due to loss of coating or non-uniform coating, can escape the macrophage to continue on its journey downstream.

CHAPTER 7

Conclusions and Recommendations

Our goal was to transform pristine SWNT, which are hydrophobic, bundled, long and non-biocompatible to hydrophilic, individual, shortened, biocompatible and opsonin resistant. We achieved this by systematically addressing each step of the process. Firstly, we identified a new compound, mAmp, which has an absorption maxima at 340nm and emission maxima at 420nm. It has detergent like properties, as tested on SWNT, evident by the van hove peaks in UV-Vis spectrum. Its structure was deciphered to resemble its parent compound, however with two more conjugate bonds which in part are responsible for its unique properties. They are negatively charged and basic in nature. QY was calculated to be 0.11, much better than the popular Cy3 dyes. Also, due to its hydrophilicity and biocompatibility it can be used to coat materials to make *in vivo* tumor targeting agents and intracellular probes.

Once we achieved control over the SWNT by making them amenable for biomedical applications, the next goal was to coat SWNT with a variety of moieties that will render SWNT, opsonin resistant. We chose Dextran sulfate. Owing to the cost effectiveness of DSS in relation to other biopolymers, this process can be used as an inexpensive way to completely wrap SWNTs using a biomaterial, thus potentially mitigating its toxicity as well as enhancing their solubility in biologically relevant aqueous solutions. We demonstrated near complete wrapping of DSS on SWNT through hydrophobic interaction. This is the first time that DSS has been shown to achieve the facile interaction with SWNT without the involvement of a third moiety. Near complete

coating of SWNT by DSS is essential to avoid any potential exposure of the SWNT sidewall to the surrounding medium. A novel lectin based affinity chromatography with MWNT as support on polypropylene microcentrifuge tubes was devised because it was near impossible to separate out free DSS from DSS-SWNT hybrids. The chromatography system was able to resolve the free DSS in solution from the DSS-SWNT hybrid.

By using EDTA to crosslink polypropylene to MWNT under specific conditions, we found out a new method to interface CNTs to not only polypropylene but also a variety of other polymers such as PDMS and polyethylene. We took advantage of this new discovery by using PEG as an opsonin repellant. PEG has been traditionally used for this purpose; however, we demonstrate a new interaction mechanism to achieve an effective PEG-SWNT hybrid.

The fourth moiety used to render SWNT opsonin resistant was inspired by a pathogen *S. aureus*. Protein A and Factor Hconjugated to SWNT, which by competitively attaching to F_c region of IgG and C3b respectively, prevents recognition my macrophages. Since we wanted the PrA and FH moieties to be on the same SWNT we came up with a new procedure that will provide opsonin resistance holistically. We, for the first time have demonstrated linking two proteins on the same SWNT using PSE as a crosslinker. This opens up new avenues for creating multimeric SWNT hybrids that can perform a wide array of functions.

The stealth CNTs are basically divided into four categories: synthetic – PEG-SWNT, semisynthetic – mAmp-SWNT, seminatural – DSS-SWNT and natural – PrA-FH-SWNT. The particles were conjugated to antibodies to make them ready for

applications where precision targeting of a tissue/organ was desired. We thus prepared four different kinds of precision targeting agents using SWNT that could also escape opsonins and macrophages.

All four were first tested on *S. aureus* to see if the coatings prevented any nonspecific interaction with the pathogen. The particles did not show any sign of attachment to the bacteria, and this served as a proof of principle to proceed with the human macrophage study. *S. aureus* however did show binding to SWNT alone, with no coating. We used Anti Protein A antibody conjugated particles on *S. aureus* to decipher whether specific attachment to pathogen was achieved. Except for PrA-FH-SWNT hybrids the remaining three particles achieved successful bacterial attachment. mAmp-SWNT more so achieved uniform distribution on the bacterial surface due to its higher stability in the complex medium. We envisage the use of these particles to target specific pathogens *in vivo*, as they have the ability to avoid any nonspecific interaction with bacteria and will only bind in the presence of a targeting moiety, specific antibodies.

We then tested the particles on human macrophages in the presence of opsonins, C3b and IgG. All four particles did not bind to the macrophages. This clearly demonstrates that the coating afforded by mAmp, PEG, DSS and PrA-FH to SWNT, renders SWNT resistant to the attachment of opsonins and thereby prevents phagocytosis by macrophages.

Finally, we have for the first time demonstrated an optical based method to prevent macrophages from engulfing SWNT. Laser induced heating of SWNT makes macrophages repel and expel already engulfed SWNT as a defense mechanism. This

noninvasive procedure can be effectively used alone or in conjunction with the coating strategies employed above to make the SWNT transparent to macrophages.

We have limited our study to *in vitro*, and there is great potential in understanding the mechanisms and processes that take place when such particles are introduced in an animal model. We can decipher if the particle that is prepared to not only evade the immune system but also reach its target tissue, is indeed functional. The functionality can be tested by using laser induced tissue ablation. There are a plethora of opsonins in the blood, even though the majority are C3b and IgG, these additional opsonins can be employed to get a complete picture of true opsonin resistance afforded by the coatings. As the particles have demonstrated tremendous potential in coating and targeting specific bacteria, *in vitro* studies that employ a mixture of bacteria will help validate this claim. In order to understand more elaborately the mechanism of SWNT repulsion by macrophage on laser treatment, different particles which have the same hat responsiveness as SWNT could be used.

REFERENCES

Abir, F., Barkhordarian, S., Sumpio, B. E., "Efficacy of Dextran Solutions in Vascular Surgery", *Vascular and Endovascular Surgery*, **2004**, *38*, 483.

Adams, D. O, Hamilton, T. A, "The cell biology of macrophage activation", *Annu. Rev. Immunol*., **1984**, *2*, 283.

Alberts, B., Johnson, A., Lewis, J., Raff, M., Roberts, K., Walter, P., *Molecular Biology of the Cell* (4th ed.), **2002**, New York and London: Garland Science.

Alexis, F., Pridgen, E., Molnar, L. K., Farokhzad, O. C., "Factors affecting the clearance and biodistribution of polymeric nanoparticles," *Molecular Pharmaceutics*, **2008**, *5*, 505.

Allen, T. M., "A study of phospholipid interactions between high-density lipoproteins and smaller unilamellar vesicles", *Biochim. Biophys. Acta*., **1981**, *640*, 385.

Allen, T.M., "The use of glycolipids and hydrophilic polymers in avoiding rapid uptake of liposomes by the mononuclear phagocyte system", *Adv. Drug Del. Rev*., **1994**, *13*, 285.

Antonsen, K. P., Hoffman, A. S., "Water structure of PEG solutions by DSC measurements", *Poly(ethylene glycol) chemistry: biotechnical and biomedical applications. New York: Plenum Press*, **1992**, 15.

Bahr, J. L., Tour, J. M., "Covalent Chemistry of Single-Wall Carbon Nanotubes, A Review," *J. Mater. Chem*., **2002**, *12*, 1952.

Bajwa, R., "Nanoparticle-based therapeutics in humans: A survey", *NanotechL & Bus.*, **2008**, *5*, 135.

Balavoine, F., Schultz, P., Richard, C., Mallouh, V., Ebbesen, T. W., Mioskowski, C., "Helical Crystallization of Proteins on Carbon Nanotubes", *Angew. Chem., Int. Ed*., **1999**, *38*, 1912.

Baughman, R. H., Zakhidovde, A. A., De Heer, W. A., "Carbon Nanotubes – The Route Towards Applications", *Science*,**2002**, *297*, 787.

Belyanskaya, L.,Manser, P., Spohn, P., Bruinink, A.,Wick, P., "The reliability and limits of the MTT conversion test for carbon nanotubes – cell interaction", *Carbon*, **2007**, *45*, 2643.

Bianco, A., Kostarelos, K., Partidos, C. D., Prato, M., "Biomedical applications of functionalised carbon nanotubes", *Chem. Commun*., **2005**, 571.

Buzea, C., Pacheco, I. I., Robbie, K., "Nanomaterials and nanoparticles: Sources and toxicity", *Biointerphases*,**2007**,*2*, MR17.

Carstensen, H., Muller, R. H., Muller, B. W., "Particle size, surface hydrophobicity and interaction with serum of parenteral fat emulsions and model drug carriers as parameters related to RES uptake", *Clin. Nutr.*, **1992**, *11*, 289.

Cathcart, H., Nicolosi, V., Hughes, J. M., Blau, W. J., Kelly, J. M., Quinn, S. J., Coleman, J. N., "Ordered DNA wrapping switches on luminescence in single-walled nanotube dispersions", *J. Am. Chem. Soc.*,**2008**, *130*, 12734.

Champion, J. A., Mitragotri, S., "Role of target geometry in phagocytosis", *Proc. Natl. Acad. Sci. USA*, **2006**, *103*, 4930.

Chen, R. J., Bangsaruntip, S., Drouvalakis, K. A., Kam, N. W. S., Shim, M., Li, Y., Kim, W., Utz, P. J., Dai, H., "Noncovalent Functionalization of Carbon Nanotubes for Highly Specific Electronic Biosensors," *Proc. Natl. Acad. Sci. USA*, **2003**, *100*, 2984.

Chen, R. J., Zhang, Y., Wang, D., Dai, H., "Noncovalent Sidewall Functionalization of Single-walled Carbon Nanotubes for Protein Immobilization", *J. Am. Chem. Soc.*, **2001**, *123*, 3838.

Chen, X., Tam, U. C., Czlapinski, J. L., Lee, G. S., Rabuka, D., Zettl, A., Bertozzi, C. R., "Interfacing carbon nanotubes with living cells", *J. Am. Chem. Soc*., **2006**, *128*, 6292.

Cherukuri, P., Gannon, C. J., Leeuw, T. K., Schmidt, H. K., Smalley, R. E., Curley, S. A., Weisman, R. B., "Mammalian pharmacokinetics of carbon nanotubes using intrinsic near-infrared fluorescence", *Proc. Natl. Acad. Sci. USA*, **2006**, *103*, 18882.

Coleman, D. L., Gregonis, D. E., Andrade, J. D., "Blood- materials interactions: the minimum interfacial free energy and the optimum polar/apolar ratio hypotheses", *J. Biomed. Mater. Res*., **1982**, *16*, 381.

Cui, D., Tian, F., Ozkan, C. S., Wang, M., and Gao, H., "Effect of single wall carbon nanotubes on human HEK293 cells", *Toxicol. Lett*., **2005**, *155*, 73.

Davis, M. E., "Nanoparticles for systemic medicines and imaging agents", *Nanotech L & Bus.*, **2006**, *3*, 255.

Demoy, M., Andreux, J. P., Weingarten, C., Gouritin, B., Guilloux, V., Couvreur, P., "In vitro evaluation of nanoparticles spleen capture", *Life Sci*., **1999**, *64*, 1329.

Dresselhaus, M. S., Dresselhaus, G., Ecklund, P. C., *Science of Fullerenes and Carbon Nanotubes, Academic Press, San Diego.***1996**.

Dumortier, H., Lacotte, S., Pastorin, G., Marega, R., Wu, W., Bonifazi, D., Briand, J. P., Prato, M., Muller, S., Bianco, A., "Functionalized carbon nanotubes are non-cytotoxic and preserve the functionality of primary immune cells", *Nano Lett*., **2006**, *6*, 1522.

Feder, J., “Random sequential adsorption”, *J. Theor.Biol.*,**1980**, *87*, 237.

Freeze, H. H., “Lectin Affinity Chromatography”, *Curr. Protoc. Protein Sci.*, **2001**, *9*, 9.1.

Fure, O.T., Karlsen, J., Waernhus, K.A., Waaler, T., “On the stability of dextran solution”, *Pharm. Acta Helv.*,**1975**, *50*, 216.

Gabizon, A., Papahadjopoulos, D., “The role of surface charge and hydrophilic groups on liposome clearance in vivo”, *Biochim. Biophys. Acta*., **1992**, *1103*, 94.

Garibaldi, S., Brunelli, C., Bavastrello, V., Ghigliotti, G., Nicolini, C., “Carbon nanotube biocompatibility with cardiac muscle cells”, *Nanotechnology*, **2006**, *17*, 391.

Goding, J. W., “Use of staphylococcal protein A as an immunological reagent”, *J. Immunol. Methods*, **1978**, *20*, 241.

Goldstein, I. J., Hughes, R. C., Monsigny, M., Osawa, T., Sharon, N., “What should be called a lectin?”, *Nature*, **1980**, *285*, 66.

Goodwin, A. P., Tabakman, S. M., Welsher, K., Sherlock, S. P., Prencipe, G., Dai, H., “Phospholipid-dextran with a single coupling point: a useful amphiphile for functionalization of nanomaterials”, *J. Am. Chem. Soc.*,**2009**, *131*, 289.

Greer, J. P., Wintrobe, M. M., Wintrobe's Clinical Hematology (12^{th} ed.), Lippincott Williams & Wilkins, **2008**.

Harashima, H., Sakata, K., Funato, K., Kiwada, H., “Enhanced hepatic uptake of liposomes through complement activation depending on the size of liposomes”, *Pharm Res*., **1994**, *11*, 402.

Hirsch, A., “Functionalization of Single-wall Carbon Nanotubes”,*Angew. Chem. Int. Edn.*, **2002**, *41*, 1853.

Huczko, A., Lange, H., “Carbon nanotubes: experimental evidence for a null risk of skin irritation and allergy”, *Fullerene Sci. Technol.*,**2001**, *9*,247.

Huczko, A., Lange, H., Bystrzejewski, M., Baranowski, P., Grubek-Jaworska, H., Nejman, P., Przybylowski, T., Czuminska, K., Glapinski, J., Walton, D. R. M., Kroto, H. W., “Pulmonary toxicity of 1-D nanocarbon materials”, *Fullerenes Nanotubes Carbon Nanostruct.*,**2005,** *13***,** 141.

Iijima, S., “Helical microtubules of graphitic carbon”, *Nature*, **1991**, *354*, 56.

Ikeda, M., Hasegawa, T., Numata, M., Sugikawa, K., Sakurai, K., Fujiki, M., Shinkai, S., "Instantaneous Inclusion of a Polynucleotide and Hydrophobic Guest Molecules into a Helical Core of Cationic b-1,3-Glucan Polysaccharide", *J. Am. Chem. Soc.*, **2007**, *129*, 3979.

Illum, L., Hunneyball, I. M., Davis, S.S., "The effect of hydrophilic coatings on the uptake of colloidal particles by the liver and by peritoneal macrophages", *Int. J. Pharma*., **1986**, *29*, 53.

Jeon, S. I., Lee, J. H., Andrade, J. D., De Gennes, P. G., "Protein—surface interactions in the presence of polyethylene oxide: I. Simplified theory", *J. Colloid Interface Sci*., **1991**, *142*, 149.

Johnson, C. A., Lenhoff, A. M., "Adsorption of Charged Latex Particles on Mica Studied by Atomic Force Microscopy", *J. Colloid Interface Sci.*,**1996**, 1*79*, 587.

Jos, A., Pichardo, S., Puerto, M., Sánchez, E., Grilo, A., Cameán, A. M., "Cytotoxicity of carboxylic acid functionalized single wall carbon nanotubes on the human intestinal cell line Caco-2". *Toxicol. In Vitro.*,**2009**, *8*, 1491.

Ju, S.Y., Doll, J., Sharma, I., Papadimitrakopoulos, F., "Selection of carbon nanotubes with specific chiralities using helical assemblies of flavin mononucleotide", *Nat. Nanotechnol*., **2008**, *3*, 356.

Kagan, V. E., Tyurina, Y. Y., Tyurin, V. A., Konduru, N. V., Potapovich, A. I., Osipov, A. N., Kisin, E. R., Schwegler-Berry, D., Mercer, R., Castranova, V., Shvedova, A. A., "Direct and indirect effects of single walled carbon nanotubes on RAW 264.7 macrophages: role of iron", *Toxicol. Lett*., **2006**, *165*, 88.

Kalb, A. J., Levitzky, A., "Metal-Binding Sites of Concanavalin A and their Role in the Binding of a-Methyl D-Glucopyranoside", *Biochem. J*., **1968**, *109*, 669.

Kam, N. W. S., Dai, H., "Carbon Nanotubes as Intracellular Protein Transporters: Generality and Biological Functionality", *J. Am. Chem. Soc*., **2005**, *127*, 6021.

Kam, N. W. S., Jessop, T. C., Wender, P. A., Dai, H., "Nanotube Molecular Transporters: Internalization of Carbon Nanotube–Protein Conjugate s into Mammalian Cells", *J. Am. Chem. Soc.*, **2004**, *126*, 6850.

Kam, N. W. S., O'Connell, M., Wisdom, J. A., Dai, H., "Carbon nanotubes as multifunctional biological transporters and near-infrared agents for selective cancer cell destruction", *Proc. Natl. Acad. Sci. USA*, **2005**, *102*, 11600.

Kamps, J. A., Scherphof, G. L., "Receptor versus non-receptor mediated clearance of liposomes", *Adv. Drug Deliv. Rev*., **1998**, *32*, 81.

Kim, J. S., Raines, R. T., “Dibromobimane as a fluorescent crosslinking reagent”, *Anal. Biochem.*, **1995**, *225*,174.

Kim, J. -W., Galanzha, E. I., Shashkov, E. V., Moon, H. M., Zharov, V. P., “Golden carbon nanotubes as multimodal photoacoustic and photothermal high-contrast molecular agents.”, *Nat. Nanotechnol.*, **2009**, *4*, 688.

Kim, J. -W., Kotagiri, N., Kim, J. H., Deaton, R., “In situ fluorescence microscopy visualization and characterization of nanometer scale carbon nanotubes labeled with 1-pyrenebutanoic acid, succinimidyl ester.”, *Appl. Phys. Lett.*, **2006**, *88*, 213110.

Kim, J. -W., Shashkov, E. V., Galanzha, E. I., Kotagiri, N., Zharov, V. P., “Photothermal antimicrobial nanotherapy and nanodiagnostics with self-assembling carbon nanotube clusters.", *Lasers Surg. Med.*,**2007**, *39*, 622.

Kim, J.-W., Tung, S., Deaton, R.,“Interfacing micro-/nano-scale biological and abiological materials for bio/abio hybrid systems”,*Proceedings of International Symposium on Nanoscale Devices, Materials, and Biological Systems: Fundamentals and Applications*, M. Cahay, M. Urquidi-Macdonald, S. Bandyopadhyay, P. Guo, H. Hasegawa, N. Koshida, J.P. Leburton, D.J. Lockwood, S. Seal, and A. Stella (eds), The Elecrochemical Society Proceedings Series, **2004**, PV-2004, Pennington, NJ.

Kinoshita, T., “Biology of the complement: the overture”, *Immunol. Today*, **1991**, *12*, 291.

Kiwada, H., Matsuo, H., Harashima, H., “Identification of proteins mediating clearance of liposomes using a liver perfusion system”, *Adv. Drug Deliv. Rev.*, **1998**, *32*, 61.

Kommareddy, S., Amiji, M., “Biodistribution and Pharmacokinetic Analysis of Long-Circulation Thiolated Gelatin Nanoparticles Following Systemic Administration in Breast Cancer-Bearing Mice”, *J. Pharm. Sci.*, **2007**, *96*, 397.

Konig, K.,“Multiphoton microscopy in life sciences”, *J. Microsc.*, **2000**, *200***,** 83.

Kotagiri, N., Kim, J. -W., "Carbon nanotubes fed on "carbs": coating of single-walled carbon nanotubes by dextran sulfate", *Macromol. Biosci.*, **2010**, *10*, 231.

Kralchevsky, P. A., Nagayama, K., “Capillary Forces between Colloidal Particles”, *Langmuir*, **1994**, *10*, 23.

Kronvall, G., Quie, P. G, Williams, R. C., “Jr Quantitation of staphylococcal protein A: Determination of equilibrium constant and number of protein A residues on bacteria”, *J. Immunol.*, **1970**, *104*, 273.

Lacerda, L., Herrero, M. A. , Venner, K., Bianco, A., Prato, M., Kostarelos, K., “Carbon nanotube shape & individualization critical for renal excretion”, *Small*, **2008**, *4*, 1130.

Lam, C. W., James, J. T., McCluskey, R., Hunter, R. L., "Pulmonary toxicity of Single-walled carbon nanotubes in mice 7 and 90 after intratracheal installation", *Toxicol. Sci.*,**2004,** *77***,** 126.

Lewinski, N., Colvin, V., Drezek, R., "Cytotoxicity of Nanoparticles", *Small*, **2008**, *4*, 26.

Linhardt, R. J., Pervin, A., "Separation of negatively charged carbohydrates by capillary electrophoresis", *J. Chromatogr. A*, **1996**, *720*, 323.

Liu, D., Hu, Q., Song, Y. K., "Liposomes Clearance from Blood: Different Animal Species Have Different Mechanisms", *Biochim. Biophys. Acta.*, **1995**, *1240*, 277.

Liu, F., Liu, D., "Serum independent liposome uptake by mouse liver", *Biochim. Biophys. Acta*., **1996**, *1278*, 5.

Liu, Z., Cai, W., He, L., Nakayama, N., Chen, K., Sun, X., Chen, X., Dai, H., "In vivo biodistribution and highly efficient tumor targeting of carbon nanotubes in mice", *Nat. Nanotech*., **2007**, *2*, 47.

Liu, Z., Tabakman, S., Welsher, K., Dai, H., "Carbon Nanotubes in Biology and Medicine: In vitro and in vivo Detection, Imaging and Drug Delivery", *Nano Res*., **2009**, *2*, 85.

Lu, Q., Moore, J. M., Huang, G., Mount, A. S., Rao, A. M., Larcom, L. L., Ke, P. C., "RNA Polymer Translocation with Single-Walled Carbon Nanotubes" *Nano Lett.*, **2004**, *4*, 2473.

Ma, W. – j., Yuan, X. – b., Kang, C. – s.,Su, T., Yuan, X. – y., Pu, P. – y., Sheng, J. , "Evaluation of blood circulation of polysaccharide surface-decorated PLA nanoparticles", *Carbohydrate Polymers*, **2008**, *72*, 75.

Male, D., Brostoff, J., Roth, D., Roitt, I., *Immunology* (7^{th} ed.), **2006**, Elsevier.

Maynard, A. D., Baron, P. A., Foley, M., Shvedova, A. A., Kisin, E. R., Castranova, V., "Exposure to Carbon Nanotube Material. Aerosol Release During the Handling of Unrefined Single Walled Carbon Nanotube Material", *J. Toxicol. Environ. Health A*,**2004**, *67***,** 87.

McDevitt, M. R., Chattopadhyay, D., Kappel, B. J., Jaggi, J. S., Schiffman, S. R., Antczak, C., Njardarson, J. T., Brentjens, R., Scheinberg, D. A., "Tumor targeting with antibody-functionalized, radiolabeled carbon nanotubes", *J. Nucl. Med*., **2007**, *48*, 1180.

Moghimi, S. M., Hunter, A. C., Murray, J. C., "Long-circulating and target-specific nanoparticles: theory to practice", *Pharmacol. Rev.*, **2001**, *53*, 283.

Moghimi, S. M., Szebeni, J., “Stealth liposomes and nanoparticles: critical issues on protein-binding properties, activation of proteolytic blood cascades and intracellular fate”, *Prog. Lipid Res*., **2003**, *42*, 463.

Moon, H. -M., Kim, J. -W., “Carbon nanotube clusters as universal bacterial adsorbents and magnetic separation agents”, *Biotechnol. Prog*., **2010**, *26*, 179.

Moreno-Herrero, F., Perez, M., Baro, A. M., Avila, J., “Characterization by Atomic Force Microscopy of Alzheimer Paired Helical Filaments under Physiological Conditions”, *Biophys. J.*,**2004**, *86*, 517.

Mujumdar, R. B., Ernst, L. A., Mujumdar, S. R., Lewis, C. J., Waggoner, A. S., “Cyanine dye labeling reagents: sulfoindocyanine succinimidyl esters”, *Bioconj. Chem.*, **1993**, *4*, 105.

Muller, R. H., Wallis, K. H., Troster, S. D., Kreuter, J., “In vitro characterization of poly(methyl-methaerylate) nanoparticles and correlation to their in vivo fate”, *J. Control. Release*, **1992**, *20*, 237.

Musso, S., Porro, S., Vinante, M., Vanzetti, L., Ploeger, R., Giorcelli, M., Possetti, B., Trotta, F., Pederzolli, C., Tagliaferro, A., “Modification of MWNTs obtained by thermal-CVD”, *Diamond and Related Materials*,**2007**, *16*, 1183.

Nagayama, S., Ogawara, K., Fukuoka, Y., Higaki, K., Kimura, T., “Time-dependent changes in opsonin amount associated on nanoparticles alter their hepatic uptake characteristics”, *Int. J. Pharm*., **2007**, *342*, 215.

Niyogi, S., Hamon, M. A., Hu, H., Zhao, B., Bhowmik, P., Sen, R., Itkis, M. E., Haddon, R. C., “Chemistry of Single-Walled Carbon Nanotubes”, *Acc. Chem. Res*., **2002**, *35*, 1105.

O'Connell, M. J., Bachilo, S. M., Huffman, C. B., Moore, V. C., Strano, M. S., Haroz, E. H., Rialon, K. L., Boul, P. J., Noon, W. H., Kittrell, C., Ma, J., Hauge, R. H., Weisman, R. B., Smalley, R. E., “Band Gap Fluorescence from Individual Single-Walled Carbon Nanotubes”, *Science*, **2002**, *297*, 593.

Otsuka, H., Nagasaki, Y., Kataoka, K., “PEGylated nanoparticles for biological and pharmaceutical applications”, *Adv. Drug Delivery Rev.*, **2003**, *55*, 403.

Owens, D. E., Peppas, N. A., “Opsonization, biodistribution, and pharmacokinetics of polymeric nanoparticles”, *Int. J. Pharm.*, **2006**, *307*, 93.

Pan, B. F., Cui, D. X., Xu, P., Huang, T., Li, Q., He, R., Gao, F., “Cellular Uptake Enhancement of Polyamidoamine Dendrimer Modified Single Walled Carbon Nanotubes”, *J. Biomed. Pharm. Eng*., **2007**, *1*, 13.

Panchapakesan, B., Lu, S., Sivakumar, K., Teker, K., Cesarone, G., Wickstrom, E.,"Single-Wall Carbon Nanotube Nanobomb Agents for KillingBreast Cancer Cells",*J. Nanobiotechnol.*, **2005**, *1*, 133.

Pandiripally, V., Wei, L., Skerka, C., Zipfel, P. F., Cue, D., "Recruitment of Complement Factor H-like Protein 1 Promotes Intracellular Invasion by Group A Streptococci", *Infect. Immun.*, **2003**, *71*, 7119.

Pangburn, M. K., "Host recognition and target differentiation by factor H, a regulator of the alternative pathway of complement", *Immunopharmacology*, **2000,** *49*, 149.

Pantarotto, D., Briand, J. P., Prato, M., Bianco, A., "Translocation of bioactive peptides across cell membranes by carbon nanotubes", *Chem. Commun*., **2004**, 16.

Panyam, J., Labhasetwar, V., "Dynamics of Endocytosis and Exocytosis of Poly (D, L-Lactide-co-Glycolide) Nanoparticles in Vascular Smooth Muscle Cells", *Pharm. Res*., **2003**, *20*, 212.

Partearroyo, M. A., Ostolaza, H., Goni, F. M., Guillem, E. B., "Surfactant-induced cell toxicity and cell lysis", *Biochem. Pharm.*, **1990**, *40*, 1323.

Patel, H. M., Moghimi, S. M., "Serum-mediated recognition of liposomes by phagocytic cells of the reticuloendothelial system – The concept of tissue specificity", *Adv. Drug Deliv. Rev*., **1998**, *32*, 45.

Poland, C. A., Duffin, R., Kinloch, I., Maynard, A., Wallace, W. A. H. , Seaton, A., Stone, V., Brown, S., MacNee, W., Donaldson, K., "Carbon nanotubes introduced into the abdominal cavity of mice show asbestos-like pathogenicity in a pilot study", *Nat. Nanotechnol*., **2008**, *3*, 423.

Porath, J., "General methods and coupling procedures", *Methods Enzymol*., **1974**, *34*, 13.

Poretz, R. D., Goldstein, I. J., "An examination of the topography of the saccharide binding sites of concanavalin A and of the forces involved in complexation", *Biochemistry,***1970**, *9*, 2890.

Puisieux, F., Barratt, G., Couarraze, G., Couvreur, P.,Devissaguet, J. P., Dubernetal, C., Polymeric biomaterials. New York: Marcel Dekker, Inc., **1994**, 749.

Pulskamp, K., Diabate, S., and Krug, H. F., "Carbon nanotubes show no sign of acute toxicity but induce intracellular reactive oxygen species in dependence on contaminants" *Toxicol. Lett*., **2007**, *168*, 58.

Rees, D. A., Scott, W. E., “Polysaccharide conformation. Pt. VI. Computer model-building for linear and branched pyranoglycans. Correlations with biological Functions. Preliminary assessment of inter-residue forces in acqueous solutions. Further interpretation of optical rotation in term of chain conformation”, *J. Chem. Soc. B*,**1971**,469.

Riegel, E. R., Kent, J. A., *Kent and Riegel's handbook of industrial chemistry and biotechnology*, **2007**, *11*, 552.

Romberg, B., Hennink, W. E., Storm, G., “Sheddable coatings for long-circulating nanoparticles”, *Pharm. Res.*, **2008**, 25, 55.

Rudt, S., Muller, R. H., “In vitro phagocytosis assay of nano- and microparticles by chemiluminescence. III. Uptake of differently sized surface-modified particles, and its correlation to particle properties and in vivo distribution”, *Eur. J. Pharma. Sci*., **1993**, *1*, 31.

Ryan, K. J., Ray, C. G., *Sherris Medical Microbiology* (4th ed.). McGraw Hill, **2004**.

Sahu, A., Lambris, J. D., “Structure and biology of complement protien C3, a connecting link between innate and acquired immunity”, *Immunol. Rev.*, **2001**,*180*, 35.

Sato, Y., Yokoyama, A., Shibata, K., Akimoto, Y., Ogino, S., Nodasaka, Y., Kohgo, T., Tamura, K., Akasaka, T., Uo, M., “Influence of length on cytotoxicity of multi-walled carbon nanotubes against human acute monocytic leukemia cell line THP-1 in vitro and subcutaneous tissue of rats in vivo”, *Mol. BioSyst.*,**2005**, *1***,** 176.

Schipper, M. L., Nakayama-Ratchford, N., Davis, C. R., Kam, N. W., Chu, P., Liu, Z., Sun, X., Dai, H., Gambhir, S. S., “A pilot toxicology study of single-walled carbon nanotubes in a small sample of mice”, *Nat. Nanotechnol*., **2008**, *3*, 216.

Shvedova, A. A., Castranova, V., Kisin, E. R., Schwegler-Berry, D., Murray, A. R., Gandelsman, V. Z., Maynard, A., Baron, P., “Exposure to carbon nanotube material, assessment of nanotube cytotoxicity using human keratinocyte cells”, *J. Toxicol. Environ. Health A*, **2003**, *66*, 1909.

Shvedova, A. A., Kisin, E. R., Mercer, R., Murray, A. R., Johnson, V. J., Potapovich, A. I, Tyurina, Y. Y., Gorelik, O., Arepalli, S., Schwegler-Berry, D., Hubbs, A. F., Antonini, J., Evans, D. E., Ku, B. K., Ramsey, D., Maynard, A., Kagan, V. E., Castranova, V., Baron, P., “Unusual inflammatory and fibrogenic pulmonary responses to single-walled carbon nanotubes in mice.”, *Am. J. Physiol. Lung Cell Mol. Physiol.*,**2005**, *5*,L698.

Singh, R., Pantarotto, D., Lacerda, L., Pastorin, G., Klumpp, C., Prato, M., Bianco, A., Kostarelos, K., “Tissue biodistribution and blood clearance rates of intravenously administered carbon nanotube radiotracers. *Proc. Nat. Acad. Sci. USA*, **2006**, *103*, 3357.

Sokolov, I., Kievsky, Y. Y., Kaszpurenko, J. M., “Self-assembly of ultra-bright fluorescent silica particles”, *Small*, **2007**, *3*, 419.

Sparrow, C. P., Parthasarathy, S., Steinberg, D., “A macrophage receptor that recognizes oxidized low density lipoprotein but not acetylated low density lipoprotein”, *J. Biol. Chem*., **1989**, *264*, 2599.

Srivastava, A., Srivastava, O. N., Talapatra, S., Vajtai, R., Ajayan, P. M., “Carbon nanotube filters”, *Nature Materials*, **2004**, *3*, 610.

Star, A., Steuerman, D. W., Heath, J. R., Stoddart, J. F., “Starched Carbon Nanotubes”, *Angew. Chem., Int. Ed*., **2002**, *41*, 2508.

Stolnik, S., Illum, L., Davis, S., “Long circulating microparticle drug carrier”, *Adv. Drug Deliv. Rev*., **1995**, *16*, 195.

Sumner, J. B., “The globulins of the jack bean, canavalia ensiformis”, *J. Biol. Chem.*,**1919**, *37*, 137.

Surolia, A., Pain, D., Khan, M. I., “Protein A: nature's universal anti-antibody”, *Trends Biochem. Sct.*, **1982**, *7*, 74.

Tabata, Y., Ikada, Y., “Effect of the size and surface charge of polymer microspheres on their phagocytosis by macrophage”, *Biomaterials*, **1988**, *9*, 356.

Tabata, Y., Ikada, Y., “Phagocytosis of polymer microspheres by macrophages”, *Adv. Polym. Sci*., **1990**, *94*, 107.

Uno, T., Masada, M., Kuroda, Y., Nakagawa, T., “Isolation and structural investigation of the fluorescent degradation products of ampicillin”, *Chem. Pharm. Bull*., **1981**, *29*, 1344.

Vivekchand, S. R. C., Jayakanth, R., Govindaraj, A., Rao, C. N. R., “The problem of purifying single-walled carbon nanotubes”, *Small*, **2005**, *1*, 920.

Vonarbourg, A., Passirini, C., Saulnier, P., Benoit, J. P., “Parameters influencing the stealthiness of colloidal drug delivery systems”, *Biomaterials*, **2006**, *27*, 4356.

Wang, H. F., Wang, J., Deng, X. Y., Sun, H. F., Shi, Z. J., Gu, Z. N., Liu, Y. F., Zhao, Y. L., “Biodistribution of carbon single-wall carbon nanotubes in mice”, *J. Nanosci. Nanotechnol*., **2004**, *4*, 1019.

Wang, H., Zhou, W., Ho, D. L., Winey, K. I., Fischer, J.,E., Glinka, C. J., Hobbie, E. K.,“ Dispersing single-walled carbon nanotubes with surfactants: A small angle neutron scattering study”, *Nano Lett*., **2004**, *4*, 1789.

Warheit, D. B., Laurence, B. R., Reed, K. L., Roach, D. H., Reynolds, G. A. M., Webb, T. R., "Gold Nanoparticles Are Taken Up by Human Cells but Do Not Cause Acute Cytotoxicity", *Toxicol. Sci.*,**2004,** *77***,** 117.

Wick, P., Manser, P., Limbach, L.K., Dettlaff-Weglikowska, U., Krumeich, F., Roth, S., Stark, W.J., Bruinink, A., "The degree and kind of agglomeration affect carbon nanotube cytotoxicity", *Toxicol. Lett.*, **2007,** *2*, 121.

Williams, A. T. R., Winfield, S. A., Miller, J. N., "Relative fluorescence quantum yields using a computer controlled luminescence spectrometer", *Analyst*, **1983**, *108*, 1067.

Wong, S., Joselevich, E., Woolley, A.T., Cheung, C. L., Lieber, C. M., "Covalently functionalized nanotubes as nanometre-sized crobes in chemistry and biology", *Nature*, **1998**,*394***,** 52.

Worle-Knirsch, J. M., Pulskamp, K., Krug, H. F., "Oops They Did It Again! Carbon Nanotubes Hoax Scientists in Viability Assays", *Nano Lett*., **2006**, *6*, 1261.

Wu, J., Wu, Y. Q., Ricklin, D., Janssen, B. J., Lambris, J. D., Gros, P., "Structure of complement fragment C3b-factor H and implications for host protection by complement regulators", *Nat Immunol.*, **2009**, *10*, 728.

Yamamoto, Y., Nagasaki, Y., Kato. Y., Sugiyama. Y, Kataoka, K., "Long-circulating poly(ethylene glycol)-poly(d,l-lactide) block copolymer micelles with modulated surface charge", *J. Controlled Release*, **2001**, *77*, 27.

Yang, W., Thordarson, P., Gooding, J. J., Ringer, S. P., Braet, F., "Carbon nanotubes for biological and biomedical applications", *Nanotechnology*, **2007**, *18*, 412001.

Yokoyama, A., Sato, Y., Nodasaka, Y., Yamamoto, S., Kawasaki, T., Shindoh, M., Kohgo, T., Akasaka, T., Uo, M., Watari, F., Tohji, K., "Biological behavior of hat-stacked carbon nanofibers in the subcutaneous tissue in rats", *Nano Lett.*,**2005**, *1***,** 157.

Zerda, A., Zavaleta, C., Keren, S., Vaithilingam, S., Bodapati, S., Liu, Z., Levi, J., Smith, B. R., Ma, T. -J., Oralkan, O., Cheng, Z., Chen, X., Dai, H., Khuri-Yakub, B. T., Gambhir, S. S., "Carbon nanotubes as photoacoustic molecular imaging agents in living mice", *Nat. Nanotechnol*., **2008**, *3*, 557.

Zhao M., Yang, M., Li, X.-M., Jiang, P., Baranov, E., Li, S., Xu, M., Penman, S., Hoffman, R. M., "Tumor-targeting bacterial therapy with amino acid auxotrophs of GFP-expressing Salmonella typhimurium", *Proc. Natl. Acad. Sci. USA*, **2005**, *102*, 755.

Zharov, V. P., Galanzha, E. I., Shashkov, E. V., Kim, J. -W., Khlebtsov, N. G., Tuchin, V. V., "Photoacoustic flow cytometry: principle and application for real-time detection of circulating single nanoparticles, pathogens, and contrast dyes in vivo", *J. Biomed. Opt.*, **2007**, *12*, 051503.

Zharov, V. P., Letfullin, R. R., Galitovskaya, E. N., “Microbubbles: overlapping mode for laser killing of cancer cells with absorbing nanoparticle clusters”, *J. Phys. D Appl. Phys.*, **2005**, *38*, 2571.

Zheng, M., Jagota, A., Semke, E. D., Diner, B. A., McLean, R. S., Lustig, S. R., Richardson, R. E., Tassi, N. G., “DNA-assisted dispersion and separation of carbon nanotubes”, *Nat. Mater.*, **2003**, *2*, 338.

APPENDIX

From Rights DE <RIGHTS-and-LICENCES@wiley-vch.de>
Sent Monday, March 14, 2011 3:56 am
To "'Nalini K. Kotagiri'" <nkotagi@uark.edu>
Cc Rights DE <RIGHTS-and-LICENCES@wiley-vch.de>
Bcc
Subject AW: AW: Request for permission

Dear Customer

Thank you for your request.

We hereby grant permission for the requested use expected that due credit is given to the original source.

Please note that we only grant rights for a printed version, but not the rights for an electronic/ online/ web/ microfiche publication, but you are free to create a link to the article in question which is posted on our website (http://onlinelibrary.wiley.com/)

If material appears within our work with credit to another source, authorisation from that source must be obtained.

Credit must include the following components:
- Books: Author(s)/ Editor(s) Name(s): Title of the Book. Page(s). Publication year. Copyright Wiley-VCH Verlag GmbH & Co. KGaA. Reproduced with permission.

- Journals: Author(s) Name(s): Title of the Article. Name of the Journal. Publication year. Volume. Page(s). Copyright Wiley-VCH Verlag GmbH & Co. KGaA. Reproduced with permission.

With kind regards

Heike Weller
****
Heike Weller
Copyright & Licensing Manager
Wiley-VCH Verlag GmbH & Co. KGaA
Boschstr. 12
69469 Weinheim
Germany

Phone: +49 (0) 62 01- 606 - 585
Fax: +49 (0) 62 01 - 606 - 332
Email: rights@wiley-vch.de
